Topics in Physics Beyond the Standard Model

A Dissertation

Presented to

The Faculty of the Department of Physics

The College of William and Mary

In Partial Fulfillment

Of the Requirements for the Degree of

Doctor of Philosophy

By

Alfredo Aranda

March 2001

UMI Number: 3012227

Bell & Howell Information and Learning Company
300 North Zeeb Road
P.O. Box 1346
Ann Arbor, MI 48106-1346

APPROVAL SHEET

This thesis is submitted in partial fulfillment of
the requirement for a degree of

Doctor of Philosophy

Alfredo Aranda

Approved, March 2001

C. D. Carone

C. E. Carlson

D. S. Armstrong

M. Sher

J. Goity
Hampton University and TJNAF

To my parents and my sisters

TABLE OF CONTENTS

ACKNOWLEDGMENTS

It is a pleasure to thank my advisor Christopher D. Carone for his guidance and support during my stay at the College, and for his infinite amount of patience.

I want to thank Rich F. Lebed who collaborated in the work related to the study of flavor physics. Also I want to thank all members of my graduate committee.

During my stay here I was able to make two very special friends, Paolo and Pibero. They both showed me lots of support and patience, and I have learned many things from them. I am very thankful to them and I hope that our friendship continues for a very long time.

I also would like to thank Jorge A. López for all the help and support he gave me during my undergraduate education. Without him it would have been impossible to get here.

Many friends have made it possible for me to have a real nice stay in Williamsburg and I am grateful to all of them. My thanks go to Hovanes, Jordi, Agus, Vittorio, and Elio.

Finally, I would like to thank some old friends who have tolerated me for many years. They are: Ricardo, Miguel, Félix, Juanete, Héctor, Carlos, and Sergio.

LIST OF FIGURES

List of Tables

ABSTRACT

Topics in Physics Beyond the Standard Model

In this dissertation we address three issues related to physics beyond the Standard model: flavor and the use of discrete gauge symmetries, the dynamical breaking of electroweak symmetry, and the addition of a U(1) gauge symmetry to the Standard model in order to suppress proton decay. We present: **i)** A model of flavor based on the double tetrahedral group that leads to acceptable quark and lepton masses as well as mixing angles. Furthermore it gives solutions for the atmospheric and solar neutrino problems. **ii)** A model of bosonic topcolor in which the breaking of electroweak symmetry occurs dynamically through the vacuum expectation value of a composite field, generated by some strong dynamics that affects third generation fields only. The mass of the top quark is also generated by this vev. All other light quarks acquire their masses through the vev of a fundamental scalar also present in the theory. **iii)** Models in which baryon number has been gauged to eliminate operators that lead to rapid proton decay. We study the phenomenology of the gauge boson associated with the new U(1). In one model we investigate the possibility of having a light leptophobic gauge boson with mass in the $1 - 10$ GeV range. In another model, constructed in the framework of extra dimensions, we explore the phenomenology of the leptophobic gauge boson and its Kaluza-Klein excitations.

Chapter 1

Introduction

The general topic of this dissertation is physics beyond the standard model (SM). In particular we address three issues:

- the use of discrete gauge symmetries in the context of flavor physics,
- topcolor models and the dynamical breaking of electroweak (EW) symmetry, and
- the addition of new U(1) gauge symmetries to the SM in order to avoid proton decay.

The first two topics are motivated by the observation that the top quark is the only with a mass ($m_t \sim 175$ GeV) that is of the order of the EW scale ($M_{EW} = 246$ GeV). In one instance (flavor) one takes the view that the O(1) top quark Yukawa coupling is of the "expected" size, while the rest of the Yukawa couplings are suppressed. One then tries to understand how this suppression comes about with the use of flavor symmetries. In the second instance (dynamical EW symmetry breaking) the opposite view is taken. Now one "expects" all Yukawa couplings to be small and thus has to explain why the top quark Yukawa coupling is large. The general idea is to assume some new strong dynamics that affect the top quark (or third generation quarks) generating a $t - \bar{t}$ bound state at a scale Λ. Below this scale the bound state will develop a vacuum expectation value (vev) and will be responsible for the breaking of EW symmetry. Finally, we explore how it is possible to avoid proton decay by adding a new U(1) gauge sector to the SM. The new U(1) is identified with baryon number and implies the existence of a new gauge boson, Z', which couples to leptons only through its mixing with the Z^0 and γ. This mixing is assumed to vanish at some high energy scale and is generated at low energies only through loop effects. Therefore the mixing is small and the Z' is leptophobic. In particular, we explore the possibilities that $M_B \ll M_Z$ and $M_B \gtrsim m_{\text{top}}$, where M_B denotes the Z' mass; in the second case the leptophobic gauge boson can propagate in extra dimensions, leading to an interesting phenomenology.

1.1 Mysteries of the Standard Model

The standard model of particle physics is very successful. In fact, it has survived every single experimental test with incredible accuracy for the last 20 or so years. For example consider the measured value of the Z^0 mass, $M_Z(\text{exp}) = 91.1872 \pm 0.0021$ GeV to be compared with the SM fit value $M_Z(SM) = 91.1879 \pm 0.0021$ GeV. The SM fit incorporates the most accurate experimentally determined observables such as M_Z, the muon decay constant (G_μ), and the fine-structure constant (α). Table 1.1 shows some of the results of the latest fit to Z−pole observables. The SM prediction for the mass of the as-yet undiscovered Higgs is also shown (for details regarding the fit see Ref. [1]). It can be seen that the SM does a remarkable job in fitting the data.

Still, even considering its success, the SM leaves many questions unanswered. It is based on the gauge group $SU(3)_C \times SU(2)_W \times U(1)_Y$, and therefore contains 12 gauge bosons: the photon γ, the Z^0, the $W^{\pm}$, and the 8 gluons. The reason for this particular gauge structure is a mystery. The matter content of the SM consists of

Observable	Value	Standard Model
m_t [GeV]	174.3 ± 5.1	172.9 ± 4.6
M_Z [GeV]	91.1872 ± 0.0021	91.1870 ± 0.0021
Γ_Z [GeV]	2.4944 ± 0.0024	2.4956 ± 0.0016
$\alpha_s(M_Z)$	0.1885 ± 0.0020	0.1192 ± 0.0028
M_H [GeV]	$---$	98^{+57}_{-38}

Table 1.1 Some $Z-$pole observables compared with the SM predictions. Also shown is the SM prediction for the Higgs mass M_H. For details about the SM fit and for more observables see Table 10.4 in Ref. [1].

three chiral families of quarks and leptons arranged as

$$\text{SU(2) doublets} \;:\; Q_L^a = \begin{pmatrix} u \\ d \end{pmatrix}_L^a, \begin{pmatrix} c \\ s \end{pmatrix}_L^a, \begin{pmatrix} t \\ b \end{pmatrix}_L^a;$$

$$L_L = \begin{pmatrix} \nu_e \\ e^- \end{pmatrix}_L, \begin{pmatrix} \nu_\mu \\ \mu^- \end{pmatrix}_L, \begin{pmatrix} \nu_\tau \\ \tau^- \end{pmatrix}_L,$$

$$\text{SU(2) singlets} \;:\; U_R^a = (u)_R^a,\ (c)_R^a,\ (t)_R^a,$$

$$:\; D_R^a = (d)_R^a,\ (s)_R^a,\ (b)_R^a,$$

$$:\; E_R = (e^-)_R,\ (\mu^-)_R,\ (\tau^-)_R,$$

where $a = 1, 2, 3$ indicates that the quarks form triplets under $SU(3)_C$. The antiparticles transform as the complex conjugate representations, i.e. the left-handed anti-leptons transform as **2**'s under $SU(2)_W$ and the anti-quarks transform as $\bar{\mathbf{3}}$'s under $SU(3)_C$. The hypercharge Y can be easily obtained using $Q = T^3 + Y$, where Q stands for electric charge (2/3 for up-type quarks, $-1/3$ for down-type quarks, 0 for all neutrinos, and -1 for all remaining leptons) and T^3 represents the third component of weak isospin ($\pm 1/2$ for left-handed particles and 0 for right-handed particles). Why there are three families satisfying this particular chiral arrangement is an open question.

The masses of the chiral fermions are also mysterious. The SM relies on the Higgs mechanism to break EW symmetry rendering the Z^0 and $W^{\pm}$ gauge bosons massive. The scalar field responsible for this breaking, the Higgs, couples to the matter fields through Yukawa interactions

$$\begin{aligned} \mathcal{L}_Y \sim & -\bar{L}^i_L(\lambda_L)_{ij} H E^j_R - \bar{Q}^i_L(\lambda_D)_{ij} H D^j_R \\ & -\bar{Q}^i_{La}(\lambda_U)_{ij}\epsilon^{ab} H^\dagger_b U^j_R + \text{h.c.}\,, \end{aligned} \quad (1.1)$$

where λ_X are 3×3 Yukawa matrices and $i = 1, 2, 3$ are generation indices. The entries in the Yukawa matrices are the Yukawa couplings and the SM does not predict them. It is clear from Eq. (1.1) that when the Higgs acquires a vev, it generates mass terms for all the fields. The mass terms can be simplified by diagonalizing the Yukawa mass matrices. For example, in the case of the quarks this is accomplished by the redefinitions

$$U_L = V_L U^m_L\,, \quad (1.2)$$

$$U_R = V_R U^m_R\,, \quad (1.3)$$

$$D_L = W_L D^m_L\,, \quad (1.4)$$

$$D_R = W_R D^m_R\,, \quad (1.5)$$

where $V_{L,R}$ and $W_{L,R}$ are 3×3 unitary matrices such that $V^\dagger_L \lambda_U V_R \equiv \lambda^D_U$, and $W^\dagger_L \lambda_D W_R \equiv \lambda^D_D$ are diagonal; $U^m_{L,R}$ and $D^m_{L,R}$ denote mass eigenstates. The diagonal entries in λ^D_U and λ^D_D correspond to the masses of the quarks and leptons. These may be chosen to reproduce the values shown in Table 1.2, but they cannot be predicted by the SM.

Due to the diagonalization of the mass matrices, the $W^{\pm}$ boson coupling to quark mass eigenstates involves the Cabibbo-Kobayashi-Maskawa (CKM) matrix

$$V_{CKM} = V_L^{\dagger} W_L \,. \tag{1.6}$$

The entries of this matrix cannot be predicted by the SM and must be determined experimentally [1],

$$V_{CKM} = \begin{pmatrix} 0.9742 \text{ - } 0.9757 & 0.219 \text{ - } 0.226 & 0.002 \text{ - } 0.005 \\ 0.219 \text{ - } 0.225 & 0.9734 \text{ - } 0.9749 & 0.037 \text{ - } 0.043 \\ 0.004 \text{ - } 0.014 & 0.035 \text{ - } 0.043 & 0.9990 \text{ - } 0.9993 \end{pmatrix} . \tag{1.7}$$

The values and patterns observed in Eq. (1.7) are also mysteries of the SM.

Another problem implied by Eq. (1.1) is that the SM includes a fundamental scalar field. Such fields receive mass squared corrections that diverge quadratically with energy. On the other hand, we know from experiments that the mass of the Higgs should be close to the EW scale (see Table 1.1). This leads to the hierarchy problem – Why is the Higgs mass $O(M_Z)$ and not the Planck scale M_P, the scale at which quantum gravity becomes relevant? Another important observation is that the standard model does not incorporate gravity. A complete (or less incomplete) description of nature should attempt to describe all known forces of nature.

One may argue that the standard model is an effective theory valid below a certain energy scale M and that the answers to some of the problems stated above can reside in physics above that scale. The hierarchy problem associated with the fundamental scalar suggests that M is not far from the electroweak scale.

m_e	m_μ	m_τ
0.511×10^{-3}	0.106	1.777
m_u	m_c	m_t
$1 - 5 \times 10^{-3}$	$1.15 - 1.35$	174.3 ± 5.1
m_d	m_s	m_b
$3 - 9 \times 10^{-3}$	$0.075 - 0.170$	$4.0 - 4.4$

Table 1.2 Experimentally determined masses of the particles in the standard model (modulo the neutrinos). All masses are in GeV [1].

All of the arguments we have presented make it clear that there is physics beyond the standard model and that it is important it be explored. Recent experimental evidence for neutrino masses [2] as well as the announcement by the Muon g-2 Collaboration [3] that there is a 2.6 σ discrepancy between the experimental measurement of the muon's anomalous magnetic moment and the prediction of the SM, support this conclusion.

1.2 Possible Solutions to the Mysteries

One of the pillars of physics beyond the standard model is grand unification [4]. The basic observation is that the running of the three gauge couplings of the SM meet at the same point at some high energy, $M_{\rm GUT}$. Theories that unify $SU(3)_C \times SU(2)_W \times U(1)_Y$ into a single gauge group at $M_{\rm GUT}$ are called grand unified theories (GUTs). The simplest GUT is based on SU(5) symmetry and it is contained in all other GUTs. By embedding all the particles of a generation into GUT representations, and thus relating leptons and quarks into a single framework, new relationships between their masses and mixings can be obtained and compared to experiments. This can in principle shed some light on the flavor problem. One aspect of unification (at least in its basic formulation) that is relevant for our discussion is that it takes place at an energy scale of $M_{GUT} \sim 2 \times 10^{16}$ GeV [1]. This implies, for instance, that the hierarchy problem we encountered in the SM remains present with M_P replaced by $M_{\rm GUT}$.

One way to solve the hierarchy problem is to make the GUTs supersymmetric. Supersymmetry is a symmetry that relates bosonic and fermionic degrees of freedom. A striking consequence of this symmetry when applied to the SM, is that it predicts the existence of a new particle for each one that has been discovered. Each SM particle has the same quantum numbers as its "superpartner" except for spin: If the SM particle is a boson (fermion), the superpartner is a fermion (boson). This symmetry can in fact be used to create a supersymmetric version of the SM, the Minimal Supersymmetric Standard Model (MSSM). In this scenario the Higgs mass squared receives radiative corrections from both the SM particles and their superpartners so that the quadratic divergences are cancelled. No great fine-tuning is required to keep the Higgs at the EW scale and not at the GUT scale. This was one of the main motivations in the use of supersymmetry. In addition to solving the hierarchy problem, the MSSM leads to more accurate unification than the SM. See Ref. [5] for a review of supersymmetry and the MSSM.

Even though supersymmetry stabilizes the hierarchy, it does not explain it. Recently, another very exciting proposal has been presented that eliminates the hierarchy altogether. The idea relates to the speculation that spacetime has more than 4 dimensions and that the extra dimensions might have large compactification radii. The idea of having more than 4 dimensions can be traced to superstring theory, which is the most promising attempt yet to construct a theory of quantum gravity and perhaps

[1] This can change dramatically when considering scenarios in which the dimensionality of spacetime is $D > 4$.

to finally incorporate it into a framework with all other forces. Superstring theory requires a spacetime with dimensionality $D = 10$ (or $D = 11$ in M−theory) in order to be physically consistent [7]. To explain why we only see 4 dimensions, the remaining $D - 4$ are compactified at very high energies leading to small compactification radii. There are several ways one can perform the compactification and they lead to different manifestations of the theory. What is interesting about the new proposal is that the extra dimensions are taken to be large and thus available for experimental exploration. In this case the Planck scale can be brought down to low energies and thus it is possible to completely eliminate the hierarchy.

There are two main scenarios discussed in the literature; in one of them only gravity can propagate in the extra dimensions and in this case the compactification scale can be very low $\sim (218\mu m)^{-1}$ [6]. In the second scenario, all gauge and Higgs fields, as well as gravity, are allowed to propagate in the extra dimensions and the compactification scale can be as low as a few TeV. An important result of this second scenario is that gauge unification can be obtained at very low energies $\sim O(10 - 100$ TeV) [8]. This is interesting because the GUT-scale particles could be explored with near future collider experiments. For a review on this fast-growing field see Ref. [9].

1.3 Our solutions

We can now discuss the main topics covered in this dissertation. A fruitful attempt at explaining the SM and MSSM mass spectra is based on the idea of a flavor symmetry, G_f, that relates the different generations of quarks and leptons. It is common to call this symmetry a horizontal symmetry. The basic idea is straightforward: let different generations transform under G_f in such a way that when the symmetry is unbroken, above some "flavor" scale, M_f, the only mass terms in the Lagrangian that one can write are those of the third generation fields. When G_f is spontaneously broken by the vevs of some scalar fields, which we call flavons, all the other mass terms are generated. More explicitly, when G_f is unbroken, the Yukawa mass matrices have the general form

$$Y \sim \begin{pmatrix} 0 & 0 & 0 \\ 0 & 0 & 0 \\ 0 & 0 & 1 \end{pmatrix}, \tag{1.8}$$

and the operators containing Yukawa couplings are given by terms like

$$\mathcal{L}_Y \sim \bar{Q}\frac{\Phi}{M_f}DH\,, \tag{1.9}$$

where $\bar{Q}$ and D represent matter fields, H represents a Higgs field, and Φ is a flavon. It is clear from Eq. (1.9) that when Φ acquires a vev, Yukawa couplings arise as ratios $\langle\Phi\rangle/M$ and add new entries in the matrix Eq. (1.8). The goal is to find a symmetry and symmetry breaking pattern that reproduces the observed patterns in the masses and mixing angles of both quarks and leptons shown in Table 1.2 and Eq. (1.7). A particularly successful supersymmetric model of flavor is based on U(2) symmetry [10]. We take this as a starting point for finding better and smaller symmetries.

In Chapter 2 we present a model based on a discrete subgroup of U(2), the double tetrahedral group T'. It is shown that the model can reproduce the observed patterns of quark and lepton masses, as well as the patterns observed in the CKM matrix. Furthermore, by introducing a right-handed neutrino, it is possible to obtain the correct mixing patterns and mass ratios required in order to solve the atmospheric and solar neutrino problems. The topic of discrete gauge symmetries is explored, and a numerical renormalization group analysis of the model is performed. In addition, a few other models based on the symmetry T' are presented and discussed.

In Chapter 3 we address the problem of EW symmetry breaking. The use of supersymmetry in the construction of the MSSM provides a mechanism for the breaking of EW symmetry. The Higgs mass, M_H, receives radiative corrections from the quark superpartners, and these corrections contribute to the running of M_H^2, making it negative at some scale that is identified with the EW scale. This is called radiative breaking of EW symmetry. While this mechanism is fairly generic for weak scale superparticles and a heavy top, there are other possibilities worth exploring. In particular we may consider the possibility that EW symmetry is broken not by a fundamental scalar, but by a fermion—anti-fermion bound state generated by some strong dynamics in a high energy theory. This scalar bound state breaks EW symmetry in the low-energy theory if it acquires a vev. Topcolor models achieve this result via a $t-\bar{t}$ bound state. The top quark mass is generated dynamically but lighter quark masses must be put in by hand via higher dimensional operators. However, such operators can also lead to flavor-changing neutral currents (FCNC) and make these models problematic.

We present a bosonic topcolor model that contains a composite scalar and also a weakly-coupled fundamental scalar. The composite field is generated by some strong dynamics above Λ_s assumed to affect only t_R and $\bar{\Psi}_L = (\bar{t}, \bar{b})_L$ generating a $\bar{t}_L t_R$ bound state, as in conventional topcolor models. The strong dynamics responsible for the generation of the composite field is assumed to come from an extra-dimensional framework, and thus Λ_s can be taken to be $\lesssim 100$ TeV. The role of the composite scalar is to break EW symmetry, while the fundamental scalar communicates the breaking to all other fields in the theory. The top quark is heavy because its dynamically-generated Yukawa coupling is naturally large. The light quarks acquire their masses from the vev of the fundamental scalar so that no higher-dimension operators need to be introduced. In this particular scenario the masses of both scalar fields obtain corrections proportional to Λ_s and since this scale is not very large, the hierarchy can be controlled. Effectively, we end up with a two Higgs doublet model at low energies and we study its phenomenology in order to impose bounds on the parameter space. This discussion will conclude the study of the first two issues mentioned at the beginning of this Chapter.

In Chapter 4 we discuss a possible mechanism for avoiding proton decay. When one takes the SM as an effective theory up to M_P, we expect non-renormalizable operators suppressed by powers of M_P that violate baryon and lepton number and lead to proton decay at an unacceptable rate. The strongest contributions come from operators with dimension 6 (or 5 if the model is supersymmetric) and thus are suppressed by two powers (or one power) M_P. It is desirable to find a mechanism that would naturally suppress or completely remove such operators. We accomplish this by gauging baryon number. In so doing, a new gauge boson is introduced into the theory and we explore its phenomenology. In particular we show that there is a possibility that a new light leptophobic gauge boson exists and has evaded detection.

The general framework can be summarized as follows. Once baryon number has been gauged, new kinetic terms arise

$$\mathcal{L}_{kin}^{new} = -\frac{1}{4}F_B^{\mu\nu}F_{B\mu\nu} - \frac{1}{2}cF_B^{\mu\nu}F_{\mu\nu}\,, \tag{1.10}$$

where $F_B^{\mu\nu}$ represents the stress-energy tensor associated with the new $\mathrm{U}(1)_B$ and $F^{\mu\nu}$ the equivalent for $\mathrm{U}(1)_Y$. The second term in Eq. (1.10) is allowed by gauge invariance and must be included. If the parameter c is assumed to be zero at some high energy scale then it is only generated radiatively, so that it is small at low energies; one can therefore treat the mixing term as a perturbation. The new Z' couples to leptons only through the resulting $Z^0 - Z'$ and $\gamma - Z'$ mixing. These corrections are proportional to the parameter c and are small, hence the name leptophobic. In Chapter 4 we present the results for a Z' in the $1 - 10$ GeV mass range.

In Chapter 5 the idea of gauging baryon number is used to solve the problem of proton decay in theories with extra dimensions. In this case the problem is accentuated because of the fact that the scale of quantum gravity is low and the operators that violate baryon number are no longer as suppressed. By gauging baryon number we show that models exist which can solve this problem by eliminating the dangerous operators, even when the symmetry is spontaneously broken. Furthermore, since we work in an extra dimensional framework, the phenomenology of this model can have interesting signatures in future collider experiments at the Tevatron.

Chapter 2

Maximal Neutrino Mixing from a Minimal Flavor Symmetry

2.1 Introduction

It is possible that the observed hierarchy of fermion masses and mixing angles originates from the spontaneous breakdown of a new symmetry G_f that acts horizontally across the three standard model generations. Ideally, all Yukawa couplings except that of the top quark are forbidden by G_f invariance at high energies; the remaining ones are generated when a set of fields ϕ that transform nontrivially under G_f develop vacuum expectation values (vevs). A hierarchy in couplings is obtained if G_f is broken sequentially at energy scales μ_i through a series of nested subgroups H_i , such that

$$G_f \xrightarrow{\mu_1} H_1 \xrightarrow{\mu_2} H_2 \xrightarrow{\mu_3} \cdots \quad \text{for } \mu_1 > \mu_2 > \mu_3 \cdots \quad . \tag{2.1}$$

At each stage of the symmetry breaking there is an associated small dimensionless parameter $\langle\phi_i\rangle/M_f$, where ϕ_i is a 'flavon' field whose vev is responsible for the breaking $H_{i-1} \to H_i$, and where M_f is the ultraviolet cutoff of the G_f-invariant effective theory. The ratios ϕ_i/M_f appear in higher-dimension operators that contribute to Yukawa couplings in the low-energy theory. For example, the superpotential term

$$\frac{1}{M_f} Q_3 H_D \phi_b D_3 \tag{2.2}$$

leads to a bottom quark Yukawa coupling of order $\langle\phi_b\rangle/M_f$. The most general set of operators involving the fields of the minimal supersymmetric standard model (MSSM) and the ϕ fields must provide for Yukawa textures that are phenomenologically viable. If flavor universality of scalar superpartner masses is not simply a consequence of the mechanism by which supersymmetry breaking is mediated [26, 27, 28, 29], then a successful model must also explain why these scalars do not contribute to flavor-changing neutral current processes at unacceptable levels.

Models with horizontal symmetries have been proposed with G_f either gauged or global, continuous or discrete, Abelian or non-Abelian, or some appropriate combination thereof [30, 31]. Abelian flavor symmetries have been used successfully to explain the absence of supersymmetric flavor-changing processes by aligning the fermion and sfermion mass matrices [30]. However, the freedom to choose a number of new U(1) charges for each MSSM matter field represents so much freedom that these models seem *ad hoc*, at least from a low-energy point of view. Non-Abelian symmetries are more restrictive, as the Yukawa matrices generally decompose into a smaller number of irreducible G_f representations. Thus, it is not unreasonable to expect that minimal models exist that are both successful and aesthetically compelling. This is the primary motivation for the current work.

In non-Abelian flavor models, the existence of three generations of matter fields, the heaviness of the top quark, and the absence of supersymmetric flavor-changing processes together suggest a $\mathbf{2}\oplus\mathbf{1}$ representation structure for the MSSM matter fields. With this choice it is not only possible to distinguish the third generation, but also to achieve an exact degeneracy between superparticles of the first two generations when G_f is unbroken. In the low-energy theory, this degeneracy is lifted by the same small symmetry-breaking parameters that determine the light fermion Yukawa couplings, so that FCNC effects remain adequately suppressed, even with superparticle masses less than a TeV.

A particularly elegant model of this type considered in the literature assumes the continuous, global symmetry G_f =U(2) [13, 14, 15]. Quarks and leptons are assigned to **2⊕1** representations, so that in tensor notation one may represent the three generations of any matter field by $F^a + F^3$, where a is a U(2) index, and F is Q, U, D, L, or E. A set of flavons is introduced consisting of ϕ_a, S_{ab}, and A_{ab}, where ϕ is a U(2) doublet, and $S(A)$ is a symmetric (antisymmetric) U(2) triplet (singlet). The doublet and triplet flavons acquire the vevs

$$\frac{\langle\phi\rangle}{M_f} = \begin{pmatrix} 0 \\ \epsilon \end{pmatrix}, \quad \text{and} \quad \frac{\langle S\rangle}{M_f} = \begin{pmatrix} 0 & 0 \\ 0 & \epsilon \end{pmatrix}, \tag{2.3}$$

the most general set of nonvanishing entries consistent with an unbroken U(1) symmetry that rotates all first generation-fields by a phase. This residual U(1) symmetry is broken at a somewhat lower scale by the flavon A

$$\frac{\langle A\rangle}{M_f} = \begin{pmatrix} 0 & \epsilon' \\ -\epsilon' & 0 \end{pmatrix}, \tag{2.4}$$

where $\epsilon' < \epsilon$. Thus, the sequential breaking

$$U(2) \xrightarrow{\epsilon} U(1) \xrightarrow{\epsilon'} nothing, \tag{2.5}$$

yields a Yukawa texture for the down quarks, for example, of the form

$$Y_D \approx \begin{pmatrix} 0 & d_1\epsilon' & 0 \\ -d_1\epsilon' & d_2\epsilon & d_3\epsilon \\ 0 & d_4\epsilon & d_5 \end{pmatrix} \xi \ , \tag{2.6}$$

where $d_1, \ldots, d_5$ are $O(1)$ coefficients. With the choice $\epsilon \approx 0.02$ and $\epsilon' \approx 0.004$, this texture achieves the correct hierarchy in down quark mass eigenvalues and gives contributions of the appropriate size to entries of the Cabibbo-Kobayashi-Maskawa

(CKM) matrix. The $O(1)$ coefficients may be determined from a global fit, as in Ref. [15]. The ratio m_b/m_t is assumed to be unrelated to U(2) symmetry breaking, and is simply put into the low-energy theory by hand. This is accomplished by choosing the free parameter ξ in Eq. (2.6).

While the form of Y_D is viable, U(2) symmetry by itself cannot explain the differences between the hierarchies within Y_D and Y_U. Quark mass ratios renormalized at the grand unified scale are given approximately by [32]

$$m_d :: m_s :: m_b = \lambda^4 :: \lambda^2 :: 1, \tag{2.7}$$

while

$$m_u :: m_c :: m_t = \lambda^8 :: \lambda^4 :: 1, \tag{2.8}$$

where $\lambda \approx 0.22$ is the Cabibbo angle. Clearly, an additional suppression factor ρ is required in Y_U for those elements that contribute most significantly to the up and charm quark mass eigenvalues,

$$Y_U \approx \begin{pmatrix} 0 & u_1\epsilon'\rho & 0 \\ -u_1\epsilon'\rho & u_2\epsilon\rho & u_3\epsilon \\ 0 & u_4\epsilon & u_5 \end{pmatrix} , \tag{2.9}$$

where $u_1 \ldots u_5$ are $O(1)$ coefficients. By embedding the U(2) model in a grand unified theory it is possible to obtain $\rho \approx \epsilon$ naturally; the model can then accommodate all the desired fermion mass hierarchies for choices of the coefficients u_i and d_i that are all of order one [15]. For example, in an SU(5) GUT, Y_U is associated with the coupling **10-10-5**, where the **10**'s represent matter fields, and the **5** is the Higgs field H. However,

$$\mathbf{10} \otimes \mathbf{10} = \overline{\mathbf{5}}_s \oplus \overline{\mathbf{45}}_a \oplus \overline{\mathbf{50}}_s \ , \tag{2.10}$$

where the subscripts indicate symmetry or antisymmetry under interchange of the two $\overline{\mathbf{10}}$'s. If we assume that the antisymmetric flavon A is an SU(5) singlet, the product AH is a $\mathbf{5}_a$, and does not contribute to Y_U. Similarly, if the flavon S is a **75** with a vev in the hypercharge direction in SU(5) space, then the part of SH that contains the Higgs doublet field transforms as a $\mathbf{45}_s$, which again does not contribute to Y_U. To obtain nonvanishing couplings of the right size in the upper two-by-two block of Y_U one introduces a singlet flavon Σ that transforms as an SU(5) adjoint. The vev of S implies that the breakings of both U(2) to U(1) and SU(5) to the standard model gauge group are associated with vevs of order ϵ. Thus, it is natural to assume $\langle\Sigma\rangle \approx \epsilon$, which provides exactly the desired value of ρ in Eq. (2.9). Moreover, the SU(5) assignments for A and S provide for a Georgi-Jarlskog mechanism [25], so that unified U(2) models successfully account for the charged lepton mass spectrum as well.

While the textures that follow from the simple two-step breaking of a U(2) flavor symmetry are indeed minimal, the original symmetry group is not. It is natural to ask whether there are small discrete groups that work equally well as horizontal symmetries. In this Chapter we show that the charged fermion Yukawa textures usually associated with U(2) models may be reproduced assuming the symmetry $G_f = T' \times Z_3$, and the breaking pattern

$$T' \otimes Z_3 \xrightarrow{\epsilon} Z_3^D \xrightarrow{\epsilon'} nothing. \qquad (2.11)$$

Here, T' is the double tetrahedral group, a discrete subgroup of SU(2) corresponding to the symmetry of a regular tetrahedron. The factor Z_3^D is the diagonal subgroup of a $Z_3 \subset T'$ and the additional Z_3 factor (see Section 2.4). Since U(2) is isomorphic to SU(2)×U(1), it is not surprising that our discrete symmetry is a product of a discrete subgroup of SU(2) and a discrete subgroup of U(1). Moreover, this symmetry is *minimal* in the sense that

- T' is the smallest discrete subgroup of SU(2) (and in fact the smallest group of any kind) with 1-, 2- and 3-dimensional representations and the multiplication rule $\mathbf{2}\otimes\mathbf{2}=\mathbf{3}\oplus\mathbf{1}$. These two ingredients are necessary to reproduce the successful U(2) textures.

- Z_3 is the smallest discrete subgroup of U(1) that allows G_f to contain a subgroup forbidding all order $O(\epsilon')$ entries in the Yukawa textures.

The latter statement applies to models in which T' is a discrete gauge symmetry (see Section 2.2); models with a global T' symmetry do not require any additional Abelian factors, as we demonstrate in Section 2.7. The use of discrete gauge rather than global symmetries is motivated by various arguments that the latter are violated at order one by quantum gravitational effects [34]. In two of the models we present, T' is an anomaly-free discrete gauge symmetry, while the additional Z_n factor is not. As in many of the Abelian models described in the literature [30], we simply assume that the Z_n factor may be embedded in a U(1) gauge symmetry whose anomalies are cancelled by the Green-Schwarz mechanism [16]. Thus, our models may be viewed as consistent low-energy effective theories for flavor symmetries that are local in a complete, high-energy theory.

On a more practical level, the different representation structure of T' allows for elegant solutions to the solar and atmospheric neutrino problems that do not alter the predictive quark and charged lepton Yukawa textures, nor require the introduction of sterile neutrinos. While similar results can be obtained in some SO(10)×U(2) models [35], we obtain our successful solutions using a much smaller symmetry structure.[1]

In addition, we propose two new models involving T' symmetry. The first model, based on the discrete gauge symmetry $T' \times Z_6$, reproduces all important features of the SU(5)×U(2) model *without requiring a field-theoretic grand unified theory.* In other words, the suppression of m_u and m_c in the SU(5)×U(2) theory described earlier is achieved in $T' \times Z_6$ without SU(5). In addition, the ratio m_b/m_t, which is not explained in SU(5)×U(2), is predicted in our model to be of $O(\epsilon) \approx 0.02$ for $\tan\beta \sim O(1)$, where $\tan\beta$ is the ratio of Higgs field vevs $\langle H_U\rangle/\langle H_D\rangle$. In a second model, we consider the implications of T' as a purely global flavor symmetry. Although in this case the symmetry may not be fundamental, it could still arise as an accidental symmetry at low energies. We show that it is possible to construct a viable model based on T' alone, with no additional Abelian factors. While it is well known that supersymmetric models with a continuous SU(2) flavor symmetry and a $\mathbf{2} \oplus \mathbf{1}$ representation structure do not have viable Yukawa textures, our global T' model demonstrates that discrete subgroups of SU(2) remain viable alternatives.

This Chapter is organized as follows. In the next section, we discuss the meaning of discrete gauge symmetries and the relevant anomaly-cancellation constraints in the low-energy effective theory. In Sections 2.3 and 2.4, we review the group theory of T' and present a minimal model [33]. In Section 2.5 we fit predictions of the model to charged fermion and neutrino masses and mixing angles, including the most significant renormalization group effects. In Section 2.6, we present the $T' \times Z_6$ model that reproduces the important features of the SU(5)×U(2) model with neither SU(5) nor U(2). In Section 2.7, we show how to construct a viable global T' model with no Abelian factors. In Section 2.8 we comment on one scenario involving sterile

[1] For a similar approach, see Ref. [36].

neutrinos, and in the final section we summarize our conclusions.

2.2 What Is a Discrete Gauge Symmetry?

Let us define a discrete gauge symmetry provisionally as a discrete remnant of a spontaneously broken continuous gauge symmetry. Below the breaking scale Λ of the continuous symmetry, the low-energy effective Lagrangian has interactions that are invariant under the unbroken discrete group, no massless gauge fields, and derivatives that transform trivially. It would seem then that this effective theory is identical to one with a purely global discrete symmetry. In this section, we review the arguments suggesting that this is not the case. We first illustrate how gauge invariance of a theory spontaneously broken to a discrete subgroup dictates the form of all terms in the low-energy effective theory, and thus renders its discrete invariance immune to wormhole dynamics. We then show that a theory with a discrete gauge symmetry predicts topological defects not present in a theory with a global symmetry, and that these play an important role in demonstrating that discrete gauge charges leave quantum-mechanical hair on black holes. Both observations suggest that discrete gauge symmetries are viable as candidates for fundamental symmetries of nature. After reviewing these arguments we summarize the anomaly-cancellation constraints relevant to low-energy theories with discrete gauge symmetries. We use these constraints in constructing models throughout this Chapter.

Following a discussion by Banks [37], let us consider the low-energy effective theory that results from spontaneously breaking a U(1) gauge symmetry to a discrete subgroup. The full theory consists of two scalar fields χ and ϕ with U(1) charges q and 1, respectively, where q is an integer. The Lagrangian is the usual one for an

Abelian Higgs model:

$$\mathcal{L} = -\frac{1}{4g^2} F_{\mu\nu} F^{\mu\nu} + |\partial_\mu \chi - iqA_\mu \chi|^2 + |\partial_\mu \phi - iA_\mu \phi|^2 + V(\chi^\dagger \chi). \tag{2.12}$$

The potential V is such that the χ field acquires a vacuum expectation value Λ. Let us rewrite the Lagrangian using the nonlinear field redefinition $\chi = (\Lambda + \sigma)e^{i\theta}/\sqrt{2}$. This yields

$$\mathcal{L} = -\frac{1}{4g^2} F_{\mu\nu} F^{\mu\nu} + \frac{1}{2}\partial_\mu \sigma \partial^\mu \sigma + \frac{1}{2}(\Lambda + \sigma)^2 (\partial_\mu \theta - qA_\mu)^2 + |\partial_\mu \phi - iA_\mu \phi|^2 + V(\sigma) \ , \tag{2.13}$$

where σ is the Higgs field and θ is the would-be longitudinal component of the U(1) gauge boson in unitary gauge. We choose to construct a low-energy effective theory in which the σ field, which has a mass of order Λ, is integrated out. However, we retain the gauge field A_μ as well as the unphysical scalar field θ. Although the gauge symmetry is spontaneously broken, the Lagrangian of the theory remains invariant under the local U(1) transformation:

$$\phi \to e^{i\alpha(x)}\phi, \quad A^\mu \to A^\mu + \partial_\mu \alpha(x), \quad \theta \to \theta + q\,\alpha(x). \tag{2.14}$$

The low-energy effective Lagrangian then consists of the kinetic terms

$$\mathcal{L} = -\frac{1}{4g^2} F_{\mu\nu} F^{\mu\nu} + |\partial_\mu \phi - iA_\mu \phi|^2 + \frac{1}{2}\Lambda^2 (\partial_\mu \theta - qA_\mu)^2 \ , \tag{2.15}$$

as well as the most general set of gauge-invariant operators involving the fields ϕ, $e^{i\theta}$, and covariant derivatives, with powers of Λ included to obtain the correct mass dimensions. We can classify the interactions in the effective Lagrangian that involve ϕ into two types: terms that are invariant under global U(1) transformations on ϕ alone (with the other fields held fixed), and those that are not. A typical term of the first type is $\phi^\dagger \phi$; terms of the second type necessarily involve the U(1) gauge-invariant product

$$e^{-i\theta}\phi^q \ , \tag{2.16}$$

or similar products with derivatives. Such terms are invariant under a Z_q phase rotation of the field ϕ alone. Thus, gauge invariance of the low-energy theory implies it must have an unbroken Z_q symmetry. Since this is a consequence of a local symmetry, it cannot be violated by wormhole dynamics.

We now show that information on discrete gauge charges is not lost when a charged particle falls into a black hole. To do so, first note that the Abelian Higgs model has stable cosmic string solutions. In the case where $\phi = 0$, the kinetic energy terms in Eq. (2.15) are minimized when

$$A_\mu = \frac{1}{q}\partial_\mu\theta \ . \tag{2.17}$$

For nonsingular gauge field configurations, this is related to $A_\mu = 0$ by a gauge transformation. However, singular solutions also exist; a cosmic string along the x^3 axis corresponds to

$$A_i = \frac{1}{q}\epsilon_{ij}\frac{x^j}{x_1^2 + x_2^2} \ , \quad i, j = 1, 2 \ , \qquad \theta = \arctan(x_2/x_1) \ . \tag{2.18}$$

If one couples the gauge field to a classical current j^μ, then the change in the action by adding one such cosmic string is

$$\delta S = (1/q)\int \partial_\mu\theta j^\mu \ , \tag{2.19}$$

which follows from Eq. (2.17). Taking j^μ to be the current of a particle with unit U(1) charge (and hence nontrivial Z_q charge) that circles the string, one finds that

$$\delta S = \frac{2\pi}{q} \ . \tag{2.20}$$

This implies an observable Aharanov-Bohm effect in the scattering of particles with discrete gauge charge off cosmic strings. Krauss and Wilczek [38] use this observation to argue that the scattering of a cosmic string off a particle with discrete gauge charge that is falling into a black hole is insensitive to the point at which the particle crosses the event horizon. Thus, the discrete charge of the particle is not lost, and the black hole grows quantum-mechanical hair.

It is interesting to note that the discussion above may be rephrased in unitary gauge by making the initial replacements

$$B_\mu = A_\mu - (1/q)\partial_\mu\theta, \quad \text{and} \quad \Phi = e^{-i\theta/q}\phi\ , \tag{2.21}$$

in Eq. (2.13), which then becomes

$$\mathcal{L} = -\frac{1}{4g^2}F_{\mu\nu}F^{\mu\nu} + \frac{1}{2}\partial_\mu\sigma\partial^\mu\sigma + \frac{1}{2}(\Lambda+\sigma)^2 q^2 B^\mu B_\mu + |\partial_\mu\Phi - iB_\mu\Phi|^2 + V(\sigma)\ . \tag{2.22}$$

Unlike the previous approach, all the fields above are gauge-invariant; one may integrate out B_μ and σ, and obtain all the possible Z_q-invariant interactions involving the light field Φ. This formulation of the low-energy theory is peculiar in that the periodicity of θ implies that

$$e^{2n\pi i/q}\Phi \equiv \Phi, \text{ for all integers } n. \tag{2.23}$$

Thus, the field manifold of ϕ is not the complex plane C, but rather the orbifold C/Z_q: Field configurations connected by Z_q transformations are identified, and hence are physically redundant, the hallmark of a gauge symmetry. Given this manifold, the field Φ has a conical singularity at the origin in field space; strings in unitary gauge correspond to Φ field configurations that wrap around this singularity as the azimuthal angle varies from 0 to 2π.

As the previous U(1) $\to Z_q$ example demonstrates, a discrete gauge symmetry can arise in a renormalizable field theory when a continuous gauge symmetry is spontaneously broken by a Higgs field vev that leaves a discrete symmetry unbroken. The same can occur for non-Abelian symmetries as well. For example, one may break a gauged SU(2) symmetry with a Higgs field transforming as a **7** (which contains a T' singlet), leaving the theory invariant under T'. On the other hand, the U(1) $\to Z_q$ example suggests how a discrete symmetry may be defined without an explicit embedding in a continuous group. In string theory, the discrete symmetry may be a remnant of general coordinate invariance, ordinary gauge invariance, or the larger gauge symmetry of string theory [37]. For our purposes, however, the nature of the high energy theory is irrelevant.

It is worth mentioning in passing that spontaneously-broken discrete gauge symmetries have domain walls that are not topologically stable. Holes bounded by strings may spontaneously nucleate, allowing the walls to tear themselves to pieces while dissipating energy through gravitational radiation [39]. The effectiveness of this mechanism at avoiding cosmological problems is not relevant to our discussion since the flavor-symmetry-breaking scale in our models is high enough (of order the unification scale) that all topological defects are eliminated by inflation.

Finally, it is relevant to consider whether there are any constraints on the low-energy particle content of theories with discrete gauge symmetries. Since continuous gauge symmetries must satisfy anomaly-cancellation conditions, the particle content of low-energy theories with discrete gauge symmetries is restricted. Ibáñez and Ross [23] were the first to consider the constraints on a discrete gauged Z_q symmetry, and their results were refined by Banks and Dine [24]: Let G_0 be a simple factor of the continuous group in which a discrete gauge symmetry is embedded, and let

G_A and G_N represent the unbroken Abelian and non-Abelian gauge symmetries of the low-energy effective theory. Cancellation of the $G_0 G_N^2$ anomaly is the only new requirement for consistency of the low-energy theory; all other anomaly-cancellation constraints involving G_0 can be satisfied by the introduction of heavy states. Banks and Dine point out that this requirement, termed the linear Ibáñez-Ross condition, is equivalent to demanding discrete gauge invariance of nonperturbative interactions generated by instantons of the unbroken continuous gauge groups. This observation demonstrates that consistency of a discrete gauge symmetry at low energies can be established without reference to any particular embedding.

2.3 The Group T'

All of the symmetries described in this Chapter contain T', the double tetrahedral group.[2] Geometrically, T' is defined as the group of all 24 proper rotations in three dimensions leaving a regular tetrahedron invariant in the SU(2) double covering of SO(3). This perhaps opaque definition may be understood in the following way. There exists a group of 12 elements called the tetrahedral group T, consisting of all proper rotations in three dimensions leaving a regular tetrahedron invariant (Fig. 2.1). It is constructed by parameterizing the group SO(3) of *all* proper rotations in three dimensions in terms of familiar Euler angles, and then restricting to those discrete values of angles describing rotations taking a regular tetrahedron into coincidence with itself. The same Euler angles describe rotations in SU(2) space, since SU(2) and SO(3) are locally isomorphic, so that T' is the subgroup of SU(2) corresponding to the same Euler angles as $T \subset \mathrm{SO}(3)$. One therefore expects that even-dimensional representations of T' are spinorial, i.e., are multiplied by -1 under a 2π rotation

[2] For a review of basic terms of discrete group theory, see Ref. [21]

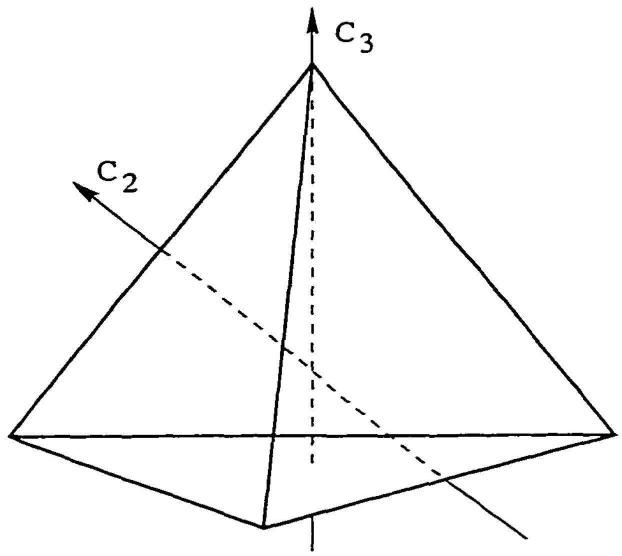

Figure 2.1 Geometrical illustration of the group T' or T. The rotations C_2 and C_3 generate all other rotations in each group.

(called R in the literature), while odd-dimensional representations of T' coincide with those of T and are invariant under this rotation, as may be verified by the character table, Table 2.1. T' is generated by the rotations C_2 and C_3 depicted in Fig. 2.1. Because of the double-valued nature of T' rotations, these elements actually have orders 4 and 6, respectively. For reasons to be described below, it turns out to be convenient to present explicit representations (*reps*) for an element of order 4 (such as C_2) and one of order 3 (such as C_3R). We label these elements as g_5 and g_9, respectively;[3] then T' is defined by the multiplication rules $g_9^3 = g_5^4 = 1$, $g_9 g_5^2 = g_5^2 g_9$, and $g_5 g_9^{-1} g_5 = g_9 g_5 g_9$. One may then show that each of the 24 elements may be written uniquely in the canonical form $g_9^p g_5^q g_9^r$, where $p = 0, \pm 1$, and if $q = 0$ or 2 then $r = 0$, while if $q = \pm 1$ then $r = 0, \pm 1$.

The group T' is central to our model building since it is the smallest with 1-,

[3]The element labels are chosen to coincide with those of Thomas and Wood, Ref. [22], where T' is seen to be isomorphic to $SL_2(F_3)$, the group of two-by-two unimodular matrices whose elements are added and multiplied as integers modulo 3.

Sample element	E	R	C_2, C_2R	C_3	C_3^2	C_3R	C_3^2R
Order of class	1	1	6	4	4	4	4
Order of element	1	2	4	6	3	3	6
$\mathbf{1}^0$	1	1	1	1	1	1	1
$\mathbf{1}^+$	1	1	1	η	η^2	η	η^2
$\mathbf{1}^-$	1	1	1	η^2	η	η^2	η
$\mathbf{2}^0$	2	-2	0	1	-1	-1	1
$\mathbf{2}^+$	2	-2	0	η	$-\eta^2$	$-\eta$	η^2
$\mathbf{2}^-$	2	-2	0	η^2	$-\eta$	$-\eta^2$	η
$\mathbf{3}$	3	3	-1	0	0	0	0

Table 2.1 Character table of the double tetrahedral group T'. The phase η is $\exp(2\pi i/3)$.

2-, and 3-dimensional reps and the multiplication rule $\mathbf{2} \otimes \mathbf{2} = \mathbf{3} \oplus \mathbf{1}$. T' models therefore allow for flavons that perform the same roles as ϕ_a, S_{ab} and A_{ab} in the U(2) model. The only other 24-element group that has reps of the same dimensions is the octahedral group O (which is isomorphic to S_4). In this case, however, the product of two doublet reps does not contain a triplet, and the analogy to U(2) is lost.

More specifically, T' has three singlets $\mathbf{1}^0$ and $\mathbf{1}^{\pm}$, three doublets, $\mathbf{2}^0$ and $\mathbf{2}^{\pm}$, and one triplet, $\mathbf{3}$. The *triality* superscript provides a concise way of stating the multiplication rules for these reps: With the identification of $\pm$ as ± 1, trialities add under addition modulo three, and the following rules hold:

$$\begin{aligned} &\mathbf{1} \otimes \mathbf{R} = \mathbf{R} \otimes \mathbf{1} = \mathbf{R} \quad \text{for any rep } \mathbf{R}, && \mathbf{2} \otimes \mathbf{2} = \mathbf{3} \oplus \mathbf{1}, \\ &\mathbf{2} \otimes \mathbf{3} = \mathbf{3} \otimes \mathbf{2} = \mathbf{2}^0 \oplus \mathbf{2}^+ \oplus \mathbf{2}^-, && \mathbf{3} \otimes \mathbf{3} = \mathbf{3} \oplus \mathbf{3} \oplus \mathbf{1}^0 \oplus \mathbf{1}^+ \oplus \mathbf{1}^- \end{aligned} \tag{2.24}$$

Note that trialities flip sign under Hermitian conjugation, so that $\mathbf{2}^+ \otimes \mathbf{2}^- = \mathbf{3} \oplus \mathbf{1}^0$ while $(\mathbf{2}^+)^\dagger \otimes \mathbf{2}^- = \mathbf{3} \oplus \mathbf{1}^+$.

The multiplication of T' representations may be made explicit by the use of Clebsch-Gordan matrices. For example, let the fields χ and ψ be column vectors that transform as $\mathbf{2}^+$ and $\mathbf{2}^-$ under T', respectively. From the rules above, we know that the product of these reps contains a trivial singlet, the $\mathbf{1}^0$, but it is not immediately clear how to construct this representation out of the given fields. Formally, we seek a matrix M such that the product

$$\chi^T M \psi \to \chi^T M \psi \tag{2.25}$$

under the transformations $\chi \to R(g)\chi$ and $\psi \to R(g)\chi$, where R is a two-dimensional matrix rep, and g runs over all elements of the group. From our earlier discussion, it is only necessary that we consider transformations associated with the defining elements, g_5 and g_9, to solve for the form of M; in the present case, one finds that M is proportional to the Pauli matrix σ_2. This algebraic procedure is easily generalized to products of other reps. Explicit matrix representations for the generating elements g_5 and g_9, as well as the complete set of Clebsch-Gordan matrices for combining T' reps are provided in Chapter 2.9. The reader should keep in mind that these Clebsch-Gordan matrices must be taken into account if one is to reproduce the Yukawa textures presented later in this Chapter. For example, without the factor of σ_2, one might not realize that a vev in the first component of χ couples only to the second component of ψ.

As mentioned in Section 2.1, we also require that our discrete flavor symmetry contain a subgroup that rotates first-generation matter fields by a phase. This subgroup plays the same role as the intermediate U(1) symmetry in the U(2) model, and must forbid all entries in the first row and column of each Yukawa matrix. The smallest discrete subgroup that one might consider is a Z_2 that flips the sign of all first generation matter fields. Unfortunately, such a transformation leaves the 11 entry of each Yukawa matrix invariant (two sign flips), so that the up and down quarks could, in principle, acquire masses that are too large. A Z_3 phase rotation, on the other hand, does not lead to the same problem, and a Z_3 subgroup of T' is generated by the element g_9 defined previously. From Section 2.9, we see that the two-dimensional representation matrices for the element g_9 are given by

$$g_9(\mathbf{2}^0) = \begin{pmatrix} \eta^2 & 0 \\ 0 & \eta \end{pmatrix}, \quad g_9(\mathbf{2}^+) = \begin{pmatrix} 1 & 0 \\ 0 & \eta^2 \end{pmatrix}, \quad g_9(\mathbf{2}^-) = \begin{pmatrix} \eta & 0 \\ 0 & 1 \end{pmatrix}, \tag{2.26}$$

where $\eta \equiv \exp(2\pi i/3)$. If matter fields of the first two generations are assigned to the $\mathbf{2}^-$ rep, one then obtains the desired phase rotation under the Z_3 subgroup. This observation is at the heart of the global T' model presented in Section 2.7.[4]

As we see below, however, models in which T' is free of discrete gauge anomalies are much easier to construct if matter fields are assigned to the $\mathbf{2}^0$ rep instead. In this case, let us consider extending the flavor symmetry group to $T' \times Z_3$. We identify a new triality index 0, + and − with the Z_3 phase rotations 1, η, and η^2, respectively. Like the T' indices, the Z_3 trialities also combine via addition modulo 3. Reps of $T' \times Z_3$ are denoted by affixing this additional triality as a superscript, e.g., $\mathbf{2}^{+-}$. We now identify the desired intermediate symmetry as the diagonal subgroup of the original Z_3, generated by the element g_9, and the new Z_3 factor. We call this subgroup Z_3^D henceforth. It is easy to see that the rep $\mathbf{2}^{0-}$ transforms under Z_3^D by the matrix

$$\begin{pmatrix} \eta & 0 \\ 0 & 1 \end{pmatrix} \tag{2.27}$$

which is simply the product of $g_9(\mathbf{2}^0)$ and η^2. The matter field assignments $\mathbf{2}^{0-} \oplus \mathbf{1}^{00}$, and the breaking pattern $T' \times Z_3 \to Z_3^D \to$ *nothing* are at the heart of the minimal flavor model discussed in the next section. It is worth pointing out that the reps $\mathbf{1}^{00}$, $\mathbf{1}^{+-}$, $\mathbf{1}^{-+}$, $\mathbf{2}^{0-}$, $\mathbf{2}^{++}$ and $\mathbf{2}^{-0}$ are special in that these singlet reps and the second

[4]One can also imagine models in which the symmetry group breaks to a non-Abelian subgroup; however, in this case the simple rephasing of multiplet components under the subgroup is not guaranteed.

component of the doublets remain invariant under Z_3^D. Thus any $\mathbf{2}\oplus\mathbf{1}$ combination of these reps is potentially useful in building models with U(2)-like textures.

Finally, we return to the issue of anomaly cancellation. We pointed out in Section 2.2 that consistency of a discrete gauge symmetry at low energies only requires the cancellation of anomalies that (1) involve the unbroken non-Abelian continuous gauge groups, and (2) are linear in a continuous group in which the discrete group is embedded. If we embed T' in SU(2), then these constraints are satisfied *automatically*, providing that the particle content of a given model fills complete SU(2) representations. Let us therefore consider the embedding of T' in SU(2) in more detail.

The group SU(2) has one rep of each nonnegative integral dimension n (the spin $(n-1)/2$ rep), while T' has only singlet, doublet, and triplet reps. It must be the case that large SU(2) reps break up into a number of T' reps with the same total dimension. To see this decomposition, consider the characteristic polynomial of matrices in each of the T' reps for any two rotations that generate the full group. The same can be done for the full SU(2) group restricted to the particular Euler angles that give T'. Then a large rep matrix of SU(2) is block-diagonalizable into smaller blocks corresponding to rep matrices of T'; in particular, the characteristic polynomial of the SU(2) matrix is the product of those of the T' matrices. It is then possible to extract which T' reps appear in a given SU(2) rep, as well as their multiplicities. The results of this decomposition are summarized in Table 2.2. There we see that the $\mathbf{1}^0$, $\mathbf{2}^0$, and $\mathbf{3}$ reps of T' correspond to the complete $\mathbf{1}$, $\mathbf{2}$, and $\mathbf{3}$ reps of SU(2). It follows, for example, that T' is non-anomalous in all models utilizing the $\mathbf{2}^{0-}\oplus\mathbf{1}^{00}$ representation structure for the matter fields (with Higgs fields as singlets). Note that there is no meaningful low-energy constraint on the Z_3 charges since Abelian

SU(2) rep multiplicity	T' rep decomposition
$12N$	$2N\,\{\mathbf{2}^0 \oplus \mathbf{2}^+ \oplus \mathbf{2}^-\}$
$12N+1$	$\mathbf{1}^0 \oplus N\,\{\mathbf{1}^0 \oplus \mathbf{1}^+ \oplus \mathbf{1}^- \oplus 3\cdot\mathbf{3}\}$
$12N+2$	$\mathbf{2}^0 \oplus 2N\,\{\mathbf{2}^0 \oplus \mathbf{2}^+ \oplus \mathbf{2}^-\}$
$12N+3$	$\mathbf{3} \oplus N\,\{\mathbf{1}^0 \oplus \mathbf{1}^+ \oplus \mathbf{1}^- \oplus 3\cdot\mathbf{3}\}$
$12N+4$	$\{\mathbf{2}^+ \oplus \mathbf{2}^-\} \oplus 2N\,\{\mathbf{2}^0 \oplus \mathbf{2}^+ \oplus \mathbf{2}^-\}$
$12N+5$	$\{\mathbf{1}^+ \oplus \mathbf{1}^- \oplus \mathbf{3}\} \oplus N\,\{\mathbf{1}^0 \oplus \mathbf{1}^+ \oplus \mathbf{1}^- \oplus 3\cdot\mathbf{3}\}$
$12N+6$	$(2N+1)\,\{\mathbf{2}^0 \oplus \mathbf{2}^+ \oplus \mathbf{2}^-\}$
$12N+7$	$\{\mathbf{1}^0 \oplus 2\cdot\mathbf{3}\} \oplus N\,\{\mathbf{1}^0 \oplus \mathbf{1}^+ \oplus \mathbf{1}^- \oplus 3\cdot\mathbf{3}\}$
$12N+8$	$\mathbf{2}^0 \oplus (2N+1)\,\{\mathbf{2}^0 \oplus \mathbf{2}^+ \oplus \mathbf{2}^-\}$
$12N+9$	$\{\mathbf{1}^0 \oplus \mathbf{1}^+ \oplus \mathbf{1}^- \oplus 2\cdot\mathbf{3}\} \oplus N\,\{\mathbf{1}^0 \oplus \mathbf{1}^+ \oplus \mathbf{1}^- \oplus 3\cdot\mathbf{3}\}$
$12N+10$	$\{\mathbf{2}^+ \oplus \mathbf{2}^-\} \oplus (2N+1)\,\{\mathbf{2}^0 \oplus \mathbf{2}^+ \oplus \mathbf{2}^-\}$
$12N+11$	$\{\mathbf{1}^+ \oplus \mathbf{1}^- \oplus 3\cdot\mathbf{3}\} \oplus N\,\{\mathbf{1}^0 \oplus \mathbf{1}^+ \oplus \mathbf{1}^- \oplus 3\cdot\mathbf{3}\}$

Table 2.2 Decomposition of SU(2) reps into reps of T'. N is any nonnegative integer.

factors may be embedded at high energies in U(1) gauge groups whose anomalies are cancelled by the Green-Schwarz mechanism [16].

2.4 A Minimal Model

In this section we present a minimal $T' \times Z_3$ model which we study in quantitative detail in Section 2.5. The three generations of matter fields are assigned to the $T' \times Z_3$ reps $\mathbf{2}^{0-} \oplus \mathbf{1}^{00}$ while the Higgs fields $H_{U,D}$ are taken to be pure G_f singlets. Given these assignments, it is easy to obtain the transformation properties of the Yukawa matrices,

$$Y_{U,D,L} \sim \left(\begin{array}{c|c} [\mathbf{3}^- \oplus \mathbf{1}^{0-}] & [\mathbf{2}^{0+}] \\ \hline [\mathbf{2}^{0+}] & [\mathbf{1}^{00}] \end{array}\right). \tag{2.28}$$

Equation (2.28) indicates the flavon reps needed to construct the fermion mass matrices, namely, $\mathbf{1}^{0-}$, $\mathbf{2}^{0+}$, and $\mathbf{3}^-$, which we call A, ϕ, and S, respectively. Once these flavons acquire vevs, the flavor group is broken. We are interested in a two-step breaking

$$T' \otimes Z_3 \xrightarrow{\epsilon} Z_3^D \xrightarrow{\epsilon'} nothing, \tag{2.29}$$

where $\epsilon' < \epsilon$ again represent ratios of flavon vevs to the scale M_f. Since we have chosen a 'special' doublet rep for the first two generations, which transforms as $diag\{\eta, 1\}$ under Z_3^D, only the 22, 23, and 32 entries of the Yukawa matrices may develop vevs of $O(\epsilon)$ originating from vevs in S and ϕ. The symmetry Z_3^D is then broken by a $\mathbf{1}^{0-}$ vev of $O(\epsilon')$. The Clebsch-Gordan coefficient that couples a $\mathbf{1}^{0-}$ to two $\mathbf{2}^{0-}$ doublets is proportional to σ_2, so the ϵ' appears in an antisymmetric matrix. These considerations yield the textures

$$Y_{U,D,L} \sim \begin{pmatrix} 0 & \epsilon' & 0 \\ -\epsilon' & \epsilon & \epsilon \\ 0 & \epsilon & 1 \end{pmatrix}, \tag{2.30}$$

where $O(1)$ coefficients have been omitted. Since the $\mathbf{1}^{0-}$ and $\mathbf{3}^{-}$ flavon vevs appear as antisymmetric and symmetric matrices, respectively, all features of the grand unified extension of the U(2) model are obtained here, assuming the same GUT transformation properties are assigned to ϕ, S, and A. One can also show readily that the squark and slepton mass-squared matrices are the same as in the U(2) model.

This simple model can be extended to describe the observed deficit of solar and atmospheric neutrinos. Models for lepton masses were constructed both with and without the assumption of SU(5) unification. The latter possibility is of interest, for example, if one is only concerned with explaining flavor physics of the lepton sector, and is provided for completeness. In either case, the proposed extensions yield viable neutrino textures with naturally large mixing between the second and third generations. Moreover, these extensions do not alter the charged fermion textures, so that all the relations between masses and mixing angles in the U(2) model are also predictions of $T' \times Z_3$. We now present two cases.

Case I: Here we do not assume grand unification, so that all flavons are SU(5) singlets. We introduce three generations of right-handed neutrinos transforming as

$$\nu_R \sim \mathbf{2}^{0-} \oplus \mathbf{1}^{-+}. \tag{2.31}$$

Note that this representation choice differs from that of the other matter fields only in the third generation. Since ν_R are singlets under the standard model gauge groups, introducing a $\mathbf{1}^-$ field by itself creates no anomaly problems. The neutrino Dirac and Majorana mass matrices then allow flavons that do not contribute to the charged fermion mass matrices. Their transformation properties are given by

$$M_{LR} \sim \left(\begin{array}{c|c} [\mathbf{3}^- \oplus \mathbf{1}^{0-}] & [\mathbf{2}^{+0}] \\ \hline [\mathbf{2}^{0+}] & [\mathbf{1}^{+-}] \end{array} \right) , \qquad M_{RR} \sim \left(\begin{array}{c|c} [\mathbf{3}^-] & [\mathbf{2}^{+0}] \\ \hline [\mathbf{2}^{+0}] & [\mathbf{1}^{-+}] \end{array} \right) . \tag{2.32}$$

Note that one obtains the same triplet and nontrivial singlet in the upper two-by-two block as in the charged fermion mass matrices, as well as one of the same flavon doublets, the $\mathbf{2}^{0+}$; the rep $\mathbf{1}^{0-}$ is not present in M_{RR}, since Majorana mass matrices are symmetric. In addition we obtain the reps $\mathbf{2}^{+0}$, $\mathbf{1}^{+-}$, and $\mathbf{1}^{-+}$, which did not appear in Eq. (2.28). New flavon fields can now be introduced with these transformation properties, and their effects on the neutrino physics explored. Let us introduce a single[5] new flavon ϕ_ν transforming as a $\mathbf{2}^{+0}$ and with a vev

$$\frac{\langle \phi_\nu \rangle}{M_f} \sim \sigma_2 \left(\begin{array}{c} \epsilon' \\ \epsilon \end{array} \right) , \tag{2.33}$$

where σ_2 is the Clebsch that couples the two doublets to $\mathbf{1}^{0-}$. This new flavon is the only extension we make to the model in order to describe the neutrino phenomenology.

[5]Assuming more than one ϕ_ν leads to the same qualitative results.

After introducing ϕ_ν, the neutrino Dirac and Majorana mass matrices read

$$M_{LR} \approx \begin{pmatrix} 0 & l_1\epsilon' & l_3 r_2 \epsilon' \\ -l_1\epsilon' & l_2\epsilon & l_3 r_1 \epsilon \\ 0 & l_4\epsilon & 0 \end{pmatrix} \langle H_U \rangle \ , \tag{2.34}$$

$$M_{RR} \approx \begin{pmatrix} r_4 r_2 \epsilon'^2 & r_4 r_1 \epsilon\epsilon' & r_2\epsilon' \\ r_4 r_1 \epsilon\epsilon' & r_3\epsilon & r_1\epsilon \\ r_2\epsilon' & r_1\epsilon & 0 \end{pmatrix} \Lambda_R \ , \tag{2.35}$$

where Λ_R is the right-handed neutrino mass scale, and we have parameterized the $O(1)$ coefficients. Furthermore, the charged lepton Yukawa matrix including $O(1)$ coefficients reads

$$Y_L \approx \begin{pmatrix} 0 & c_1\epsilon' & 0 \\ -c_1\epsilon' & 3c_2\epsilon & c_3\epsilon \\ 0 & c_4\epsilon & c_5 \end{pmatrix} \xi \ . \tag{2.36}$$

The factor of 3 in the 22 entry is simply assumed at present, but originates from the Georgi-Jarlskog mechanism in the grand unified case considered next.

The left-handed Majorana mass matrix M_{LL} follows from the seesaw mechanism

$$M_{LL} \approx M_{LR} M_{RR}^{-1} M_{LR}^T \ , \tag{2.37}$$

which yields

$$M_{LL} \sim \begin{pmatrix} (\epsilon'/\epsilon)^2 & \epsilon'/\epsilon & \epsilon'/\epsilon \\ \epsilon'/\epsilon & 1 & 1 \\ \epsilon'/\epsilon & 1 & 1 \end{pmatrix} \frac{\langle H_U \rangle^2 \epsilon}{\Lambda_R}, \tag{2.38}$$

where we have suppressed the $O(1)$ coefficients. It is clear by inspection that we naturally obtain large mixing between second- and third-generation neutrinos. It is also important to point out that the two eigenvalues of Eq. (2.38) that appear to be of $O(1)$ depend sensitively on the products of a large number of order one coefficients. It is easy to obtain a hierarchy of order 10 in the two largest mass eigenvalues, without allowing any of the coefficients defined in Eqs. (2.34)–(2.36) to deviate from unity by more than a factor of 2. This comment is important in understanding how the reasonable coefficients given above Eq. (2.43) account for the differing mass scales associated with atmospheric and solar neutrino oscillations.

In order to determine neutrino oscillation parameters precisely one needs to compute the neutrino CKM matrix. If M_{LL} and Y_L are diagonalized by $M_{LL} = W M_{LL}^0 W^\dagger$, $Y_L = U_L Y_L^0 U_R^\dagger$, then

$$V = U_L^\dagger W. \tag{2.39}$$

We parameterize this matrix as in Ref. [40],

$$V = \begin{pmatrix} c_{12}c_{13} & c_{13}s_{12} & s_{13} \\ -c_{23}s_{12}e^{i\phi} - c_{12}s_{13}s_{23} & c_{12}c_{23}e^{i\phi} - s_{12}s_{13}s_{23} & c_{13}s_{23} \\ s_{23}s_{12}e^{i\phi} - c_{12}c_{23}s_{13} & -c_{12}s_{23}e^{i\phi} - c_{23}s_{12}s_{13} & c_{13}c_{23} \end{pmatrix}, \tag{2.40}$$

where $c_{ij}(s_{ij})$ stands for $\cos\theta_{ij}(\sin\theta_{ij})$. Then one finds

$$\sin^2(2\theta_{12}) = 4\frac{V_{11}^2 V_{12}^2}{(V_{11}^2 + V_{12}^2)^2}, \tag{2.41}$$

$$\sin^2(2\theta_{23}) = 4\frac{V_{23}^2 V_{33}^2}{(V_{23}^2 + V_{33}^2)^2}. \tag{2.42}$$

The observed atmospheric neutrino fluxes may be explained by ν_μ-ν_τ mixing if $\sin^2 2\theta_{23} \gtrsim 0.8$ and $10^{-3} \lesssim \Delta m_{23}^2 \lesssim 10^{-2}$, while the solar neutrino deficit may be accommodated by $\nu_e - \nu_\mu$ mixing assuming the small-angle MSW solution $2 \times 10^{-3} \lesssim \sin^2 2\theta_{12} \lesssim 10^{-2}$ for $4 \times 10^{-6} \lesssim \Delta m_{12}^2 \lesssim 10^{-5}$, where all squared masses are given in eV^2 [2, 41]. These regions of parameter space are the ones obtained most naturally from our models.[6] Since Λ_R is not determined from symmetry considerations, it is only necessary to reproduce $\Delta m_{23}^2/\Delta m_{12}^2$. Assuming the previous values

[6]The experimental ranges for neutrino mixing parameters follow from a two-neutrino mixing approximation which is valid only if the mixing angle $\theta_{13} < 15°$ [40]. This condition is satisfied in all our models.

$\epsilon = 0.02$ and $\epsilon' = 0.004$ and the parameter set $(l_1, \ldots, l_4, r_1, \ldots, r_4, c_1, \ldots, c_4, c_5, \xi) =$ $(0.5, 1.0, -1.2, 2.3, 1.0, 1.0, 1.0, 1.0, 1.0, 1.0, 1.0, 1.0, 1.0, 1.0)$, we find:

$$\frac{\Delta m^2_{23}}{\Delta m^2_{12}} = 105, \qquad \sin^2 2\theta_{12} = 5 \times 10^{-3}, \qquad \sin^2 2\theta_{23} = 0.9, \tag{2.43}$$

which fall in the desired ranges. While all our coefficients are of natural size, we have arranged for an $O(15\%)$ cancellation between 12 mixing angles in U_L and V to reduce the size of $\sin^2 2\theta_{12}$ to the desired value.

Case II: Here we assume SU(5) unification and that the flavons transform non-trivially under the GUT group, namely, $A \sim \mathbf{1}$, $S \sim \mathbf{75}$, $\phi \sim \mathbf{1}$, and $\Sigma \sim \mathbf{24}$. Note that since $\overline{H} \sim \overline{\mathbf{5}}$, the products $S\overline{H}$ and $A\overline{H}$ transform as a $\overline{\mathbf{45}}$ and $\overline{\mathbf{5}}$, respectively, ultimately providing a factor of 3 enhancement in the 22 entry of Y_L (the Georgi-Jarlskog mechanism). In addition, two $\mathbf{2}^{+0}$ doublets are introduced, $\phi_{\nu 1}$ and $\phi_{\nu 2}$, since the texture obtained for the neutrino masses by adding only one extra doublet is not viable. Both doublets ϕ_ν have vevs of the form displayed in Eq. (2.33). As before, the presence of these two new doublets does not alter the form of any charged fermion Yukawa texture.

The neutrino Dirac and Majorana mass matrices now take the forms

$$M_{LR} \approx \begin{pmatrix} 0 & l_1\epsilon' & l_5 r_2\epsilon' \\ -l_1\epsilon' & l_2\epsilon^2 & l_3 r_1\epsilon \\ 0 & l_4\epsilon & 0 \end{pmatrix} \langle H_U \rangle \ , \tag{2.44}$$

$$M_{RR} \approx \begin{pmatrix} r_3\epsilon'^2 & r_4\epsilon\epsilon' & r_2\epsilon' \\ r_4\epsilon\epsilon' & r_5\epsilon^2 & r_1\epsilon \\ r_2\epsilon' & r_1\epsilon & 0 \end{pmatrix} \Lambda_R \ , \tag{2.45}$$

while the charged lepton mass matrix is the same as in Eq. (2.36). Using Eq. (2.37) one obtains the texture:

$$M_{LL} \sim \begin{pmatrix} (\epsilon'/\epsilon)^2 & \epsilon'/\epsilon & \epsilon'/\epsilon \\ \epsilon'/\epsilon & 1 & 1 \\ \epsilon'/\epsilon & 1 & 1 \end{pmatrix} \frac{\langle H_U \rangle^2}{\Lambda_R} \ . \tag{2.46}$$

If we now choose $(l_1, \ldots, l_5, r_1, \ldots, r_5, c_1, \ldots, c_5, \xi) = (-1.0,\ 1.0,\ 1.0,\ 0.5,\ 1.0,\ 0.5,\ 1.0,\ 1.0,\ 1.0,\ -2.0,\ 1.0,\ 1.0,\ 1.0,\ 1.0,\ 1.0,\ 1.0)$, we find

$$\frac{\Delta m^2_{23}}{\Delta m^2_{12}} = 282, \qquad \sin^2 2\theta_{12} = 6 \times 10^{-3}, \qquad \sin^2 2\theta_{23} = 0.995. \tag{2.47}$$

Again these values fall in the desired ranges to explain the atmospheric and solar neutrino deficits, assuming an appropriate choice for Λ_R.

While the texture in Eq. (2.46) appears to be the same as the one in Eq. (2.38) (up to an overall factor of ϵ), there is in fact an important difference: the $O(1)$ entries in Eq. (2.46) have a vanishing determinant at lowest order. The ratio of the two largest eigenvalues are therefore determined by higher order corrections, which must be taken into account to obtain the correct numerical results.[7] While the zero determinant is lifted at $O(\epsilon)$ in the superpotential, it is interesting that, in this particular case, a comparable correction comes from D-terms that alter the canonical form of the neutrino kinetic energy

$$\int d^4\theta [\nu_L^\dagger \nu_L + \nu_L^\dagger B \nu_L] \ . \tag{2.48}$$

Here B is a Hermitian matrix that depends on the flavons in the model. The kinetic terms may be put back into canonical form by the superfield redefinition $\nu_L \to \sqrt{1-B}\nu_L \approx (1 - B/2)\nu_L$. This in turn leads to a correction to M_{LL},

$$M_{LL} \to M_{LL} - 1/2\{B, M_{LL}\}. \tag{2.49}$$

Numerically, it is only necessary that we retain the largest elements of B

$$B \approx \begin{pmatrix} \cdot & \cdot & \cdot \\ \cdot & \cdot & a\epsilon \\ \cdot & a\epsilon & \cdot \end{pmatrix}, \tag{2.50}$$

[7] In fact, the analysis made for the model in Case I included higher order terms, which did not contribute in any significant way.

which also leads to an $O(\epsilon)$ correction to the determinant discussed above. The parameter a is included in the quantitative analysis of the model presented in the next section.

2.5 Numerical Analysis

The numerical check of the unified $T' \times Z_3$ model presented in Section 2.4 relied on two assumptions. The first is that there exist $O(1)$ coefficients c_i, d_i, and u_i for the charged fermion Yukawa matrices that, when combined with the particular choice of neutrino Yukawa parameters l_i and r_i, yield charged fermion mass eigenvalues and mixing angles in agreement with the values observed. This should not be a problem since the textures of the $T' \times Z_3$ model for the charged fermions agree completely with those of the U(2) model[15], in which all of these observables are accommodated in detailed fits. Second, the textures as written in the last section are defined at the scale $M_{\rm GUT} \approx 2 \times 10^{16}$ GeV, while the observables are of course measured below the electroweak scale. A truly meaningful fit requires running the gauge and Yukawa couplings over this range. While the textures renormalized at $M_{\rm GUT}$ and m_t should not differ wildly in form, a global fit is required to properly compare the predictions of our model to the experimental data. The purpose of this section is to report on the necessary steps in these fits and the numerical results.

In order to study the renormalization of gauge and Yukawa couplings, we run the one-loop renormalization group equations (RGE's) of the MSSM [42] from $M_{\rm GUT}$ down to the electroweak scale taken to be $m_t = 175$ GeV. This analysis does not include two-loop corrections nor threshold effects at either end of the spectrum. In particular, this approach does not differentiate between the scales M_f, $\epsilon M_f \approx M_{\rm GUT}$,

$\epsilon' M_f \approx \epsilon' M_{\rm GUT}/\epsilon$, and $\Lambda_R \approx \epsilon M_{\rm GUT}$.[8] In any case, both the two-loop and threshold effects are formally of subleading order, and therefore are taken into account by permitting theoretical uncertainties in the gauge and Yukawa couplings of $O(1/16\pi^2) \approx 1\%$.

Values of the gauge couplings at $M_{\rm GUT}$ are obtained by starting with the precision values extracted at the scale M_Z [1],

$$\begin{aligned} \alpha_1^{-1}(M_Z) &= 59.99 \pm 0.04, \\ \alpha_2^{-1}(M_Z) &= 29.57 \pm 0.03, \\ \alpha_3^{-1}(M_Z) &= 8.40 \pm 0.13. \end{aligned} \tag{2.51}$$

The gauge couplings are run from M_Z to m_t using the one-loop Standard Model (SM) RGE's, and then from m_t to $M_{\rm GUT}$ using the one-loop MSSM RGE's.[9] The GUT scale couplings are taken directly from the textures of Eqs. (2.6), (2.9), (2.36), and (2.44), given numerical values for the dimensionless coefficients c_i, d_i, l_i, r_i, u_i, and a (collectively k_i), and for ϵ, ϵ', ρ, and ξ. The Yukawa matrices are then run down to m_t and diagonalized.[10]

Experimental values for the low-energy Yukawa couplings are extracted from the physical masses and mixing angles compiled by the Particle Data Group [1], where

[8] Notice that $\Lambda_R \approx \epsilon M_{\rm GUT}$ yields the appropriate mass scale in Eq. (2.46) for atmospheric neutrino oscillations.

[9] It should be pointed out that, while the SM RGE's make use of the $\overline{MS}$ scheme, the MSSM RGE's in Ref. [42] make use of the $\overline{DR}$ scheme [43], which differ at the matching scale (m_t by our choice) by an amount

$$\frac{4\pi}{\alpha_i^{\overline{DR}}} = \frac{4\pi}{\alpha_i^{\overline{MS}}} - \frac{1}{3}(C_A)_i, \tag{2.52}$$

where $C_A = \{0, 2, 3\}$ for $i = 1, 2, 3$.

[10] The RGE's are integrated by means of the Runge-Kutta method with adaptive stepsize control[44]. The results of this method were cross-checked against the results of using Richardson extrapolation with Bulirsch-Stoer stepping[44] and were found to agree to the limits of the expected accuracy of either solution.

entries of Y_U are obtained by dividing quark masses by $v \sin\beta/\sqrt{2}$ and those of $Y_{D,L}$ by dividing quark and lepton masses by $v \cos\beta/\sqrt{2}$, where $v = 246$ GeV.

The experimental uncertainties on the observables (or estimates for the quark masses) used in the fits are either those appearing in Ref. [1] or 1% of the central value, whichever is larger; since the lepton masses are measured with extraordinary precision, they are sensitive to the two-loop RGE and threshold corrections that we have ignored.

The RGE for the neutrino Majorana mass matrix M_{LL} was computed in Ref. [45] and is included here in order to complete the RGE evolution for all observables. The low-energy neutrino observables are taken to be

$$\begin{aligned} &100 \lesssim \frac{\Delta m_{23}^2}{\Delta m_{12}^2} \lesssim 2500, \\ &\sin^2 2\theta_{23} \gtrsim 0.8, \\ &2 \times 10^{-3} \lesssim \sin^2 2\theta_{12} \lesssim 10^{-2}. \end{aligned} \tag{2.53}$$

For the sake of having meaningful uncertainties, a parameter whose lower bound is much smaller than its upper bound is converted into its logarithm. Instead of Eq. (2.53), we use

$$\begin{aligned} \ln\left(\frac{\Delta m_{23}^2}{\Delta m_{12}^2}\right) &= 6.22 \pm 1.61, \\ \sin^2 2\theta_{23} &= 0.9 \pm 0.1, \\ \ln\left(\sin^2 2\theta_{12}\right) &= -5.41 \pm 0.80. \end{aligned} \tag{2.54}$$

Summarizing to this point, we have discussed the details of how inputs consisting of the gauge couplings at M_Z and Yukawa matrix parameters at a high scale are manipulated using one-loop RGE's to produce output values for fermion masses and mixing angles observed at low energy. Of course, the salient question is whether one can find a choice of parameters k_i, where all of these coefficients are $O(1)$, and yet the output quantities are all in agreement with their observed values.[11] This is accomplished through a χ^2 minimization; thus, the complete simulation consists of choosing a set of parameters k_i (relevant at M_{GUT}), running the RGE's down to m_t, and comparing with observation to compute a figure of merit, χ^2. If χ^2 is too large, the parameters k_i are adjusted and the procedure is repeated until convergence of χ^2 to a minimum is achieved.

The χ^2 function assumes a somewhat nonstandard form. Fermion masses and mixing angles are converted to Yukawa couplings $k_i^{\text{expt}} \pm \Delta k_i$, and contribute an amount

$$\Delta\chi^2 = \left(\frac{k_i^{\text{expt}} - k_i}{\Delta k_i}\right)^2 \tag{2.55}$$

to χ^2, as usual. There are 15 observables (6 quark masses, 3 quark CKM elements [since CP violation is neglected], 3 lepton masses, 2 neutrino mixing angles, and 1 neutrino mass ratio) and 26 parameters k_i; on the surface, it seems that the fit is always under-constrained. However, our demand that the parameters k_i lie near unity imposes additional restrictions, which we include by adding terms to χ^2 of the form

$$\Delta\chi^2 = \left(\frac{\ln|k_i|}{\ln 3}\right)^2 \tag{2.56}$$

for each i. Thus, the parameters k_i are effectively no longer free, but are to be treated analogously to pieces of data, each of which contributes one unit to χ^2 if it is as large as 3 or as small as 1/3. The particular choice of 3 for this purpose is, of course, a

[11] We also allow for variation of the parameters ϵ, ϵ', ρ, and ξ by hand, but do not minimize with respect to them. Changes in these parameters are equivalent to redefinitions of the $O(1)$ coefficients, so that they merely set the scale for the other parameters of the fit.

matter of taste. In effect, the inclusion of such terms renders the parameters k_i no longer as true degrees of freedom. On the other hand, they are not true pieces of data either, since a value of say, $k_i = 0.8$ is just as valid as a value of -1.1 for our purposes. Thus, the value of $\chi^2_{\rm min}$ determining a 'good' fit is 15, since there are 15 pieces of true data and effectively no *unconstrained* fit parameters.

The numerical minimization is carried out using the MINUIT minimization package. As a cross check, minimization using Powell's direction set method[44] is carried out to make sure that the same minimum is achieved. Since the topography of the χ^2 function is complicated due to the numerous parameters involved, it is important to try a number of initial choices for the input parameters k_i in order to have confidence that the minimum obtained is close to global. Once convergence is achieved, a parabolic minimum is assumed and a Hessian matrix is computed in order to gauge uncertainties of the parameters.

Detailed numerical fits show that it is not difficult to find parameters k_i that satisfy the constraint $\chi^2_{\rm min} < 15$. However, in the $T' \times Z_3$ model, the ratio m_b/m_t must be accommodated either by a small value of ξ or a large value of $\tan\beta$. For definiteness, we choose $\tan\beta = 2$ as a representative value, and find a best fit with $\chi^2_{\rm min}$ of 2.77. The complete set of parameters is listed in Table 2.3 and a comparison to data appears in Table 2.4. Note especially that the parameters ϵ, ϵ', and ρ are somewhat larger (a factor of 2 or more) than their values in the U(2) model of Ref. [14], where neutrino physics was not considered. From the excellent χ^2, one concludes that the $T' \times Z_3$ model has little difficulty satisfying all of the required constraints including the naturalness of the coefficients, allowing for the small parameter ξ that distinguishes the scale of Y_U from $Y_{D,L}$.

While we have seen that the minimal scenario is extremely successful at reproduc-

$c_1 = -0.93 \pm 0.01$	$d_1 = +1.33 \pm 0.45$	$l_1 = +0.85 \pm 0.62$
$c_2 = -0.46 \pm 0.03$	$d_2 = -0.81 \pm 0.26$	$l_2 = -1.01 \pm 1.11$
$c_3 = -1.02 \pm 1.13$	$d_3 = +1.55 \pm 0.67$	$l_3 = -0.97 \pm 0.75$
$c_4 = -1.03 \pm 1.15$	$d_4 = +1.14 \pm 1.33$	$l_4 = -1.09 \pm 1.04$
$c_5 = -0.90 \pm 0.01$	$d_5 = -1.29 \pm 0.12$	$l_5 = -1.11 \pm 0.79$
$r_1 = +0.94 \pm 0.84$	$u_1 = +0.92 \pm 0.31$	$\epsilon = 0.04$
$r_2 = +1.06 \pm 0.95$	$u_2 = +1.48 \pm 0.70$	$\rho = 0.08$
$r_3 = +1.03 \pm 1.12$	$u_3 = -0.90 \pm 0.91$	$\epsilon' = 0.004$
$r_4 = -1.07 \pm 1.05$	$u_4 = +1.07 \pm 1.21$	$\xi = 0.017$
$r_5 = -0.97 \pm 1.03$	$u_5 = +1.84 \pm 0.95$	$a = +0.98 \pm 1.06$

Table 2.3 Best fit parameters for the $T' \times Z_3$ model with $\tan\beta = 2$. The minimum χ^2 = 2.77.

Observable	Expt. value	Fit value
m_u	$(3.3 \pm 1.8) \times 10^{-3}$	3.5×10^{-3}
m_d	$(6.0 \pm 3.0) \times 10^{-3}$	4.0×10^{-3}
m_s	0.155 ± 0.055	0.136
m_c	1.25 ± 0.15	1.24
m_b	4.25 ± 0.15	4.25
m_t	173.8 ± 5.2	170.4
m_e	$(5.11 \pm 1\%) \times 10^{-4}$	5.11×10^{-4}
m_μ	$0.106 \pm 1\%$	0.106
m_τ	$1.78 \pm 1\%$	1.78
$\|V_{us}\|$	0.221 ± 0.004	0.221
$\|V_{ub}\|$	$(3.1 \pm 1.4) \times 10^{-3}$	2.3×10^{-3}
$\|V_{cb}\|$	$(3.9 \pm 0.3) \times 10^{-2}$	3.9×10^{-2}
$\Delta m_{23}^2/\Delta m_{12}^2$	100 – 2500	526
$\ln(\Delta m_{23}^2/\Delta m_{12}^2)$	6.22 ± 1.61	6.27
$\sin^2 2\theta_{12}$	2×10^{-3} – 10^{-2}	4.5×10^{-3}
$\ln(\sin^2 2\theta_{12})$	-5.41 ± 0.80	-5.40
$\sin^2 2\theta_{23}$	$\gtrsim 0.8$	0.90
$\sin^2 2\theta_{13}$	—	1.4×10^{-3}

Table 2.4 Experimental values versus fit central values for observables using the inputs of Table 2.3. Masses are in GeV and all other quantities are dimensionless. Error bars indicate the larger of experimental or 1% theoretical uncertainties, as described in the text.

ing fermion masses and mixing angles, there are nonetheless a number of interesting variant models based on T' symmetry. We explore these models in the next three sections.

2.6 SU(5)×U(2) with neither SU(5) nor U(2)

As discussed in Section 2.1, the U(2) model must be embedded in a grand unified theory to reproduce all of the observed quark mass hierarchies. In this section we present a model that does exactly the same, without the need for a GUT, by extending the discrete gauged flavor group to $T' \times Z_6$. We show that this model explains the ratio m_b/m_t, which is merely parameterized in the U(2) model (and in our other T' models). Before presenting the model we comment on notation. As before, we use the triality superscripts $+, -$, and 0 for the different representations of T'. For the Z_6 reps we now introduce the indices $i = 0, 1, \ldots, 5$, which combine through addition modulo 6. For example, $\mathbf{2}^{+4} \otimes \mathbf{1}^{+2} = \mathbf{2}^{-0}$, etc. Since Z_6 is isomorphic to $Z_3 \times Z_2$, one may view the new flavor symmetry as a Z_2 extension of the $T' \times Z_3$ flavor group defined in the model of Section 2.4; denoting the Z_2 reps by $+$ and $-$, one identifies

Z_3	Z_2	Z_6
0	+	0
−	−	1
+	+	2
0	−	3
−	+	4
+	−	5

That is, the Z_6 charge is $2 \times (Z_3 \text{ charge}) + 3 \times (Z_2 \text{ charge})$ modulo 6. In the remainder of this section we use the more compact $T' \times Z_6$ notation.

The three generations of matter fields transform as

$$Q, U, D \sim \mathbf{2}^{04} \oplus \mathbf{1}^{00} \; , \tag{2.57}$$

$$L \sim \mathbf{2}^{04} \oplus \mathbf{1}^{+4} \,, \tag{2.58}$$

$$E \sim \mathbf{2}^{+2} \oplus \mathbf{1}^{-2} \,, \tag{2.59}$$

$$\nu_R \sim \mathbf{2}^{04} \oplus \mathbf{1}^{+1} \,. \tag{2.60}$$

The matter fields have transformation properties that differ from those in our previous models, and in particular, the electroweak doublet leptons are no longer anomaly free by themselves. The third-generation L field is assigned to a nontrivial T' singlet, the $\mathbf{1}^+$, which does not form a complete SU(2) representation. Given the discussion in Section 2.2, the T' $\mathrm{SU}(2)_W^2$ anomaly is not automatically cancelled. However, we remedy this problem by assigning non-trivial transformation properties to the Higgs fields:

$$H_U \sim \mathbf{1}^{00}, \;\; H_D \sim \mathbf{1}^{-2}. \tag{2.61}$$

The fields H_D and L_3 are both electroweak doublets and, as far as the non-Abelian quantum numbers are concerned, form a vector-like pair when H_D is a $\mathbf{1}^-$ under T'. The remaining fields, E and ν_R, do not transform under any unbroken non-Abelian continuous gauge groups and thus their $T' \times Z_6$ quantum numbers may be assigned freely.

In order to break the flavor symmetry and obtain the fermion mass matrices we introduce the following flavons:

$$S \sim \mathbf{3}^0, \;\; A \sim \mathbf{1}^{-0}, \;\; \phi \sim \mathbf{2}^{02}, \tag{2.62}$$

$$\Delta \sim \mathbf{1}^{+4}, \;\; \Delta^{'} \sim \mathbf{1}^{-2} \,. \tag{2.63}$$

In addition to these flavon fields, we introduce two more in the neutrino sector of the theory. Their transformation properties are such that they do not alter the form of the charged fermion Yukawa textures:

$$\phi_\nu \sim \mathbf{2}^{+3}, \ \Delta_\nu \sim \mathbf{1}^{+1} \ . \tag{2.64}$$

Together with ν_R, these fields are the only ones that transform nontrivially under the Z_2 subgroup of Z_6 (i.e., the only ones with odd Z_6 charges). Again, we are interested in a two-step breaking:

$$T' \times Z_6 \xrightarrow{\epsilon} Z_3^D \xrightarrow{\epsilon'} nothing, \tag{2.65}$$

where Z_3^D is precisely the same subgroup as in the minimal $T' \times Z_3$ model. Thus, by the same arguments presented in Section 2.4, we obtain the following patterns of vevs:

$$\frac{\langle S \rangle}{M_f} \sim \begin{pmatrix} 0 & 0 \\ 0 & \epsilon \end{pmatrix}, \ \frac{\langle A \rangle}{M_f} \sim \begin{pmatrix} 0 & \epsilon' \\ -\epsilon' & 0 \end{pmatrix}, \tag{2.66}$$

$$\frac{\langle \phi \rangle}{M_f} \sim \sigma_2 \begin{pmatrix} 0 \\ \epsilon \end{pmatrix}, \ \frac{\langle \Delta \rangle}{M_f} \sim \epsilon, \ \frac{\langle \Delta' \rangle}{M_f} \sim \epsilon, \tag{2.67}$$

$$\frac{\langle \phi_\nu \rangle}{M_f} \sim \sigma_2 \begin{pmatrix} \epsilon' \\ \epsilon \end{pmatrix}, \ \frac{\langle \Delta_\nu \rangle}{M_f} \sim \epsilon. \tag{2.68}$$

Unlike the minimal model described in the previous two sections, the flavons here contribute to the Yukawa matrices in some cases only at quadratic order

$$\begin{aligned} Y_U &\sim \left(\begin{array}{c|c} [\mathbf{3}^4 \oplus \mathbf{1}^{04}] & [\mathbf{2}^{02}] \\ \hline [\mathbf{2}^{02}] & [\mathbf{1}^{00}] \end{array} \right) \\ &\sim \left(\begin{array}{c|c} \Delta S + \Delta A + \phi^2 & \phi \\ \hline \phi & 1 \end{array} \right) \approx \begin{pmatrix} 0 & \epsilon\epsilon' & 0 \\ -\epsilon\epsilon' & \epsilon^2 & \epsilon \\ 0 & \epsilon & 1 \end{pmatrix}, \end{aligned} \tag{2.69}$$

$$
\begin{aligned}
Y_D &\sim \left(\begin{array}{c|c} [\mathbf{3}^2 \oplus \mathbf{1}^{+2}] & [\mathbf{2}^{+0}] \\ \hline [\mathbf{2}^{+0}] & [\mathbf{1}^{+4}] \end{array}\right) \\
&\sim \left(\begin{array}{c|c} \Delta' S + \Delta' A & \Delta\phi \\ \hline \Delta\phi & \Delta \end{array}\right) \approx \begin{pmatrix} 0 & \epsilon' & 0 \\ -\epsilon' & \epsilon & \epsilon \\ 0 & \epsilon & 1 \end{pmatrix} \epsilon\,,
\end{aligned} \tag{2.70}
$$

$$
\begin{aligned}
Y_L &\sim \left(\begin{array}{c|c} [\mathbf{3}^4 \oplus \mathbf{1}^{04}] & [\mathbf{2}^{-4}] \\ \hline [\mathbf{2}^{-4}] & [\mathbf{1}^{+4}] \end{array}\right) \\
&\sim \left(\begin{array}{c|c} \Delta S + \Delta A + \phi^2 & \Delta'\phi + \Delta_\nu \phi_\nu \\ \hline \Delta'\phi + \Delta_\nu \phi_\nu & \Delta \end{array}\right) \approx \begin{pmatrix} 0 & \epsilon' & \epsilon' \\ -\epsilon' & \epsilon & \epsilon \\ \epsilon' & \epsilon & 1 \end{pmatrix} \epsilon\,.
\end{aligned} \tag{2.71}
$$

We see that the flavons Δ and Δ' appear in precisely the right way to recover approximate SU(5) $\times$ U(2) textures for Y_D and Y_L, *with an additional overall factor of* ϵ. The only difference is a relatively uninteresting ϵ' entry in the 13 and 31 elements of Y_L. Notice that the vev of the Σ field has been replaced by $\langle\Delta\rangle$ in Eq. (2.69). Thus, all important features of the SU(5) $\times$ U(2) model are reproduced.

Note that the ratio m_b/m_t, which is experimentally observed to be in the range $0.023 < m_b/m_t < 0.026$, is predicted to be of order $\epsilon \approx 0.02$ for $\tan\beta \approx O(1)$, as can be seen from the ratio of the 33 entries in Y_U and Y_D. This is promising since $\tan\beta \approx O(1)$ is the naive expectation if the Higgs potential is not fine-tuned.

Before proceeding to the analysis of the neutrino sector, a few comments are warranted on the possible supersymmetric contributions to FCNC's in this model. As mentioned in Section 2.1, scalar superpartners of the first two generations are exactly degenerate in our models when the flavor symmetry is unbroken. The amount of scalar nondegeneracy at low energies is determined by the order at which flavons contribute to the scalar mass matrices. In the minimal model, the flavons contribute quadratically to the scalar masses of the first two generations, as a consequence of the flavons' nontrivial Z_3 charges. The scalar mass-squared matrices of the U(2) model are then reproduced. In the current model, however, the flavon S may contribute linearly, since $\mathbf{3}^0$ is in the product of $(\mathbf{2}^{04})^\dagger \otimes (\mathbf{2}^{04})$. The important point is that this effect provides an $O(\epsilon)$ correction to the *diagonal* entries of the scalar mass matrices. In the fermion mass-eigenstate basis, a Cabibbo-like rotation $\theta_C \sim \epsilon'/\epsilon$ leads to 12 entries in the scalar mass matrices of order $\epsilon' \tilde{m}_0^2$, where $\tilde{m}_0^2$ is an average scalar mass, and $\epsilon' \approx 0.004$. Taking into account uncertainty in $O(1)$ coefficients, this result is in marginal agreement with the bounds from CP-conserving flavor-changing processes, assuming superpartner masses less than a TeV [12]. While bounds from CP-violating precesses are generically stronger, the $O(1)$ coefficients have unknown phases that one may simply choose in order to avoid these bounds. Without a firm understanding of the origin of CP violation, saying more about these phases entails a degree of speculation that we choose to avoid. Of course, if scalar superpartners are heavy (as in the 'more minimal MSSM' [46]) or flavor universal (as in gauge mediation [26], anomaly mediation [27, 28], or Scherk-Swartz mechanism [29]) the current T' model is completely safe.

Next we examine the neutrino sector of the model. Given the transformation properties of ν_R, we calculate the neutrino Dirac and Majorana mass matrices

$$M_{LR} \sim \left(\begin{array}{c|c} [\mathbf{3}^4 \oplus \mathbf{1}^{04}] & [\mathbf{2}^{-1}] \\ \hline [\mathbf{2}^{-4}] & [\mathbf{1}^{+1}] \end{array}\right) \sim \left(\begin{array}{c|c} \Delta S + \Delta A + \phi^2 & \Delta\phi_\nu \\ \hline \Delta'\phi + \Delta_\nu\phi_\nu & \Delta_\nu \end{array}\right) \langle H_U \rangle$$
$$\approx \begin{pmatrix} 0 & l_1\epsilon' & l_2 r_1 \epsilon' \\ -l_1\epsilon' & l_3\epsilon & l_2 r_3 \epsilon \\ l_4\epsilon' & l_5\epsilon & l_6 \end{pmatrix} \epsilon \langle H_U \rangle \, , \tag{2.72}$$

$$M_{RR} \sim \left(\begin{array}{c|c} [\mathbf{3}^4] & [\mathbf{2}^{-1}] \\ \hline [\mathbf{2}^{-1}] & [\mathbf{1}^{+4}] \end{array}\right) \sim \left(\begin{array}{c|c} \Delta S & \Delta\phi_\nu \\ \hline \Delta\phi_\nu & \Delta \end{array}\right) \Lambda_R \approx \begin{pmatrix} 0 & 0 & r_1\epsilon' \\ 0 & r_2\epsilon & r_3\epsilon \\ r_1\epsilon' & r_3\epsilon & r_4 \end{pmatrix} \epsilon\Lambda_R \, , \tag{2.73}$$

where r_i and l_i are $O(1)$ coefficients. To leading order, the seesaw mechanism gives

$$M_{LL} \sim \begin{pmatrix} \epsilon'^2/\epsilon & \epsilon' & \epsilon' \\ \epsilon' & 1 & 1 \\ \epsilon' & 1 & 1 \end{pmatrix} \frac{\epsilon \langle H_U \rangle^2}{\Lambda_R} . \tag{2.74}$$

Note that the texture in Eq. (2.74) is not changed if higher-order corrections are included that lift the zeroes in Eqs. (2.72)–(2.73). Following the same procedure as before, we diagonalize M_{LL} and Y_L and extract the neutrino masses and mixing angles. A global fit of the parameters in this model can in principle be done; however we just present a viable set of parameters for simplicity. Using the set of values for the $O(1)$ coefficients in M_{LL} ($r_1, \ldots, r_4, l_1, \ldots, l_6$) $=$ (1.0, 1.0, 1.0, -1.0, 1.2, 1.2, 1.3, -1.0, -2.0, 1.0) and assuming all coefficients in Y_L are 1.0 except that of the 22 entry, which we set to 3.0, we obtain

$$\frac{\Delta m^2_{23}}{\Delta m^2_{12}} = 125, \qquad \sin^2 2\theta_{12} = 3.5 \times 10^{-3}, \qquad \sin^2 2\theta_{23} = 0.88. \tag{2.75}$$

This agrees with the allowed ranges described in the previous sections. It is worth mentioning that the texture Eq. (2.74) is the same as obtained in Ref. [17], and thus the claim in Ref. [18] that this texture cannot account for solar neutrino oscillations is not correct.

2.7 A Global T' Model

As pointed out in Section 2.1, it is not possible to construct a realistic supersymmetric model with a continuous SU(2) flavor symmetry if scalar universality is not assumed. The argument is straightforward: The left- and right-handed up quark fields must be embedded in **2**$\oplus$**1** representations to maintain the heaviness of the top quark, as well as degeneracy of squarks of the first two generations. Given this assignment, the coupling $Q^a U^b \epsilon_{ab} H_u$ is allowed by the unbroken flavor symmetry, which implies the unacceptable relation $m_u = m_c \approx m_t$. The T' model below demonstrates that discrete subgroups of SU(2) are viable for building models of fermion masses, although they are more dangerous than models with additional Abelian factors, as far as supersymmetric FCNC processes are concerned. We first present the model, and then explain how it evades the problem described above.

The crucial feature that allows one to build a successful $T' \times Z_3$ model is the existence of a doublet representation $\mathbf{2}^{0-}$, whose first generation component alone rotates by a phase under the Z_3^D subgroup. This choice is unique in models where T' is a discrete gauge symmetry, since the $\mathbf{2}^0$ rep is the only doublet that fills a complete SU(2) representation if we embed T' in SU(2). The $\mathbf{4}$ of SU(2) decomposes into the reps $\mathbf{2}^+$ and $\mathbf{2}^-$, which implies that each is separately anomalous. While it might still be possible to construct models involving anomaly-free combinations of $\mathbf{2}^+$ and $\mathbf{2}^-$ reps, we have found no examples that are particularly compelling. On the other hand, if T' is assumed to be a global symmetry, then matter fields can be assigned to any of the doublet representations freely. This provides an opportunity for constructing economical models, as we now demonstrate.

Consider the Z_3 subgroup of T' generated by the element g_9 that acts on the $\mathbf{2}^0$ rep as $diag\{\eta^2, \eta\}$, with η defined as in Section 2.3. In the $\mathbf{2}^-$ rep, this element takes the form $diag\{\eta, 1\}$, which we identify as the desired phase rotation matrix for matter fields of the first two generations. Given our freedom to assign matter fields to any of the doublet reps in a global T' model, it is no longer necessary to extend the flavor symmetry by an Abelian factor in order to find a subgroup that forbids the order ϵ' Yukawa entries. Thus, one is naturally led to the charge assignment

$$\psi \sim \mathbf{2}^- \oplus \mathbf{1}^0 \quad \text{for} \quad \psi = Q, U, D, L \text{ and } E, \tag{2.76}$$

and $H_{U,D} \sim \mathbf{1}^0$, which yields

$$Y_{U,D,L} \sim \left(\begin{array}{c|c} [\mathbf{3} \oplus \mathbf{1}^-] & [\mathbf{2}^+] \\ \hline [\mathbf{2}^+] & [\mathbf{1}^0] \end{array}\right). \tag{2.77}$$

Introducing flavons, A, ϕ and S transforming as $\mathbf{1}^-$, $\mathbf{2}^+$, and $\mathbf{3}$, respectively, one reproduces the canonical U(2) textures assuming the breaking pattern

$$T' \xrightarrow{\epsilon} Z_3 \xrightarrow{\epsilon'} nothing, \tag{2.78}$$

together with the dynamical assumption that only the $\mathbf{1}^-$ rep participates in the last step of symmetry breaking. The resulting textures are identical to those in our original model of Section 2.4. One difference, however, is that the S flavon in this model contributes to the squark mass matrices at first order in ϵ, just as in the $T' \times Z_6$ model. However, this is not a concern for the same reasons discussed at length in Section 2.6.

Turning to neutrino physics, recall that successful results were obtained in the $T' \times Z_3$ model by altering the charge assignment of the third-generation right-handed neutrino field. Thus, we are motivated here to consider

$$\nu_R \sim \mathbf{2}^- \oplus \mathbf{1}^- \ , \tag{2.79}$$

which implies

$$M_{LR} \sim \left(\begin{array}{c|c} [\mathbf{3} \oplus \mathbf{1}^-] & [\mathbf{2}^-] \\ \hline [\mathbf{2}^+] & [\mathbf{1}^+] \end{array}\right) \ , \qquad M_{RR} \sim \left(\begin{array}{c|c} [\mathbf{3}] & [\mathbf{2}^-] \\ \hline [\mathbf{2}^-] & [\mathbf{1}^-] \end{array}\right) \ . \tag{2.80}$$

We identify the flavon ϕ_ν with the representation $\mathbf{2}^-$, which does not appear in any of the charged fermion Yukawa textures. However, there is an important difference between this model and the one discussed in Section 2.4: The third generation ν_R field transforms by a phase under the Z_3 subgroup, so that, for example, the 13 and

31 entries of M_{RR} are left invariant under this intermediate symmetry. This implies an inversion in the hierarchy of vevs in the third row and column of M_{RR}. In the non-unified version of the model, it is somewhat remarkable that we still obtain a viable form for M_{LL}:

$$M_{LR} \approx \begin{pmatrix} 0 & l_1\epsilon' & l_5 r_1 \epsilon \\ -l_1\epsilon' & l_2\epsilon & l_3 r_2 \epsilon' \\ 0 & l_4\epsilon & 0 \end{pmatrix} \langle H_U \rangle \ , \qquad M_{RR} \approx \begin{pmatrix} 0 & 0 & r_1\epsilon \\ 0 & r_3\epsilon & r_2\epsilon' \\ r_1\epsilon & r_2\epsilon' & r_4\epsilon' \end{pmatrix} \Lambda_R \ , \tag{2.81}$$

$$M_{LL} \sim \begin{pmatrix} (\epsilon'/\epsilon)^2 & \epsilon'/\epsilon & \epsilon'/\epsilon \\ \epsilon'/\epsilon & 1 & 1 \\ \epsilon'/\epsilon & 1 & 1 \end{pmatrix} \frac{\langle H_U \rangle^2 \epsilon}{\Lambda_R}, \tag{2.82}$$

Unfortunately, this result does not persist in the simplest unified version of the model, which includes additional suppression factors in the 22 entries of M_{LR} and M_{RR}. Fortunately, a simple modification of the flavon charge assignments in the unified theory allows us to recover the previous result. We introduce two ϕ_ν flavons that transform differently under $T' \times$ SU(5):

$$\phi_\nu \sim (\mathbf{2}^-, \mathbf{24}) \quad , \quad \phi'_\nu \sim (\mathbf{2}^-, \mathbf{1}) \ . \tag{2.83}$$

Furthermore, we assume the pattern of vevs

$$\langle \phi_\nu \rangle \sim \begin{pmatrix} 0 \\ \epsilon \end{pmatrix} \ , \ \langle \phi'_\nu \rangle \sim \begin{pmatrix} \epsilon' \\ 0 \end{pmatrix} \ . \tag{2.84}$$

This is consistent with the breaking pattern in Eq. (2.78), but includes a dynamical assumption that the doublet ϕ'_ν does not participate in the first stage of sequential symmetry breaking and its second component acquires no vev.[12] Since ϕ_ν transforms as an SU(5) adjoint, it can contribute directly to M_{LR}, but only to M_{RR} if, for

[12]We consistently assume that a flavon that transforms nontrivially under a subgroup H_i either acquires a vev of order the scale at which H_i is spontaneously broken, or acquires no vev at all.

example, the adjoint flavon Σ is also present; the corresponding entries of M_{RR} are therefore suppressed by an additional factor of ϵ:

$$M_{LR} \approx \begin{pmatrix} 0 & l_1\epsilon' & l_5 r_1 \epsilon \\ -l_1\epsilon' & l_2\epsilon^2 & l_3 r_2 \epsilon' \\ 0 & l_4\epsilon & 0 \end{pmatrix} \langle H_U \rangle \ , \qquad M_{RR} \approx \begin{pmatrix} 0 & 0 & r_1\epsilon^2 \\ 0 & r_3\epsilon^2 & r_2\epsilon' \\ r_1\epsilon^2 & r_2\epsilon' & r_4\epsilon' \end{pmatrix} \Lambda_R \ . \tag{2.85}$$

The seesaw mechanism then yields

$$M_{LL} \sim \begin{pmatrix} (\epsilon'/\epsilon)^2 & \epsilon'/\epsilon & \epsilon'/\epsilon \\ \epsilon'/\epsilon & 1 & 1 \\ \epsilon'/\epsilon & 1 & 1 \end{pmatrix} \frac{\langle H_U \rangle^2 \epsilon}{\Lambda_R}, \tag{2.86}$$

where we used the numerical fact that ${\epsilon'}^2/\epsilon^3 \sim O(1)$. It is important to note that we have only displayed the contributions to Eq. (2.85) linear in ϕ, S and A, for convenience; quadratic and higher order corrections lift the zero entries of these textures, but do not change the result in Eq. (2.86) qualitatively. Note that Eq. (2.86) is the same successful texture obtained in our original $T' \times Z_3$ model.

Finally, we return to the no-go theorem presented at the beginning of this section. It is not possible to construct a realistic model with a continuous SU(2) flavor symmetry and $\mathbf{2} \oplus \mathbf{1}$ rep structure because an unwanted flavor-invariant operator may be formed from the product of two doublet matter fields. In our global T' model we have the freedom to assign matter fields to new doublet representations whose products contain no trivial singlets, thus avoiding the problem.

2.8 T' with Sterile Neutrinos

In this section we comment briefly on the possibility of four light neutrino species. Rather than investigating the (vast) space of possible models, we simply show how the results of a successful extension of the U(2) model with a sterile neutrino proposed by Hall and Weiner (HW) [18] can be reproduced with T' symmetry instead.

Consider a U(2) model with all matter fields, including three generations of right-handed neutrinos, in $\mathbf{2} \oplus \mathbf{1}$ representations. Given the canonical pattern of flavon vevs, one obtains a right-handed neutrino mass matrix of the form

$$M_{RR} = \begin{pmatrix} 0 & 0 & 0 \\ 0 & \epsilon & \epsilon \\ 0 & \epsilon & 1 \end{pmatrix} \Lambda_R \ . \tag{2.87}$$

Since M_{RR} is symmetric, there is no contribution from the flavon A, leading to a singular matrix. It is important to emphasize that the zero entries of Eq. (2.87) are not lifted at any order in ϵ and ϵ' as a consequence of the holomorphicity of the superpotential. From consideration of the U(2) indices of the flavon fields (or alternatively their charges under a U(1) subgroup of U(2)), it is possible to show that any contribution to the vanishing entries of Eq. (2.87) requires the complex conjugation of a flavon field, which is not allowed by unbroken supersymmetry. If the pattern of flavon vevs is not altered, the first-generation right-handed neutrino remains in the low-energy theory as a sterile neutrino.

This sterile neutrino mixes with the second-generation left-handed neutrino at order ϵ' in M_{LR}. After integrating out the two heavy right-handed neutrino flavors, one obtains a four-by-four neutrino mass matrix of the form

$$M^{(4)} = \left(\begin{array}{ccc|c} & & & 0 \\ & M_{LL}^{(3)} & & c\epsilon' \langle H_U \rangle \\ & & & 0 \\ \hline 0 & c\epsilon' \langle H_U \rangle & 0 & 0 \end{array} \right) \ , \tag{2.88}$$

where the three-by-three block $M_{LL}^{(3)}$ has entries of order $\langle H_U \rangle^2 / \Lambda_R$, which can be found in Ref. [18]. HW observe that the 24 and 42 entries of $M^{(4)}$ are much larger than all others, leading naturally to maximal mixing between ν_μ and the sterile neutrino. As it stands, however, both would have masses of order of the electroweak scale unless c is taken to be of $O(10^{-8})$. To obtain a viable model, HW extend the flavor symmetry by an additional U(1) factor, under which all the right-handed neutrinos have charge +1. A charge −1 flavon is introduced with the vev $\epsilon_N \sim 10^{-8}$, which breaks this symmetry weakly. One then finds that $c \approx \epsilon_N$, while $M^{(3)}$ remains unchanged.

The main obstacle to implementing this solution in a $T' \times Z_3$ model with all matter fields assigned to $\mathbf{2}^{0-} \oplus \mathbf{1}^{00}$ reps is that higher-order corrections to the first row and column of Eq. (2.87) are not forbidden by holomorphicity; the complex conjugate of any non-trivial Z_3 phase rotation is the same as its square. Thus, we are led to promote our Z_3 symmetry to a continuous U(1).[13] The appropriate embedding is given by

$$\psi \sim \mathbf{2}^{0-} \oplus \mathbf{1}^{00} \longrightarrow \mathbf{2}^0_{+1} \oplus \mathbf{1}^0_0$$

$$\phi \sim \mathbf{2}^{0+} \longrightarrow \mathbf{2}^0_{-1} \quad , \quad S \sim \mathbf{3}^- \longrightarrow \mathbf{3}_{-2} \quad , \quad A \sim \mathbf{1}^{0-} \longrightarrow \mathbf{1}^0_{-2} \, , \tag{2.89}$$

where the subscript indicates the U(1) charge. Assuming the breaking pattern

$$T' \times U(1) \xrightarrow{\epsilon} Z_3^D \xrightarrow{\epsilon'} nothing, \tag{2.90}$$

we reproduce the textures of the U(2) model, including Eq. (2.87), identically. The HW predictions for solar, atmospheric and LSND [19] neutrino oscillations are then recovered by extending the symmetry by an additional U(1) factor, implemented precisely as before. We are thus able to reproduce the results of Ref. [18] with the flavor symmetry $T' \times \mathrm{U}(1)^2$. Although we find this model less compelling than the other three already discussed, it may be of some relevance if the LSND oscillation result is independently confirmed.

[13] We could also promote Z_3 to a much larger Z_n that adequately suppresses corrections to the zero entries in Eq. (2.87); we leave this possibility implicit in our discussion.

2.9 Explicit Details of T'

As described in the text, the group T' is generated by the elements labeled g_5 and g_9. We begin by exhibiting explicit matrices representing these elements in each of the seven reps listed in Table I. The singlets are $g_5(\mathbf{1}^{0,\pm}) = 1$, $g_9(\mathbf{1}^0) = 1$, $g_9(\mathbf{1}^+) = \eta$, $g_9(\mathbf{1}^-) = \eta^2$, where $\eta = \exp(2\pi i/3)$. The doublets are

$$g_5(\mathbf{2}^{0,\pm}) = M_1, \quad g_9(\mathbf{2}^0) = \eta M_2, \quad g_9(\mathbf{2}^+) = \eta^2 M_2, \quad g_9(\mathbf{2}^-) = M_2, \tag{2.91}$$

where

$$M_1 = -\frac{1}{\sqrt{3}} \begin{pmatrix} +i & +\sqrt{2}e^{i\pi/12} \\ -\sqrt{2}e^{-i\pi/12} & -i \end{pmatrix}, \quad M_2 = \begin{pmatrix} \eta & 0 \\ 0 & 1 \end{pmatrix}, \tag{2.92}$$

and the triplet rep is generated by

$$g_5(\mathbf{3}) = \frac{1}{3} \begin{pmatrix} -1 & 2\eta & 2\eta^2 \\ 2\eta^2 & -1 & 2\eta \\ 2\eta & 2\eta^2 & -1 \end{pmatrix}, \quad g_9(\mathbf{3}) = \begin{pmatrix} 1 & 0 & 0 \\ 0 & \eta & 0 \\ 0 & 0 & \eta^2 \end{pmatrix}. \tag{2.93}$$

The Clebsch-Gordan (CG) coefficient matrices $\mathcal{O}_i$ coupling an n_x-plet $\mathbf{x}$ and an n_y-plet $\mathbf{y}$ to form an n_z-plet $\mathbf{z}$ consist of n_z matrices of dimensions $n_x \times n_y$ satisfying the condition

$$R_x^T \mathcal{O}_i R_y = \sum_{j=1}^{n_z} (R_z)_{ij} \mathcal{O}_j, \quad i = 1, \dots, n_z, \tag{2.94}$$

where R_i denotes the group rotation R in rep i. In a perhaps more familiar notation, the CGs above may be written

$$(\mathcal{O}_i)_{jk} = \left(\begin{array}{cc|c} \mathbf{x} & \mathbf{y} & \mathbf{z} \\ j & k & i \end{array} \right). \tag{2.95}$$

Note from Eq. (2.95) that the CG matrices for $\mathbf{R}_1 \otimes \mathbf{R}_2$ are simply the transposes of those for $\mathbf{R}_2 \otimes \mathbf{R}_1$, and thus are omitted below. The coefficients c below indicate multiplicative constants arbitrary in the definition Eq. (2.94). The CG coefficients for two singlet reps or any rep with $\mathbf{1}^0$ are all unity; the remaining CGs for products involving singlets are

$$\mathbf{1}^{t_1} \otimes \mathbf{2}^{t_2} = \mathbf{2}^{t_1+t_2}, \text{ with } \mathcal{O}_1 = c(1\ 0),\ \mathcal{O}_2 = c(0\ 1). \tag{2.96}$$

$$\mathbf{1}^{+} \otimes \mathbf{3} = \mathbf{3}, \text{ with } \mathcal{O}_1 = c(0\ 0\ 1),\ \mathcal{O}_2 = c(1\ 0\ 0),\ \mathcal{O}_3 = c(0\ 1\ 0). \tag{2.97}$$

$$\mathbf{1}^{-} \otimes \mathbf{3} = \mathbf{3}, \text{ with } \mathcal{O}_1 = c(0\ 1\ 0),\ \mathcal{O}_2 = c(0\ 0\ 1),\ \mathcal{O}_3 = c(1\ 0\ 0). \tag{2.98}$$

Next, let

$$\begin{aligned} M_3 &= \frac{1}{2}(1-i)\begin{pmatrix} 0 & 1 \\ 1 & 0 \end{pmatrix}, \quad M_4 = \begin{pmatrix} i & 0 \\ 0 & 0 \end{pmatrix}, \\ M_5 &= \begin{pmatrix} 0 & 0 \\ 0 & 1 \end{pmatrix}, \quad M_6 = \begin{pmatrix} 0 & 1 \\ -1 & 0 \end{pmatrix}. \end{aligned} \tag{2.99}$$

Then

$$\mathbf{2}^0 \otimes \mathbf{2}^0 \supset \mathbf{3},\ \ \mathbf{2}^{\pm} \otimes \mathbf{2}^{\mp} \supset \mathbf{3}:$$

$$\mathcal{O}_1 = cM_3,\ \ \mathcal{O}_2 = cM_4,\ \ \mathcal{O}_3 = cM_5. \tag{2.100}$$

$$\mathbf{2}^0 \otimes \mathbf{2}^0 \supset \mathbf{1}^0,\ \ \mathbf{2}^{\pm} \otimes \mathbf{2}^{\mp} \supset \mathbf{1}^0:$$

$$\mathcal{O} = cM_6. \tag{2.101}$$

$$\mathbf{2}^0 \otimes \mathbf{2}^+ \supset \mathbf{3},\ \ \mathbf{2}^- \otimes \mathbf{2}^- \supset \mathbf{3}:$$

$$\mathcal{O}_1 = cM_5,\ \ \mathcal{O}_2 = cM_3,\ \ \mathcal{O}_3 = cM_4. \tag{2.102}$$

$$\mathbf{2}^0 \otimes \mathbf{2}^+ \supset \mathbf{1}^+,\ \ \mathbf{2}^- \otimes \mathbf{2}^- \supset \mathbf{1}^+:$$

$$\mathcal{O} = cM_6. \tag{2.103}$$

$$\mathbf{2}^0 \otimes \mathbf{2}^- \supset \mathbf{3},\ \ \mathbf{2}^+ \otimes \mathbf{2}^+ \supset \mathbf{3}:$$

$$\mathcal{O}_1 = cM_4,\ \ \mathcal{O}_2 = cM_5,\ \ \mathcal{O}_3 = cM_3. \tag{2.104}$$

$$\mathbf{2}^0 \otimes \mathbf{2}^- \supset \mathbf{1}^-,\ \ \mathbf{2}^+ \otimes \mathbf{2}^+ \supset \mathbf{1}^-:$$

$$\mathcal{O} = cM_6. \tag{2.105}$$

The remaining combinations are:

$$\mathbf{2}^{0,\pm}\otimes\mathbf{3}\supset\mathbf{2}^{0,\pm}:$$

$$\mathcal{O}_1=c\begin{pmatrix}1&0&0\\0&1+i&0\end{pmatrix},\ \mathcal{O}_2=c\begin{pmatrix}0&0&1-i\\-1&0&0\end{pmatrix}. \tag{2.106}$$

$$\mathbf{2}^{0}\otimes\mathbf{3}\supset\mathbf{2}^{+},\ \mathbf{2}^{+}\otimes\mathbf{3}\supset\mathbf{2}^{-},\ \mathbf{2}^{-}\otimes\mathbf{3}\supset\mathbf{2}^{0}:$$

$$\mathcal{O}_1=c\begin{pmatrix}0&1&0\\0&0&1+i\end{pmatrix},\ \mathcal{O}_2=c\begin{pmatrix}1-i&0&0\\0&-1&0\end{pmatrix}. \tag{2.107}$$

$$\mathbf{2}^{0}\otimes\mathbf{3}\supset\mathbf{2}^{-},\ \mathbf{2}^{+}\otimes\mathbf{3}\supset\mathbf{2}^{0},\ \mathbf{2}^{-}\otimes\mathbf{3}\supset\mathbf{2}^{+}:$$

$$\mathcal{O}_1=c\begin{pmatrix}0&0&1\\1+i&0&0\end{pmatrix},\ \mathcal{O}_2=c\begin{pmatrix}0&1-i&0\\0&0&-1\end{pmatrix}. \tag{2.108}$$

$$\mathbf{3}\otimes\mathbf{3}\supset\mathbf{3}_s\oplus\mathbf{3}_a:$$

$$\begin{aligned}\mathcal{O}_1&=c_1\begin{pmatrix}2&0&0\\0&0&-1\\0&-1&0\end{pmatrix}+c_2\begin{pmatrix}0&0&0\\0&0&-1\\0&1&0\end{pmatrix},\\ \mathcal{O}_2&=c_1\begin{pmatrix}0&-1&0\\-1&0&0\\0&0&2\end{pmatrix}+c_2\begin{pmatrix}0&-1&0\\1&0&0\\0&0&0\end{pmatrix},\\ \mathcal{O}_3&=c_1\begin{pmatrix}0&0&-1\\0&2&0\\-1&0&0\end{pmatrix}+c_2\begin{pmatrix}0&0&1\\0&0&0\\-1&0&0\end{pmatrix}.\end{aligned} \tag{2.109}$$

$$\begin{aligned}\mathbf{3}\otimes\mathbf{3}\supset\mathbf{1}^{0}:&\quad \mathcal{O}=c\begin{pmatrix}1&0&0\\0&0&1\\0&1&0\end{pmatrix},\\ \mathbf{3}\otimes\mathbf{3}\supset\mathbf{1}^{+}:&\quad \mathcal{O}=c\begin{pmatrix}0&1&0\\1&0&0\\0&0&1\end{pmatrix},\\ \mathbf{3}\otimes\mathbf{3}\supset\mathbf{1}^{-}:&\quad \mathcal{O}=c\begin{pmatrix}0&0&1\\0&1&0\\1&0&0\end{pmatrix}.\end{aligned} \tag{2.110}$$

2.10 Conclusions

We have shown in this Chapter how to reproduce the quark and charged lepton Yukawa textures of the U(2) model using a *minimal* non-Abelian discrete symmetry, the double tetrahedral group T'. The first model we discuss, based on the discrete gauge symmetry $T' \times Z_3$, not only successfully accommodates the observed charged fermion masses and CKM angles, but also accounts for solar (small-angle MSW) and atmospheric neutrino oscillations. In particular, a large ν_μ-ν_τ mixing angle is predicted in the model, even though all charged fermion Yukawa textures are hierarchical. A global fit including neutrino parameters was performed in a grand unified version of the model, and results with extremely good χ^2 were obtained.

In addition, two variant T' models were discussed. In the first, the flavor group was extended to $T' \times Z_6$, and all important features of the SU(5)$\times$U(2) model were reproduced without the need for a field-theoretic unification. This model provided a successful prediction (with order-one uncertainty) of the bottom to top Yukawa coupling ratio, which is merely parameterized in the U(2) model and in the other T' models we discuss. The second variant theory was based on a global T' symmetry and demonstrates that the successful U(2) textures can be obtained without including an Abelian factor in the flavor group. In both variant models, large ν_μ-ν_τ mixing is predicted, and solutions to the solar and atmospheric neutrino problems are naturally obtained.

It is worth pointing out that the viable neutrino textures predicted by our models are achieved without altering the predictive textures of the charged fermions, and without introducing sterile neutrinos. Interestingly, the solutions we present have no simple analogy in the U(2) model: the right-handed neutrino fields in our models do not fill complete U(2) representations. In particular, the third generation ν_R transforms as a $\mathbf{1}^-$, which forms only *part* of a $\mathbf{5}$ in U(2). Aside from the possibility of very nonminimal U(2) models (e.g. with seven generations of right-handed neutrinos), the desired neutrino T' reps do not naturally occur. The key advantage of discrete groups is that the large, phenomenologically unused representations of the continuous embedding group break up into sets of small phenomenologically useful representations of the discrete group. If discrete gauge symmetries arise as fundamental symmetries of nature, then we see from the example of T' that their richer representation structure makes it possible to construct simple and elegant models of flavor.

Chapter 3
Bosonic Topcolor

3.1 Introduction

In spite of the quantitative success of the standard model, the mechanism of electroweak symmetry breaking remains unclear. Only a few years ago, bosonic technicolor models provided a relatively unconventional approach to solving this problem [47, 48, 49]: electroweak symmetry was broken dynamically by a fermion condensate triggered by new strong forces, while a fundamental scalar field was responsible for transmitting these effects to the fermions through ordinary Yukawa couplings. These models did not require a conventional extended technicolor sector, and hence were freed from the associated flavor changing neutral current (FCNC) problems. Unfortunately, precision electroweak constraints rule out bosonic technicolor models at least in models where the strong dynamics is QCD-like and the S-parameter can be reliably estimated [50].

In this Chapter, we point out that a very similar scenario, bosonic topcolor, also provides a very simple low-energy effective theory, but one that is not in conflict with electroweak constraints. In this scenario, electroweak symmetry is partly broken by new strong dynamics that affects fields of the third generation, as in conventional topcolor scenarios [51, 52], while a weakly-coupled scalar doublet transmits the symmetry breaking to the fermions via Yukawa couplings. Since this scenario involves both a fundamental (H) and a composite (Σ) Higgs field that both contribute to electroweak symmetry breaking, the usual problematic relation [51] between the dynamical top quark mass and the electroweak symmetry breaking scale is not obtained. The result is a viable two Higgs doublet model of type III, which we will show survives the bounds from flavor changing neutral current processes and may provide interesting flavor-changing signals as well.

The possibility of topcolor models involving fundamental scalars has been considered in Refs. [53, 54]. In these papers, however, the fundamental Higgs field was strongly coupled, and the authors considered whether the fundamental field itself could trigger the formation of a $t\bar{t}$ condensate. Here we introduce H as a weakly-coupled field and investigate the phenomenological consequences.

It is worth pointing out that a philosophical objection to the original bosonic technicolor scenarios, and the bosonic topcolor models described here, is that strong dynamics was originally intended to eliminate the need for a fundamental Higgs field altogether, as well as the associated problem with quadratic divergences. Recent theoretical developments relating to the possibility of low-scale quantum gravity [55] renders these objections hollow: The presence of a low string scale eliminates the conventional desert so that nonsupersymmetric low-energy theories with fundamental scalars are not unnatural. Moreover, in this setting there are new origins for the strong dynamics, namely the exchange of a nonperturbatively large number of gluon Kaluza-Klein excitations [56]. While we will not consider an explicit extra-dimensional embedding of the scenario described here, it seems that these considerations make the investigation of models with dynamical electroweak symmetry breaking and fundamental scalar fields well motivated.

In the next section we will present a simple realization of the bosonic topcolor idea following the Nambu-Jona-Lasinio approach [51]. Our first model is non-generic in the sense that we do not specify the most general set of higher-dimension operators that could appear in an arbitrary high-energy theory. However, it does provide a very convenient framework for parameterizing and exploring the basic phenomenological features of the scenario. After considering the phenomenological bounds, we will describe how to study the same type of scenario in a more general effective field theory approach. While we will not consider every phenomenological detail in this study, we hope to obtain an accurate overall picture of the allowed parameter space. Finally, we will discuss flavor changing signals for the model, notably a potential contribution to D^0-$\overline{D^0}$ mixing that can be as large as the current experimental bound. We then summarize our conclusions.

3.2 Minimal Bosonic Topcolor

Our high-energy theory is defined by

$$\mathcal{L} = \mathcal{L}_{\mathrm{H}} + \mathcal{L}_{\mathrm{NJL}} \ , \tag{3.1}$$

where

$$\mathcal{L}_{\mathrm{H}} = D_\mu H^\dagger D^\mu H - m_H^2 H^\dagger H - \lambda (H^\dagger H)^2 - h_t(\overline{\psi}_L H t_R + h.c.) \ , \tag{3.2}$$

and

$$\mathcal{L}_{\mathrm{NJL}} = \frac{\kappa}{\Lambda^2} \overline{\psi}_L t_R \bar{t}_R \psi_L \ . \tag{3.3}$$

The field H is a fundamental scalar doublet, and Λ characterizes the scale at which new physics is present that generates the nonrenormalizable interaction in Eq. (3.3). In light of our introductory remarks, we will assume henceforth that $\Lambda \lesssim 100$ TeV. In this minimal scenario we assume that the right-handed top, and left-handed top-bottom doublet ψ_L experience the new strong interactions. Immediately beneath the scale Λ we may rewrite Eqs. (3.2) and (3.3) as

$$\begin{aligned}\mathcal{L} &= D_\mu H^\dagger D^\mu H - m^2 H^\dagger H - \lambda \left(H^\dagger H\right)^2 - c\Lambda^2 \Sigma^\dagger \Sigma \\ &\quad -h_t(\bar{\Psi}_L t_R H + h.c.) - g_t(\bar{\Psi}_L t_R \Sigma + h.c.)\end{aligned} \tag{3.4}$$

where Σ is a non-propagating auxiliary field. Using the equations of motion, $\Sigma = -g_t(\bar{t}_R \psi_L)/(c\Lambda^2)$ and one recovers Eqs. (3.2) and (3.3) with the identification $\kappa = g_t^2/c$.

At energies $\mu \ll \Lambda$, quantum corrections induce a kinetic term for Σ, so that it becomes a dynamical field, a composite Higgs doublet in the low-energy theory. In order to study the quantum corrections to Eq. (3.4) it is convenient for us to define the column vector

$$\Phi = \begin{pmatrix} \Sigma \\ H \end{pmatrix} . \tag{3.5}$$

Then the kinetic term at the scale μ may be written $\partial_\mu \Phi^\dagger Z \partial^\mu \Phi$, with

Then the kinetic term at the scale μ may be written $\partial_\mu \Phi^\dagger Z \partial^\mu \Phi$, with

$$Z = \begin{pmatrix} \frac{g_t^2 N_C \ln(\Lambda/\mu)}{8\pi^2} & \frac{g_t h_t N_C \ln(\Lambda/\mu)}{8\pi^2} \\ \frac{g_t h_t N_C \ln(\Lambda/\mu)}{8\pi^2} & 1 + \frac{h_t^2 N_C \ln(\Lambda/\mu)}{8\pi^2} \end{pmatrix} \approx \begin{pmatrix} \frac{1}{r^2} & 0 \\ 0 & 1 \end{pmatrix} . \tag{3.6}$$

In [illegible] terms assume the canonical form. However, in most of the parameter space that we consider later in this Chapter h_t is small enough that the off-diagonal elements of Z are numerically irrelevant; thus we use the simpler approximate form parameterized by r in Eq. (3.6). Properly normalized kinetic terms are then obtained via the substitution $\Sigma \to r\Sigma$. Quantum corrections also induce quartic self interactions, and mixing in the Φ mass matrix. We retain the largest self-coupling, $(\Sigma^\dagger\Sigma)^2$ with coefficient $\lambda_\Sigma = g_t^4 N_C \ln(\Lambda/\mu)/(4\pi^2)$; the Φ mass matrix is given by

$$\mathcal{L}_{mass} = -\Phi^\dagger \mathcal{M}^2 \Phi , \tag{3.7}$$

with

$$\mathcal{M}^2 = \begin{pmatrix} r^2 m_\Sigma^2 & r\delta m^2 \\ r\delta m^2 & m_H^2 \end{pmatrix}, \tag{3.8}$$

where $\delta m^2 = -\frac{N_c}{8\pi^2} g_t h_t \Lambda^2$. Eq. (3.8) reflects the fact that both the diagonal and off-diagonal entries receive quadratically divergent radiative corrections. For the diagonal elements, the tree-level mass terms present in Eq. (3.4) can be fine-tuned against these radiative corrections (as in the standard model) so that m_Σ and m_H are well beneath the cutoff scale Λ. On the other hand, there is no tree-level $H\Sigma$ mass mixing term given the way we defined our high-energy theory in Eqs. (3.2)-(3.3). However, since we are considering the situation where the scale Λ is relatively low ($<$ 100 TeV) and where the coupling h_t is small (see Figs. 3.1 and 3.2), the off-diagonal elements will also be much smaller than the cut off. For the case where such tree-level mass mixing is present at the scale Λ, the reader should refer to Section 3. Electroweak symmetry will be broken in this model if Σ and/or H acquire vacuum expectation values (vevs). There are several ways this can happen depending on the values of the different parameters in the model. We are principally interested in the case where $m_H^2 > 0$, so that electroweak symmetry breaking is triggered by the strong dynamics and the vev of H can be interpreted as a subsidiary effect. Thus, it is necessary to study the scalar potential,

$$\begin{aligned} V(\Sigma, H) &= r^2 m_\Sigma^2 \Sigma^\dagger \Sigma + m_H^2 H^\dagger H + r\delta m^2 \left(\Sigma^\dagger H + h.c.\right) \\ &\quad + \lambda \left(H^\dagger H\right)^2 + \lambda_\Sigma r^4 \left(\Sigma^\dagger \Sigma\right)^2 . \end{aligned} \tag{3.9}$$

Rather than search directly for minima in a five-dimensional parameter space (m_Σ^2, m_H^2, δm^2, λ, λ_Σ) we extremize the potential and solve for m_Σ^2 and m_H^2 in terms of the Σ and H vevs. It is much more manageable to study the remaining constrained three-dimensional parameter space and determine which points correspond to stable local minima. If we denote the vevs of Σ and H by $v_1/\sqrt{2}$ and $v_2/\sqrt{2}$, one finds

$$m_\Sigma^2 = -\frac{1}{rv_1}\left(\delta m^2 v_2 + \lambda_\Sigma r^3 v_1^3\right) , \tag{3.10}$$

$$m_H^2 = -\frac{1}{v_2}\left(\delta m^2 r v_1 + \lambda v_2^3\right) . \tag{3.11}$$

From Eq. (3.9), one may obtain the mass matrices for the scalars, pseudoscalars, and charged scalars:

$$M_S = \frac{1}{2}\begin{pmatrix} m_\Sigma^2 r^2 + 3\lambda_\Sigma r^4 v_1^2 & \delta m^2 r \\ \delta m^2 r & m_H^2 + 3\lambda v_2^2 \end{pmatrix} , \tag{3.12}$$

$$M_P = \frac{1}{2}\begin{pmatrix} m_\Sigma^2 r^2 + \lambda_\Sigma r^4 v_1^2 & \delta m^2 r \\ \delta m^2 r & m_H^2 + \lambda v_2^2 \end{pmatrix} , \tag{3.13}$$

$$M_+ = \begin{pmatrix} m_\Sigma^2 r^2 + \lambda_\Sigma r^4 v_1^2 & \delta m^2 r \\ \delta m^2 r & m_H^2 + \lambda v_2^2 \end{pmatrix} . \tag{3.14}$$

The Higgs field vevs are responsible for producing the proper gauge boson masses, *i.e.*

$$v_1^2 + v_2^2 = (246 \text{ GeV})^2 , \tag{3.15}$$

as well as the mass of the top quark

$$m_t = (rg_t v_1 + h_t v_2)/\sqrt{2} . \tag{3.16}$$

This expression shows that the top quark receives both an ordinary and a dynamical contribution. Since we focus on small values of h_t in this Chapter, the top quark mass is mostly dynamical, originating from the first term in Eq. (3.16). In this limit, the vevs v_1 and v_2 are determined by the choice of scales Λ and μ, since the quantity rg_t is independent of g_t.

3.3 Phenomenology

Notice that all the freedom in Eqs. (3.10)-(3.14) is fixed by specifying Λ, μ, h_t and λ. Thus, for a fixed choice of $\Lambda < 100$ TeV and μ of order the weak scale, we may map our results onto the λ-h_t plane. Fig. 3.1 displays results for $\Lambda = 10$ TeV and Fig. 3.2 for $\Lambda = 100$ TeV, with $g_t = 1$. In each case, the intersecting solid lines indicate where m_Σ^2 or m_H^2 change sign, with positive values lying above the corresponding line. Figs. 3.1a and 3.2a provide mass contours for the lightest neutral scalar and charged scalar states; Figs. 3.1b and 3.2b display constant contours for the electroweak parameters S and T. These were computed using formulae available in the literature for general two Higgs doublet models [57],

$$\begin{aligned} S &= \frac{1}{12\pi}\left(s^2_{\alpha-\beta}\left[\ln\frac{M_2^2}{M_H^2} + g(M_1^2, M_3^2) - \frac{1}{2}\ln\frac{M_+^2}{M_1^2} - \frac{1}{2}\ln\frac{M_+^2}{M_3^2}\right]\right. \\ &\quad \left. + c^2_{\alpha-\beta}\left[\ln\frac{M_1^2}{M_H^2} + g(M_2^2, M_3^2) - \frac{1}{2}\ln\frac{M_+^2}{M_2^2} - \frac{1}{2}\ln\frac{M_+^2}{M_3^2}\right]\right), \end{aligned} \tag{3.17}$$

and

$$\begin{aligned} T &= \frac{3}{48\pi s^2 m_W^2}\left(s^2_{\alpha-\beta}\left[f(M_1^2, M_+^2) + f(M_3^2, M_+^2) - f(M_1^2, M_3^2)\right]\right. \\ &\quad \left. + c^2_{\alpha-\beta}\left[f(M_2^2, M_+^2) + f(M_3^2, M_+^2) - f(M_2^2, M_3^2)\right]\right), \end{aligned} \tag{3.18}$$

where M_1, M_2, M_3, and M_+ are the light scalar, heavy scalar, pseudoscalar, and charged scalar masses respectively, and $\beta = \tan^{-1}(v_2/v_1)$. The scalar mixing angle α and the functions f and g are defined in Ref. [57]. Figs. 3.3c and 2c show regions excluded by (i) the current LEP bound on neutral Higgs production, (ii) bounds on the S and T parameters, (iii) bounds on the charged scalar mass from $b \to s\gamma$. In the first case, we compute the production cross section for the lightest scalar state ϕ_s,

$$\sigma(e^+e^- \to Z\phi_s) = s^2_{\alpha-\beta}\sigma_{SM}(e^+e^- \to ZH^0) \tag{3.19}$$

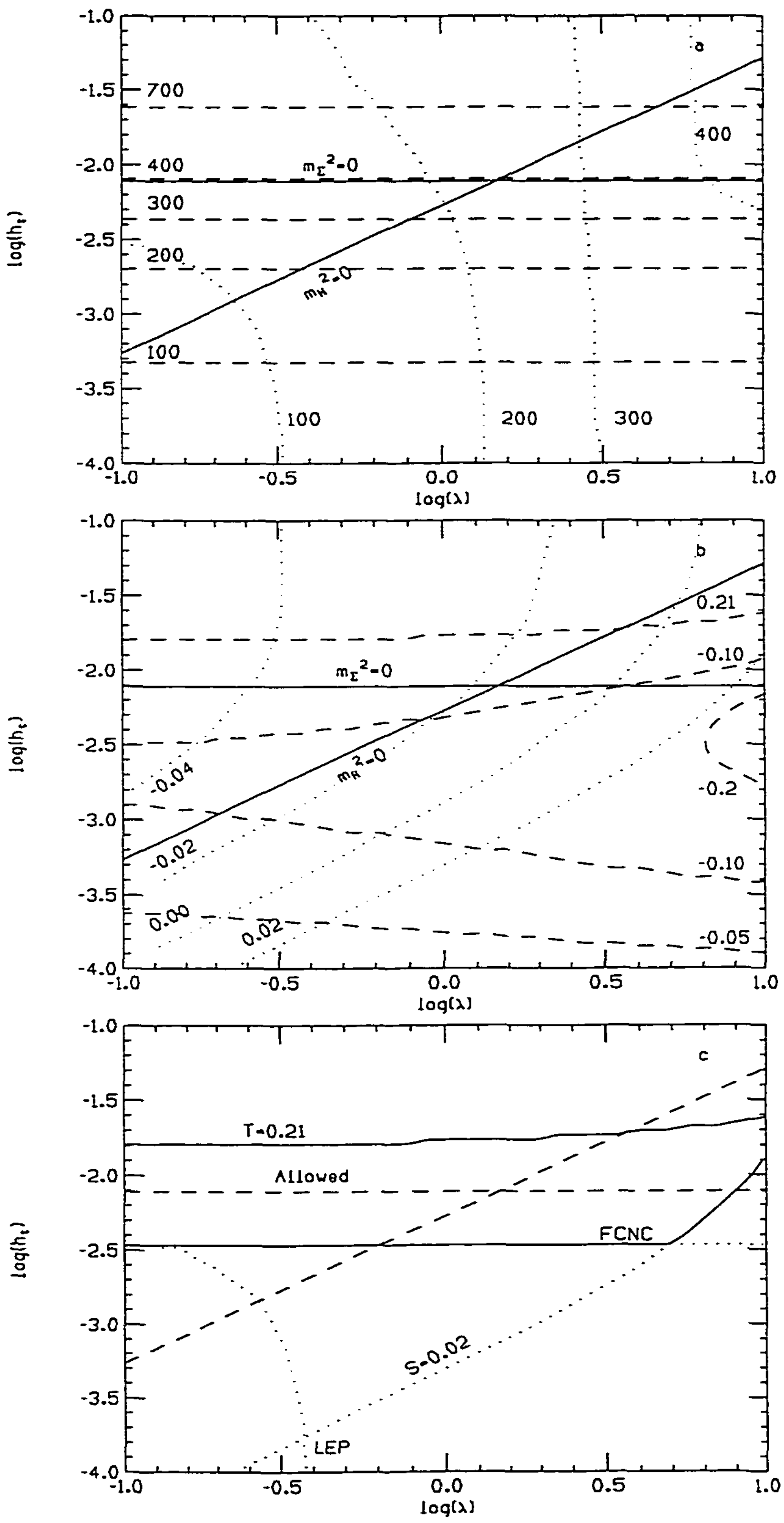

Figure 3.1 Minimal model, $\Lambda = 10$ TeV.(a) Neutral (dashed) and charged (dotted) mass contours, units of GeV, (b) S (dotted) and T (dashed) parameter contours, (c) Exclusion regions.

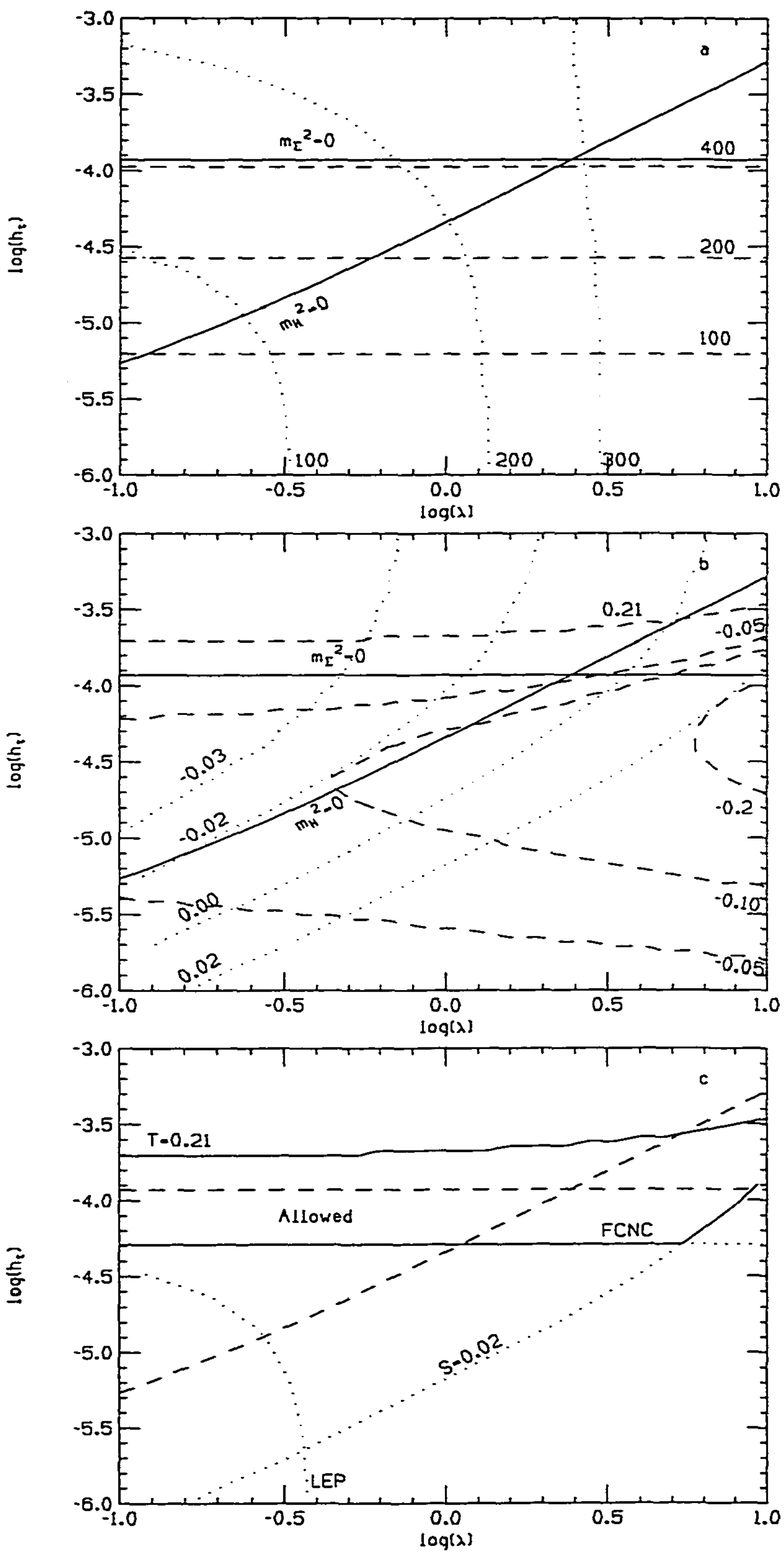

Figure 3.2 Same as Fig. 3.1, with $\Lambda = 100$ TeV.

and compare to the corresponding standard model cross section for a Higgs boson with mass equal to the current LEP bound, $m_H < 107.9$ GeV, 95% CL [58]. In the case of the S and T bounds, we consider the results of global electroweak fits quoted in the Review of Particle Properties [1], $S = -0.26 \pm 0.14$ and $T = -0.11 \pm 0.16$ [50], which assume a reference Higgs mass of 300 GeV. We show the two standard deviation limit contours for S and T separately wherever an upper or lower limit is exceeded. (Note that we don't take into account correlations between S and T in determining this exclusion region.) Finally, we plot the charged Higgs mass limit $m_{H^+} > [244 + 63/(\tan\beta)^{1.3}]$ GeV from $b \to s\gamma$ [59]. This is the strongest, albeit indirect, charged Higgs mass limit listed in Ref. [1]. Although, strictly speaking, this bound applies to a type II two-Higgs doublet model, the leading top quark loop contribution is the same in our model; the top quark-charged scalar coupling is given by

$$\begin{aligned} \Phi^+ \frac{g}{2\sqrt{2}M_W} & \left[\bar{t}(m_t^H \cot\beta - m_t^\Sigma \tan\beta) V_{tq} (1-\gamma^5) q \right. \\ & - \left. \bar{t} \cot\beta V_{tq} m_q^H (1+\gamma^5) q \right] \end{aligned} \tag{3.20}$$

in the case where the Cabibbo-Kobayashi-Maskawa (CKM) matrix V originates from diagonalization of the down quark Yukawa matrix alone (the reason for this assumption is given in the following section). Here m_t^H and m_t^Σ refer to contributions to the top mass from the H and Σ vevs, respectively. For most of the parameter range of interest to us, $m_t^H \ll m_t^\Sigma$ and the interaction in Eq. (3.20) reduces to that of a type II model, and the $b \to s\gamma$ bound is approximately valid. In both Figs. 3.1 and 3.2 a rectangular region is shown in which the charged scalars are heavy enough to weaken the flavor changing neutral current bounds, without exceeding that of the T parameter.

3.4 Flavor Changing Signals

The fact that one of our two Higgs doublets (Σ) couples preferentially to the top quark leads to a potentially interesting source of flavor violation in the model. While the charge $-1/3$ quark masses and neutral scalar interactions both originate via couplings to H (and hence are simultaneously diagonalizable), the same is not true in the charge 2/3 sector, where the mass matrix depends on both the H and Σ vevs,

$$M^U = Y_\Sigma^U \frac{v_1}{\sqrt{2}} + Y_H^U \frac{v_2}{\sqrt{2}} \ . \tag{3.21}$$

For concreteness, let us consider a definite Yukawa texture:

$$M^U = \begin{pmatrix} 0 & 0 & 0 \\ 0 & 0 & 0 \\ 0 & 0 & rg_t \end{pmatrix} \frac{v_1}{\sqrt{2}} + \begin{pmatrix} \lambda^8 & \lambda^5 & \lambda^3 \\ \lambda^5 & \lambda^4 & \lambda^2 \\ \lambda^3 & \lambda^2 & h_t \end{pmatrix} \frac{v_2}{\sqrt{2}} \ . \tag{3.22}$$

Here $\lambda = 0.22$ is the Cabibbo angle, and we have picked a symmetric texture for the fundamental Higgs Yukawa couplings that approximately reproduces the correct CKM angles. Dropping the factors of $v_i/\sqrt{2}$, the matrices shown give the neutral scalar couplings in our original field basis. In the quark (and Higgs) mass eigenstate basis, there will be flavor-changing top and charm quark interactions. Here, we focus only on the latter. CKM-like rotations that diagonalize the mass matrices yield 1-2 neutral scalar couplings of order λ^5. It is straightforward to estimate the contribution to D^0-$\overline{D^0}$ mixing,

$$|\frac{\Delta m_D}{m_D}|_{\rm new} \approx \lambda^{10} \frac{f_D^2}{12 M_\phi^2} \left[-1 + 11 \frac{m_D^2}{(m_c + m_u)^2} \right] \ . \tag{3.23}$$

For $f_D \approx 200$ MeV, this contribution saturates the current experimental bound, $\Delta m_D < 1.58 \times 10^{-10}$ MeV [1], for $M_\phi \lesssim 495$ GeV. The reason that we do not include this as a bound is that the 1-2 neutral scalar couplings need not be $O(\lambda^5)$; they could in principle be zero, if the CKM matrix results from the diagonalization of the down quark Yukawa matrix alone. Since this is the least constrained possibility, we adopted this assumption in Eq. (3.20) for computing the $b \to s\gamma$ exclusion region. Generically, however, we see that bosonic topcolor models predict significant contributions to D^0-$\overline{D^0}$ mixing, potentially as large as the current experimental bound.

3.5 Generalizations

The scenario described in the previous section is particularly convenient in that the basic phenomenology can be described in a two-dimensional parameter space, for fixed Λ and μ. However, a realistic high-energy theory is likely to provide more than the single higher-dimension operator in Eq. (3.3). In this section we briefly describe the effective field theory approach for constructing the most general low-energy effective bosonic topcolor theory. Given our assumption that ψ_L and t_R experience the new strong dynamics, the strongly-coupled sector of the theory possesses a global symmetry $G =$SU(2)$_L\times$U(1)$_R$, that is spontaneously broken by the $t\bar{t}$ condensate to the U(1) that counts top quark number. If we denote the elements of this SU(2)$\times$U(1) by U and V, respectively, then the transformation properties of the fields are given by

$$\psi_L \to U\psi_L, \qquad t_R \to Vt_R, \qquad \text{and} \qquad \Sigma \to U\Sigma V^\dagger \ , \tag{3.24}$$

where V is a phase. The Yukawa couplings of the fundamental Higgs field explicitly break G, so we may treat h_tH as a 'spurion' transforming as

$$h_tH \to U(h_tH)V^\dagger \ . \tag{3.25}$$

We may now include $h_t H$ systematically in an effective Lagrangian by forming all possible G-invariant terms. At the renormalizable level,

$$
\begin{aligned}
\mathcal{L}_{eff} &= D^\mu H^\dagger D_\mu H + D^\mu \Sigma^\dagger D_\mu \Sigma \\
&- m_H^2 H^\dagger H - m_\Sigma^2 \Sigma^\dagger \Sigma + m_{H\Sigma}^2 h_t (H^\dagger \Sigma + h.c.) \\
&- \lambda (H^\dagger H)^2 - \lambda_0 (\Sigma^\dagger \Sigma)^2 + h_t (h^\dagger \Sigma) \Sigma^\dagger \Sigma + \cdots \\
&- h_t \overline{\psi}_L H t_R - g_\Sigma \overline{\psi}_L \Sigma t_R + h.c. \ . \qquad (3.26)
\end{aligned}
$$

Note that we have eliminated a possible kinetic mixing term by field redefinitions, which do not affect the form of the other terms. The $\cdots$ represent all the other possible quartic terms which are higher order in h_t. Unlike the model described in the previous section, we no longer have a boundary condition at the scale Λ that sets $\lambda_0(\Lambda) = 0$ and $m_{H\Sigma}^2(\Lambda) = 0$, thus introducing two additional degrees of freedom into the scalar potential. Since we are now working directly with the low-energy theory, the scale Λ is not input directly, but rather can be computed by determining the scale at which the wavefunction renormalization of the Σ field vanishes. At this scale, Σ again becomes an auxiliary field, and may be eliminated using the equations of motion, leaving a more general set of higher-dimension operators than we had assumed originally in Eq. (3.3).

A complete investigation of the parameter space of this generalized model is beyond the scope of this study. Before closing, we point out that there are reasonable parameter choices in Eq. (3.26) where the resulting phenomenology is similar to the minimal model considered in Section 2. In Fig. 3.3 we provide the same information given in Figs. 3.1 and 3.2 for the general bosonic topcolor model, with $m_{H\Sigma}^2 = (400 \text{ GeV})^2$ and $\lambda_0 = 1$. It is interesting that in this case the allowed band delimited by the FCNC and T parameter lines lies mostly in the region where both

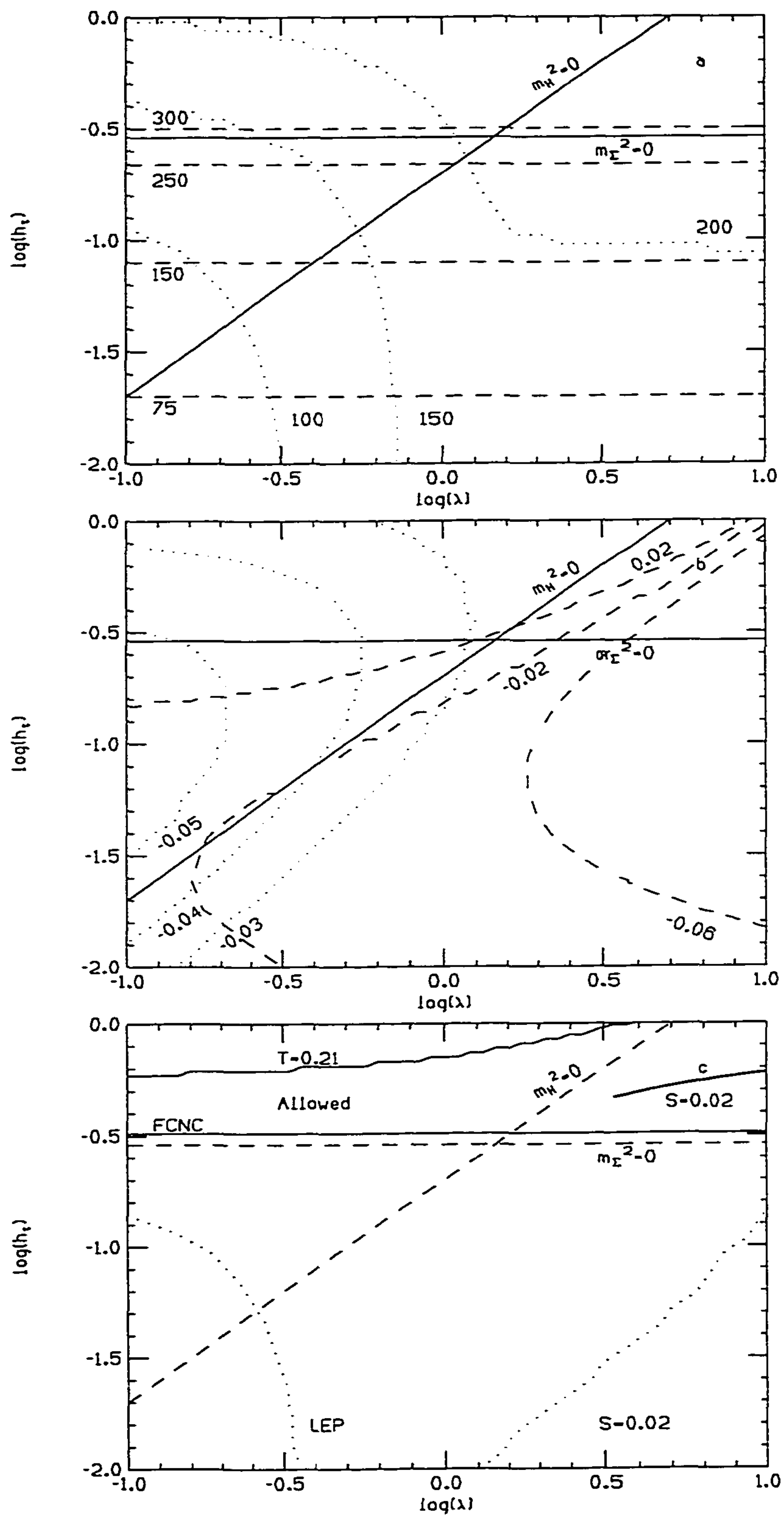

Figure 3.3 General model, $m_{H\Sigma}^2 = (400\text{ GeV})^2$, $\lambda_0 = 1$. Notation is the same as in Figs. 3.1 and 3.2.

m_Σ^2 and m_H^2 are positive; in this region the mixing term in Eq. (3.8) drives one of the scalar mass squared eigenvalues negative so that electroweak symmetry is broken. A full exploration of this parameter space will be provided elsewhere [60].

3.6 Conclusions

In this Chapter, we have described models in which electroweak symmetry breaking is triggered by strong dynamics affecting the third generation but transmitted to the fermions by a weakly-coupled, fundamental Higgs doublet. We have argued in Section 3.1 that such models are not unnatural given recent developments in low-scale quantum gravity. Our minimal scenario, while probably not representing the ultimate high-energy theory, has the virtue of allowing a simple parameterization of the basic phenomenology of the model. It is our hope that others will adopt it as the basis for further phenomenological study. Issues that one could address include relaxation of our small h_t approximation, flavor-changing top quark processes, and the collider physics of the model. We also described how the scenario may be generalized using effective field theory techniques. Unlike bosonic technicolor models, bosonic topcolor is not excluded by current phenomenological bounds. Moreover, the model has interesting flavor-changing signals such as a contribution to D^0-$\overline{D^0}$ mixing that could be as large as current experimental bounds.

Chapter 4

Limits on a Light Leptophobic Gauge Boson

4.1 Introduction

In the past few years, the possibility of new leptophobic gauge bosons has been explored as a means of explaining apparent discrepancies in electroweak observables measured with high precision at LEP [61, 62], as well as an apparent high E_T excess in the inclusive dijet spectrum at the Tevatron [63]. While for the most part these anomalies have since gone away, the possibility remains that a Z-prime boson (Z') coupling mostly to quarks and with a mass smaller than m_Z could exist while evading experimental detection [64, 65, 66]. Given the assumptions that (1) the leptons are not charged under the new U(1) gauge interaction, and (2) the couplings to quarks are generation independent (to avoid large flavor-changing neutral current effects) then the normalization of the U(1) can be chosen so that the Z' couples precisely to baryon number. Anomaly cancellation can be achieved at the expense of introducing new exotic states. Two explicit examples of viable, anomaly-free models were presented in Refs. [64, 65], and these models presumably don't exhaust the possible ways in which anomalies can be cancelled. Therefore, we will set model-building issues aside and focus instead on the phenomenology of the Z'. This is of timely interest given the recent stringy suggestion that the Planck scale and weak scale might be identified [67, 68]. In these scenarios, the dimension-5 baryon and lepton number violating operators that arise generically at the string scale would only be suppressed by a TeV, and hence would be phenomenologically lethal. Barring a higher-dimensional solution to the proton decay problem [68], additional gauge symmetries could provide a more prosaic, though equally effective, resolution.

In Ref. [65], a specific mechanism was proposed for maintaining leptophobia in models with gauged baryon number, and we will adopt this mechanism here. The reason that leptophobia is not automatic is that the baryon number and hypercharge gauge fields mix via their kinetic terms

$$\mathcal{L}_{kin} = -\frac{1}{4}(F_Y^{\mu\nu}F_{\mu\nu}^Y + 2cF_B^{\mu\nu}F_{\mu\nu}^Y + F_B^{\mu\nu}F_{\mu\nu}^B) \ . \tag{4.1}$$

We assume there are no Higgs fields that carry both baryon number and electroweak quantum numbers, so that mass mixing terms are not present. Below the electroweak symmetry breaking scale, there are separate kinetic mixing parameters for the photon and Z, which we will call c_γ and c_Z, respectively. In order that leptophobia be preserved, c_γ and c_Z must be sufficiently small at experimental energies. This can be arranged if the parameter c is forced to zero at some high scale Λ, so that c_γ and c_Z are only generated at the one-loop level, via renormalization group running. The boundary condition $c(\Lambda) = 0$ can be achieved, for example, by embedding $U(1)_B$ into a non-Abelian group, as was shown explicitly in Ref. [65]. Here we will be more general and not assume the specific mechanism for achieving this boundary condition. Thus, the boundary condition, together with assumptions (1) and (2) given above, define a class of models that we will consider further in the present analysis.

In Ref. [65], the Z' mass range $m_\Upsilon < m_B < m_Z$ was studied, primarily because the coupling α_B could be taken as large as ~ 0.1 at points within this interval, without conflicting with the experimental bounds. Possible high energy collider signatures were then considered. Here we will focus instead on Z' masses between ~ 1 GeV and m_Υ, with the initial goal of determining how tightly we can bound the parameter space of the model. Although the coupling α_B cannot be as large as 0.1 within this mass range, we will show that current experiment does allow it to be comparable to $\alpha_{EM} \approx 1/137$. Given this result, we consider the possibility of detecting the Z' at charm and bottom meson factories via the decays of various quarkonium states which would be plentifully produced. We will not consider smaller values of m_B, but instead refer the interested reader to the discussion in Ref [69].

This Chapter is organized in two parts. We will first discuss the current bounds on the parameter space of the model. With the boundary condition on the kinetic mixing terms described above, both the hadronic and leptonic signatures of the Z' are completely determined by its mass, m_B, and gauge coupling $g_B = \sqrt{4\pi\alpha_B}$. Therefore, these bounds can be translated into boundaries of excluded regions on a two-dimensional mass-coupling plane. We will then consider possible discovery signals for a Z' living within these allowed regions.

4.2 Parameter Space

Most of the important phenomenological bounds follow directly from the Z-prime's gauge coupling to quarks. In addition, we take into account the small kinetic mixing effects by treating the mixing term in $\mathcal{L}_{kin}$ as a perturbative interaction. The Feynman rules corresponding to the $Z' - \gamma$ and $Z' - Z$ vertices are

$$-ic_\gamma \cos\theta_w (p^2 g^{\mu\nu} - p^\mu p^\nu), \tag{4.2}$$

and

$$ic_Z \sin\theta_w (p^2 g^{\mu\nu} - p^\mu p^\nu), \tag{4.3}$$

respectively, where $c_\gamma = c_Z = c$ above the electroweak scale, and where $c = 0$ at some ultraviolet cutoff Λ. We will initially set $\Lambda = m_{top} \approx 180$ GeV, since this is probably the lowest scale at which the new physics responsible for the boundary condition $c(\Lambda) = 0$ might itself remain undetected. We will describe how our results change with different choices for Λ as needed. Note that choosing a somewhat higher value for Λ, for example 500 GeV, has only a small effect on the mixing since the dependence on Λ is only logarithmic.

At any desired renormalization scale μ, we may rewrite $c_\gamma(\mu)$ and $c_Z(\mu)$ as an explicit function of α_B by solving the one-loop renormalization group equations. These equations follow from the one quark-loop diagrams that connects the Z' to the γ and Z, respectively [65]:

$$\mu\frac{\partial}{\partial\mu}c_\gamma(\mu) = -\frac{2}{9\pi}\frac{\sqrt{\alpha_B\alpha}}{c_w}[2N_u - N_d] \tag{4.4}$$

and

$$\mu\frac{\partial}{\partial\mu}c_Z(\mu) = -\frac{1}{18\pi}\frac{\sqrt{\alpha_B\alpha}}{s_w^2 c_w}[3(N_d - N_u) + 4(2N_u - N_d)s_w^2] \; . \tag{4.5}$$

Here c_w (s_w) represents the cosine (sine) of the weak mixing angle, α is the electromagnetic fine structure constant, and N_u (N_d) is the numbers of charge 2/3 ($-1/3$) quarks that are lighter than the renormalization scale. It is straightforward to show, for example

$$c_\gamma(m_b) = 0.033\sqrt{\alpha_B} \qquad c_Z(m_b) = 0.116\sqrt{\alpha_B}$$

$$c_\gamma(m_c) = 0.047\sqrt{\alpha_B} \qquad c_Z(m_c) = 0.130\sqrt{\alpha_B} \tag{4.6}$$

We will use expressions like these to translate bounds on leptonic processes to exclusion regions on the m_B-α_B plane.

The experimental bounds on the model from hadronic decays are summarized in Fig. 4.1. Beginning with the $\Upsilon(1S)$, the new contribution to the hadronic decay width is given by [64]

$$\Delta R_\Upsilon = \frac{4}{3}\left[\frac{\alpha_B}{\alpha}\frac{m_\Upsilon^2}{m_B^2 - m_\Upsilon^2} + \left(\frac{\alpha_B}{\alpha}\frac{m_\Upsilon^2}{m_B^2 - m_\Upsilon^2}\right)^2\right] \; , \tag{4.7}$$

where $R_\Upsilon \equiv \Gamma(\Upsilon \to \text{hadrons})/\Gamma(\Upsilon \to \mu^+\mu^-)$, and the interference with s-channel photon exchange is included. The most stringent bound on this quantity follows from an ARGUS limit on the non-electromagnetic (NE) contribution to the $\Upsilon(1S) \to 2$ jets branching fraction [70],

$$BF(\Upsilon(1S) \to 2\,\text{jets},\ \text{NE}) < 0.053 \quad (95\%\ \text{CL}) \; ,$$

which we find corresponds to $\Delta R_\Upsilon < 2.48$. This bound is stronger than the one obtained from the $\Upsilon(1S)$ hadronic width, discussed in Ref. [64]. Note that we have chosen to restrict Fig. 4.1 to values of the coupling $\alpha_B > 10^{-3}$, where direct experimental detection of the Z' via rare decays might be feasible. With this choice, finite width effects omitted from Eq. (4.7) have a negligible effect on the segments of the exclusion curves shown.

We may place additional bounds on the parameter space of the model by considering the hadronic decay widths of the $\Upsilon(2S)$ and $\Upsilon(3S)$ respectively. Since no direct experimental bounds exist on the non-electromagnetic, two jet branching fraction, we compare $R_{\Upsilon(2S)}$ and $R_{\Upsilon(3S)}$ to the perturbative QCD prediction [71],

$$R = \frac{10(\pi^2 - 9)}{9\pi}\frac{\alpha_s^3}{\alpha^2}\left(1 + \frac{\alpha_s}{\pi}\left\{-18.2 + \frac{3}{2}\beta_0[1.161 + \ln(\frac{2\mu}{m_\Upsilon})]\right\}\right) \tag{4.8}$$

where $\beta_0 = 11 - 2n_f/3 = 23/3$. We evaluate this expression using $\alpha_s(m_b)$ as determined from the world average value $\alpha_s(m_Z) = 0.119 \pm 0.002$ [1]. We extract the

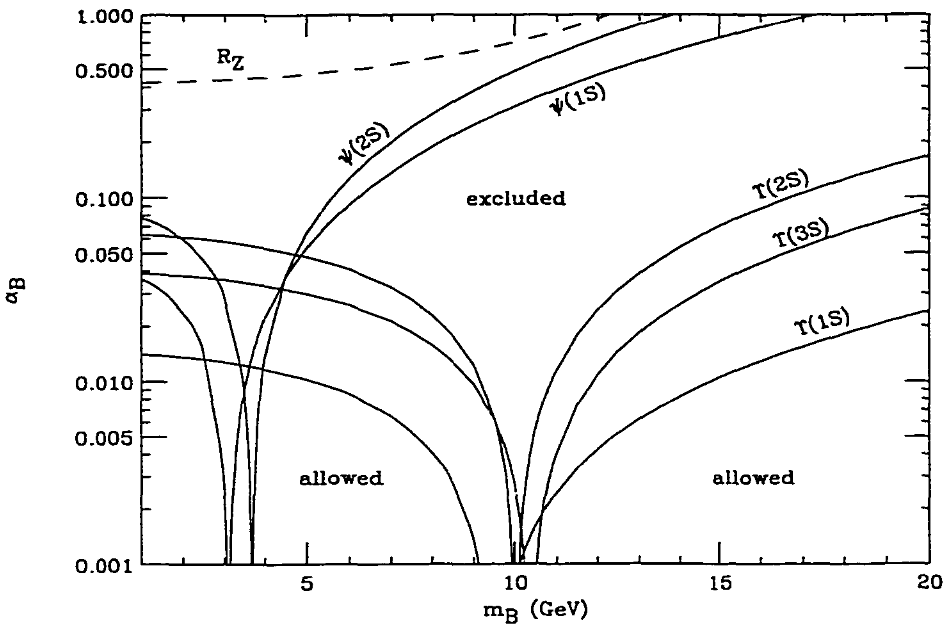

Figure 4.1 Bounds from hadronic decays.

experimental values of R from branching fraction data in the 1998 Review of Particle Properties [1]. This is straightforward, except in the case of the $\Upsilon(3S)$, where the branching fraction to $\mu^+\mu^-$ has not been measured. We assume in this case that $\Gamma(\mu^+\mu^-)$ is approximately equal to $\Gamma(e^+e^-)$, which has been measured. Taking into account experimental uncertainties, we find $\Delta R \lesssim 92$ and $\Delta R \lesssim 33$ for the $\Upsilon(2S)$ and $\Upsilon(3S)$ respectively, at the 95% confidence level. Although these bounds are weak, they nonetheless exclude some additional region of the parameter space immediately around the resonance masses.

Similar bounds may be determined from the hadronic decay widths of the J/ψ and the $\psi(2S)$. Here, however, it is not so straightforward to determine the standard model expectation. The perturbative QCD prediction for the gluonic decay width in Eq. (4.8) is derived in a nonrelativistic bound state approximation, and is therefore subject to $O(v^2/c^2)$ corrections, which are expected to be significant. Therefore, we will use the results of a recent relativistic potential model analysis [72] as as our standard model expectation. In Ref. [72], the J/ψ hadronic decay width was used to extract $\alpha_s(m_c)$, yielding 0.29 ± 0.02. Comparing to the world average value, we find that the difference $\Delta\alpha_s(m_c) < 0.068$ can be tolerated, allowing two-standard deviation uncertainties. Thus, any new contribution to R_ψ is bounded by $\Delta R \lesssim 3(\Delta\alpha_s/\alpha_s)R \approx 34$, yielding the contour shown in Fig. 4.1. We determine the gluonic contribution to $R_{\psi(2S)}$ from branching fraction data in the Review of Particle Physics [1], and obtain $R_g = 123.6 \pm 27.3$. Since this is so large and uncertain, the bound on the model's parameter space will clearly be weak. Thus, we simply compare $R_{\psi(2S)}$ to the perturbative QCD prediction, including a theoretical uncertainty comparable in size to the relativistic corrections in the J/ψ case; we find $\Delta R \lesssim 162$, yielding the curve shown.

Finally, Fig. 4.1 displays the bound from the hadronic decay width of the Z, labelled R_Z, which we find provides the strongest constraint from the Z-pole observables. This result includes the contributions from (i) direct Z' production $Z \to q\bar{q}Z'$, (ii) the $Zq\bar{q}$ vertex correction, and (iii) the $Z - Z'$ mixing. These contributions were discussed in detail in Refs. [64, 65], using old LEP data, and here we simply include an updated bound. We will say nothing further on this point, since the corresponding exclusion curve is superceded by the others shown in Fig. 4.1.

Other bounds on the parameter depend more crucially on the kinetic mixing. We consider (i) the e^+e^- cross section to hadrons, (ii) deep inelastic scattering, and (iii) the muon anomalous magnetic moment. In each case, however, we find that the constraints on the model are always weaker than those presented in Fig. 4.1. Let us briefly consider these topics in turn:

The contribution of the Z' to $R = \sigma(e^+e^- \to \text{hadrons})/\sigma(e^+e^- \to \mu^+\mu^-)$ was considered in Ref. [65], and was bounded by the two-standard deviation uncertainty in the experimental data, using a compilation of the experimental data points. While this is a reasonable approximation, it does not take into account that a tighter bound on any new positive contribution to R from a resonance effect is obtained when the central value of a given data point lies *below* the standard model prediction. Here we will take this into account, using the most precise measurements of R in the 5–10 GeV range obtained by the Crystal Ball experiment [73]. Given the standard model prediction for R in the continuum region between the J/ψ and the Υ,

$$R = \frac{10}{3}(1 + \alpha_s/\pi) \approx 3.54 \tag{4.9}$$

we evaluate the upper bound on the difference between theory and experiment taking into account two standard deviation uncertainties. The tightest bound we obtained from any data point was $\Delta R/R < 0.05$, from the measurement $R = 3.31 \pm 0.10 \pm 0.03 \pm 0.17$ at $\sqrt{s} = 6.25$ GeV [73]. The first two experimental errors are statistical and systematic errors for the given datum, while the third is an overall systematic uncertainty of 5.2%, which takes into account any average offset of the data. Note that within the allowed parameter space of Fig. 4.1, α_B is not much larger than 10^{-2}, and hence the Z' width is typically of order 10 MeV, or smaller. On the other hand, the experimental resolution at Crystal Ball is $\sigma_E/E = (2.7 \pm 0.2)\%/\sqrt{E/\text{GeV}}$ for electromagnetically showering particles [74], so that the resolution in the Z' invariant mass is comparable or larger to the Z' width. Assuming that $m_B = 6.25$ GeV and $\alpha_B \approx 0.01$ (the largest value allowed for this mass in Fig. 4.1), we compute the contribution to $\Delta R/R$ by integrating the resonant and background cross-sections over an energy bin equal to the detector resolution, which we set equal to the Z' width,

$\Gamma = 4\alpha_B m_B/9 \approx 28$ MeV. We find

$$\Delta R/R \approx 0.03$$

which is below the experimental bound. Since the other experimental data points present weaker bounds on $\Delta R/R$ than the one just considered, we conclude that R does not allow us to exclude any additional parameter space in Fig. 4.1. Note that at lower values of $\sqrt{s}$ above the charm threshold, R is not as precisely measured, and no useful bounds on the model can be determined.

Deep inelastic νN scattering, parity violating eN scattering, and the muon $g-2$ provide only weak bounds the Z' coupling. Using the results of Ref. [65], together with the boundary condition described earlier, we find the corresponding exclusion regions are given by

$$\alpha_B < 0.33(1+[m_B/4.47\ \text{GeV}]^2) \quad \nu\ \text{N scattering} \tag{4.10}$$

$$\alpha_B < 0.35(1+[m_B/4.47]^2) \quad \text{parity-violating e N scattering} \tag{4.11}$$

$$\alpha_B < 1.13(m_B/1\ \text{GeV})^2 \quad \text{muon } g-2 \tag{4.12}$$

which are not even visible in Fig. 4.1. Finally, we point out that resonant Bhabha scattering places no additional bounds on the model since the nonstandard contribution to the amplitude is proportional to c_γ^2, and hence the number of events near the resonance are suppressed relative to the electromagnetic background by a factor of $c_\gamma^4 \sim 10^{-10}$.

Finally, we can ask how our conclusions change if the cutoff scale Λ is pushed to its largest possible value. We may use the accurate measurement the Z-hadronic width to first bound the mixing parameter $c_Z(m_Z)$; we find for $\alpha_B = 0.01$ that $c_Z(m_Z) \lesssim 0.02$. This corresponds to the bound $\Lambda < 68$ TeV. We may obtain similar bounds from consideration of R; however these are strongly dependent on the value of m_B, as well as on the assumptions made in combining uncertainties from different, and often conflicting, experiments. Setting Λ to this maximum value, we find $c_\gamma(m_b) \approx 0.007$, a factor of 2 enhancement over the value obtained from Eq. (4.6) for the same choice of α_B. Clearly, this is not significant enough to change our qualitative conclusion that the processes involving the kinetic mixing in Eqs. (4.10–4.12) do little to constrain the parameter space of the model.

4.3 Rare Decays

What we gather from the preceding discussion is that Fig. 4.1 by itself gives a reasonable picture of the allowed parameter space of the model. We also learn that for $m_\psi < m_B < m_\Upsilon$ and for $m_B < m_\psi$, there are regions where the Z' coupling can be comparable to α_{EM}. Thus, the gauge coupling need not be so small in these models as to require a separate leap of faith. In this section, we will assume that $\alpha_B \approx \alpha$, and consider whether the Z' might eventually be detected via rare two-body decays of charm and bottom mesons.

Since the Z' coupling to fermions is purely vectorial, the Lagrangian is charge conjugation invariant if the Z' is C odd. This discrete symmetry forbids the decays of either the J/ψ or Υ to $\gamma Z'$ or $Z'Z'$ final states. Therefore, we consider instead the possible two-body decays of B and D mesons, as well as the decays of the lowest-lying C even quarkonium states, the η_c, χ_c, η_b, and χ_b.

In the first case, we know that for every B or D meson decay involving a photon in the final state, there is an analogous process involving the Z'. The only two-body decays involving a photon are the various $b \to s\gamma$ exclusive modes. We estimate

$$\frac{\Gamma(b \to sZ')}{\Gamma(b \to s\gamma)} = \frac{\alpha_B}{\alpha}(1 + \frac{1}{2}\frac{m_B^2}{m_b^2})(1 - \frac{m_B^2}{m_b^2})^2 \tag{4.13}$$

where $m_b \approx 4.3$ GeV is the bottom quark mass. While this ratio is not necessarily small, $b \to sZ'$ is probably not the easiest place to look for the Z'. Unlike $b \to s\gamma$ which is discerned experimentally by study of the photon energy spectrum, $b \to sZ'$ yields only hadrons in the final states, and would be overwhelmed by the larger background from $b \to s$ glue [75]. On the other hand, the contribution to the (yet unobserved) process $b \to se^+e^-$ involves the kinetic mixing, so that for $\alpha_B \approx \alpha$ any resonance effect in the e^+e^- invariant mass spectrum would be suppressed relative to the QED background by $c_\gamma^2 \sim 10^{-5}$. The standard model prediction for the corresponding radiative decays in the D meson system yield drastically smaller branching fractions, and thus, these decays are not likely to aid in the Z' search.

The situation is more promising in the case of the C-even quarkonia states. For example, the decay $\eta_c \to \gamma Z'$ is allowed, with

$$\frac{\Gamma(\eta_c \to \gamma Z')}{\Gamma(\eta_c \to \gamma\gamma)} \approx \frac{1}{4}\frac{\alpha_B}{\alpha}(1 - m_B^2/m_{\eta_c}^2) \tag{4.14}$$

There is an overall suppression factor of 1/4 relative to the purely electromagnetic decay from the squared ratio of baryon number to electric charge of the charm quark. In this case, one could consider $\eta_c \to \gamma X$, and search for a peak in the photon momentum spectrum. Note that the η_c branching fraction to γ+hadrons is dominated by the decay to $\gamma Z'$; the decay $\eta_c \to \gamma g$, where g is a gluon, is forbidden by color conservation, while $\eta_c \to \gamma gg$ is forbidden by charge conjugation invariance. The next possibility $\eta_c \to \gamma ggg$ is down by $\sim (\alpha_s^3/\alpha_B)/(2\pi)^4 \sim 0.001$ relative to the Z' decay due mostly to phase space suppression, and is therefore negligible. It is simply an experimental question of whether single photons from other backgrounds processes can be adequately suppressed. This at least seems possible given that searches of exactly this type for lighter neutral gauge bosons have been undertaken in π, η and η' decays [76]. A possible scenario at an e^+e^- machine is to sit on the $\psi(2S)$ resonance, and look for the decay chain

$$\psi(2S) \to \gamma\eta_c \to \gamma\gamma X \ .$$

One would retain events where one photon has precisely the right energy to come from the desired initial two body decay of the $\psi(2S)$, and then study the energy spectrum of the remaining photon. Exactly the same procedure could be applied to $\psi(2S) \to \gamma\chi_c \to \gamma\gamma X$, for the various χ_c states. At a charm factory with a typical beam luminosity of $10^{34}\mathrm{cm}^{-2}\mathrm{sec}^{-1}$ [77], and taking the $\psi(2S)$ production cross section to be ~ 600 nb from published data [78], we find $\sim 10^4$ $\gamma Z'$ events per year via χ_c decays, and $\sim 10^3$ events per year via η_c decays. Here we have taken the branching fraction of the χ_c and η_c states to $\gamma Z'$ to be approximately 1/4 the $\gamma\gamma$ branching fractions *i.e.* $\sim 10^{-4}$. The analogous decay chains of the $\Upsilon(2S)$ in the b-quark system could be studied in the same way. However, compared to the charmonium case, one would expect a factor of 400 reduction in the event rates: the production cross section for the $\Upsilon(2S)$ [79] is approximately two orders of magnitude smaller that of the $\psi(2S)$, and the $\gamma Z'$ branching fraction is down by a factor of 4 relative to the same decay in the charmonium case, due to the smaller electric charge of the b quark. Hence, one might still expect ~ 25 events/year from χ_b decays. but the (yet unobserved) η_b seems less promising.

4.4 Conclusions

In this Chapter we have defined a generic class of naturally leptophobic Z' models, and considered the Z' phenomenology in the 1–10 GeV mass range, a lower range than considered in Ref. [65]. In this mass interval, decays of various quarkonia states present additional bounds on the Z' coupling, but new opportunities for its discovery as well. We found that the experimental bound on $\Upsilon(1S)$ decay to two jets is primarily responsible for defining the allowed parameter space of the model. Bounds from the hadronic decays of the J/ψ, $\psi(2S)$, $\Upsilon(2S)$, and $\Upsilon(3S)$ only limit the parameter space in the immediate vicinity of the resonance masses; this is a consequence of larger experimental and (in the case of the charmonium states) theoretical uncertainties. We find that a Z' coupling $\alpha_B \approx \alpha_{EM}$ is allowed in mass intervals above and below the charmonium threshold. This opens the possibility of discovering the Z' in rare two-body quarkonia decays. We've suggested that perhaps the most interesting place to look is in the decay chain $\psi(2S) \to \gamma(\eta_c \text{ or } \chi_c) \to \gamma\gamma Z'$, as well as in analogous decays of the $\Upsilon(2S)$. If one photon has the right energy to indicate an initial two-body decay to the desired quarkonium state, one could search for a peak in the momentum distribution of the other photon. This could provide a stunning signal of a light and not so weakly-coupled Z', which, given the current experimental bounds, remains a viable possibility.

Chapter 5

Orthogonal U(1)'s, Proton Stability and Extra Dimensions

5.1 Introduction

It is a general principle of effective field theory that one should include all operators consistent with symmetry constraints when constructing a low-energy effective Lagrangian [80]. Such operators are suppressed by powers of the ultraviolet cutoff, so that each has the appropriate mass dimension, and multiplied by coefficients that parameterize the unknown physics relevant at higher energy scales. When this approach is applied to models with a low quantum gravity scale [81], one obtains a multitude of phenomenological disasters, unless specific mechanisms are invoked to suppress contributions to processes that are suppressed or absent in the standard model [82]. In this Chapter, we consider the possibility that baryon-number-violating operators are present generically in such theories [83], but are suppressed by an additional, non-anomalous, spontaneously-broken U(1) gauge symmetry that is orthogonal to hypercharge [65]. We will argue that the natural scale for the breaking of this symmetry is $\mathcal{O}(1)$ TeV, so that our scenario may have testable consequences at the Fermilab Tevatron, or at the next generation of collider experiments.

We focus on baryon number violation since it is by far the most dangerous of nonstandard model processes. Even if the Planck scale has its conventional value $M_{Pl} \approx 10^{19}$ GeV, the most general set of Planck-suppressed, baryon-number-violating operators lead to proton decay at a rate that is much too fast, unless there is some additional parametric suppression. For example, the superpotential operator $(Q_1 Q_{1,2})Q_2 L_i/M_{Pl}$ must be suppressed by an additional factor of $\mathcal{O}(10^{-6})$ to avoid conflict with the proton lifetime bounds from SuperKamiokande [84]. For a high Planck scale, this additional suppression factor can originate from the same sequential breaking of flavor symmetries that may account for the smallness of the Yukawa couplings of the first two generations [85]. However, if M_{Pl} is in the $1 - 100$ TeV range, which can be the case in models with extra spacetime dimensions compactified at the TeV-scale, then a much higher degree of suppression is required. We will show that a flavor-universal U(1) gauge symmetry, isomorphic to baryon number on the standard model particle content and spontaneously broken only slightly above the weak scale, is sufficient to avoid any phenomenological problems stemming from baryon-number-violating operators.

It is worth stressing that there are probably many possible ways of suppressing or eliminating proton decay in theories with a low Planck scale. One elegant suggestion made by Arkani-Hamed and Schmaltz is that quarks and leptons may be localized at different points in an extra dimension, so that proton decay operators are suppressed by the tiny overlap of the quark and lepton wave functions [86]. The approach that we consider here is complementary in that it applies also to the case when quarks and leptons are fixed to a single brane, with no separation. No doubt, this possibility has met considerable interest in the recent literature [87].

There is some relationship between the present work and earlier papers on the possibility of gauged baryon number, in which the scale of spontaneous symmetry breaking was taken *below* M_Z [65, 64, 88, 89]. While the proton decay issue was discussed in Ref. [65], the model used as a basis for the argument is now excluded at above the 95% confidence level from bounds on the electroweak S parameter – the model required a fourth chiral generation to cancel gauge anomalies. Other possibilities for anomaly cancellation discussed in the first version of Ref. [64] are excluded by S, and are also inconsistent with gauge coupling unification. Here we will present a supersymmetric model that is consistent with unification (in the case where all gauge and Higgs fields live in the bulk [90, 91]) as well as the anomaly-cancellation constraints. The required extra matter is chiral under the full gauge group, but vector-like under the standard model gauge factors, so that the S parameter bound may be avoided. The extra matter fields get masses of order the U(1) breaking scale Λ_B, which in principle could be decoupled from the weak scale. We suggest, however, that a natural possibility for generating Λ_B is a radiative breaking scenario that relates this scale to the scale of supersymmetry breaking. In this case, the new physics we introduce becomes relevant for TeV-scale collider experiments.

One of the distinctive features of the Z' boson in the class of models we consider is its natural leptophobia. While it may be tempting to think that a model with gauged baryon number is leptophobic by design, it is not hard to see that this statement is patently false. Generically, any additional U(1) symmetry will mix with hypercharge via the kinetic interaction

$$\mathcal{L} = -\frac{1}{2} c_B F_Y^{\mu\nu} F_{\mu\nu}^{new} \ , \tag{5.1}$$

which is not forbidden by any symmetry of the low-energy theory. Even if c_B is identically zero at the ultraviolet cutoff of the theory M_{Pl}, it will be renormalized at one loop by all particles that carry both hypercharge and the additional U(1) charge, so that $c_B(\mu) \neq 0$ for $\mu < M_{Pl}$. The class of models that we consider here have the property that $c_B(M_{Pl}) = 0$, and in addition

$$Tr(BY) = 0 \ , \tag{5.2}$$

where B and Y are the baryon number and hypercharge matrices, and the trace sums over all fields in the theory. It is in this sense that we say the additional U(1) is orthogonal to hypercharge. Such orthogonal U(1)'s are known to arise in string theory [92], though we will not commit ourselves to any specific string-theoretic embedding. The constraint $Tr(BY) = 0$ assures that the mixing parameter $c_B(\mu)$ remains zero until the heaviest particle threshold is crossed. In our models, the heaviest particle threshold includes all the nonstandard particles introduced to cancel anomalies; thus the running of $c_B(\mu)$ begins after the exotic states are integrated out, and hence is controlled *solely* by the standard model particle content. This gives our phenomenological analysis a high degree of model independence: a similar model with different nonstandard matter content would have identical Z' phenomenology.[1]

It is worth stressing that the leptophobia of the Z' in this model (as well as the leptophobia of its Kaluza-Klein excitations) is quite robust. For example, one might think that the Z' could be made less leptophobic by taking the scale Λ_B to be high (so that $c_B(\mu)$ would have a greater distance to run). However, this possibility is inconsistent with the assumption that (a) the Z' zero mode is phenomenologically relevant and (b) the model is consistent with unification. Since we don't know the string normalization of the new U(1) gauge coupling, we only require that it not differ wildly in strength from hypercharge at low energies. For a Z' with mass $M_B < 1$ TeV, and coupling $g_B \lesssim g_Y$, the associated symmetry breaking scale M_B/g_B cannot be arbitrarily high. Since this is also the scale of the exotic matter content, $c_B(\mu)$

[1]For Z' models that suppress proton decay and have a different phenomenology, see Ref. [93].

cannot run over very large intervals. If one takes g_B to be smaller, the scale at which running begins is pushed up, but $c_B(\mu)$ runs more slowly due to the reduced coupling. We study this effect quantitatively in Section 3.

Finally, if one is willing to sacrifice simple power-law unification, as in the original scenario of Arkani-Hamed, Dimopoulos and Dvali [81], then it is possible to consider a scenario where only gravity and the additional U(1) may propagate into the extra dimensional bulk space. What is interesting about this possibility is that strongest bounds on the compactification scale come solely from the effects of the new U(1). As a consequence, the Z' and its Kaluza-Klein (KK) excitations may be brought within the kinematic reach of the Tevatron. We show that for gauge couplings not much smaller than that of hypercharge, the Z' and its first few KK modes could remain invisible at Run I of the Tevatron, but be discerned easily at Run II. For this model, the ability of a collider experiment to probe weak couplings is as important as mass reach; we show that the enhanced luminosity of Run II could allow the Tevatron to probe a significant region of the model's parameter space.

In the next section, we highlight the points discussed above by presenting a concrete example. We do not view this model as unique, but rather as a representative example of a class of orthogonal U(1) models that have similar low-energy physics. In Section 3 we discuss the low-energy phenomenology of our scenario, and in the final section present our conclusions.

5.2 A Model

The gauge group is that of the standard model with an additional U(1) factor:

$$G = SU(3) \times SU(2) \times U(1)_Y \times U(1)_B \ . \tag{5.1}$$

We normalize the gauge coupling g_B such that all standard model quarks have charge 1/3, while all leptons and standard model Higgs fields have charge 0; these are the conventional charge assignments for baryon number in the standard model. Gauging this symmetry requires the introduction of exotic matter to cancel chiral gauge anomalies, as well as additional Higgs fields to spontaneously break the symmetry and avoid long-range forces. The aim of this section is to show that this can be done in a relatively simple way, consistent with a number of important phenomenological constraints. In particular, we show that exotic matter can be chosen such that the model (1) is consistent with gauge unification, (2) is anomaly free, (3) suppresses proton decay sufficiently, (4) has no unwanted stable colored or charged states, and (5) has a mechanism for giving the exotic matter mass. We present the model by considering these issues systematically:

Gauge Unification. We would like our model to be consistent with power-law unification [91], at least in the case where all the gauge and Higgs fields are allowed to propagate into the extra-dimensional space. Since the string normalization of the additional U(1) is uncertain [95], we seek to preserve unification of the ordinary standard model gauge factors while allowing g_B to assume values at low energies that do not differ wildly from that of hypercharge. We therefore require that the exotic matter fields fall in complete SU(5) representations. While there are of course other possibilities [94], this is the simplest. We introduce an extra generation that is vector-like under the standard model gauge factors but chiral under $\mathrm{U}(1)_B$:

$$\left.\begin{array}{l} Q_L \\ U_R \\ D_R \end{array}\right\} b_Q \quad \left.\begin{array}{l} \overline{Q}_R \\ \overline{U}_L \\ \overline{D}_L \end{array}\right\} b_{\bar{Q}}$$
$$\left.\begin{array}{l} L_L \\ E_R \\ N_R \end{array}\right\} b_L \quad \left.\begin{array}{l} \overline{L}_R \\ \overline{E}_L \\ \overline{N}_L \end{array}\right\} b_{\bar{L}} \quad . \tag{5.2}$$

Although we assume supersymmetry, we show only the fermionic components above. The overlines indicate Dirac adjoints, and the b's represent the $\mathrm{U}(1)_B$ charges, yet to be specified. (Four distinct $\mathrm{U}(1)_B$ charges is the smallest number we found that could produce a viable model.) The charges under the standard model gauge factors for fields in the first column are precisely the same as those of fields in an ordinary standard model generation; the only exception is N_R which is a standard model singlet. The fields in the second column have conjugate standard model charges so that, for example, $\overline{Q}_R Q_L$ would be invariant if $b_Q + b_{\bar{Q}} = 0$. As we will see below, our choices for the b_i are such that all the fields in Eq. (5.2) obtain masses of order the $\mathrm{U}(1)_B$ breaking scale.

Anomaly Cancellation We now aim to restrict the b_i so that the model is free of gauge anomalies. We first note that triangle diagrams involving only standard model gauge factors remain vanishing since the additional matter is introduced in complete generations. We therefore must consider anomalies of the form $\mathrm{U}(1)_B^3$, $G_{SM}\mathrm{U}(1)_B^2$ and $G_{SM}^2\mathrm{U}(1)_B$, where G_{SM} represents any of the standard model group factors. Given the tracelessness of the non-Abelian generators, this reduces the relevant anomalies to the set: $\mathrm{U}(1)_Y\mathrm{U}(1)_B^2$, $\mathrm{SU}(3)^2\mathrm{U}(1)_B$, $\mathrm{SU}(2)^2\mathrm{U}(1)_B$, $\mathrm{U}(1)_Y^2\mathrm{U}(1)_B$, and $\mathrm{U}(1)_B^3$. It is easy to see that the $\mathrm{SU}(3)^2\mathrm{U}(1)_B$ anomaly vanishes since all colored matter with the same $\mathrm{U}(1)_B$ charge comes in groups with equal numbers of left- and right-handed fields.

The same can be said of the $U(1)_B^3$ anomaly, since the additional $N_{L,R}$ states assure that the exotic 'leptons' with the same $U(1)_B$ charge again come in equal numbers of left- and right-handed fields. Finally, we can dispense with the $U(1)_Y U(1)_B^2$ anomaly by noting that every group of particles with the same $U(1)_B$ charge separately satisfies $Tr(Y) = 0$. The remaining two anomaly cancellation conditions, $SU(2)^2 U(1)_B$ and $U(1)_Y^2 U(1)_B$, give exactly the same constraint

$$3\Delta_Q + \Delta_L = -3 \ , \tag{5.3}$$

where we have defined

$$\Delta_Q = b_Q + b_{\bar{Q}} \quad \text{and} \quad \Delta_L = b_L + b_{\bar{L}} \ . \tag{5.4}$$

Given the charges defined in Eq. (5.2), we impose Eq. (5.3) to render our theory free of anomalies.

Notice that $-\Delta_Q$ and $-\Delta_L$ also represent the charges of Higgs fields that we require to give the exotic matter fields masses when $U(1)_B$ is spontaneously broken. The most economical exotic Higgs sector is obtained by setting

$$\Delta_Q = \pm \Delta_L \ . \tag{5.5}$$

Then all the desired mass terms may be formed by introducing a single pair of Higgs fields

$$S_B \quad \text{and} \quad S_{\bar{B}} \ , \tag{5.6}$$

with charges $+\Delta_Q$ and $-\Delta_Q$, respectively. This is the minimal possibility, since, as in the minimal supersymmetric standard model (MSSM), a vector-like pair of Higgs superfields is required to avoid additional anomalies. The choice of Eq. (5.5) together with the constraint Eq. (5.3) implies that either

$$\Delta_Q = \Delta_L = -3/4 \quad \text{or} \quad \Delta_Q = -\Delta_L = -3/2 \ . \tag{5.7}$$

The remaining freedom to choose exotic $\mathrm{U}(1)_B$ charges will be important in satisfying the other phenomenological constraints below.

Proton decay. If our additional U(1) symmetry were unbroken, then it would be clear that all operators contributing to proton decay would be exactly forbidden. When the symmetry is spontaneously broken, the form of baryon-number-violating operators in the low-energy effective theory depends on the charge assignment of the Higgs fields which break $\mathrm{U}(1)_B$, as well as on the size of their vacuum expectation values (vevs). Let us work in the very low-energy limit, below the scales of extra dimensions, exotic matter, and supersymmetry breaking, which we will take to be ~ 1 TeV universally for the purposes of the present argument. In this effective nonsupersymmetric theory, operators that could contribute to proton decay have the form [65]

$$\mathcal{O} = q^k \ell^m \chi^n \ , \tag{5.8}$$

where q and ℓ represent generic quark and lepton fields, respectively, and χ represents the vev of either S_B or $S_{\bar{B}}$. Here we have suppressed both the Dirac structure of the operator and the standard model gauge indices for convenience. First, we note that since the lepton electric charge is integral, k must be a multiple of 3, *i.e.* $k = 3p$. It follows that the baryon number of $q^k \equiv q^{3p}$ is p, which is an integer. On the other hand, this must be compensated by the baryon number of χ, which is either $\pm 3/2$ or $\pm 3/4$, given the charges of the S_B fields already discussed. Thus we conclude that the operators represented by Eq. (5.8) must be of the form

$$(q^9 \chi^2)^r \ell^m \quad \text{or} \quad (q^9 \chi^4)^r \ell^m \ , \tag{5.9}$$

where r and m are integers. The point is simple: the fact that the possible symmetry breaking 'spurions' have fractional $U(1)_B$ charges forces the baryon-number-violating operators to contribute to no less than $\Delta B = 3$ transitions. This renders our model safe from proton decay as well as N-$\overline{N}$ oscillations. The operators in Eq. (5.9) are suppressed by high powers of mass scales that are either 1 TeV or M_{Pl}, and thus are unlikely to have any observable effects on stable matter at low energies.

Avoiding Stable Charged Exotic Matter. We will now further restrict our charge assignments b_i to assure that we have no stable heavy states that are charged under any of the standard model gauge factors. This allows us to evade bounds on stable charged matter from searches for anomalously heavy isotopes in sea water [1]. In both the exotic lepton and quark sectors separately, it is always possible to choose Yukawa couplings such that one exotic state is lightest, and ordinary weak decays to this state are kinematically allowed. For example, the exotic lepton superpotential couplings (in terms of left-handed chiral superfields)

$$W \supset L\bar{L}S_{\bar{B}} + (E\bar{E} + N\overline{N})S_B + (LE + \bar{L}\bar{N})H_D + (\bar{L}\bar{E} + LN)H_U \tag{5.10}$$

lead to mass terms of the form

$$\begin{pmatrix} \bar{e}_H & E \end{pmatrix} \begin{pmatrix} M_1 & m_2 \\ m_1 & M_2 \end{pmatrix} \begin{pmatrix} e_H \\ \overline{E} \end{pmatrix} + \begin{pmatrix} \bar{\nu}_H & N \end{pmatrix} \begin{pmatrix} M_1 & m_4 \\ m_3 & M_3 \end{pmatrix} \begin{pmatrix} \nu_H \\ \overline{N} \end{pmatrix} , \tag{5.11}$$

where the M_i are masses of order the $U(1)_B$ breaking scale, while m_i are of order the weak scale. Here we have written the component superfields in the doublets L ($\overline{L}$) as ν_H ($\bar{\nu}_H$) and e_H ($\bar{e}_H$). Clearly one has the freedom to arrange for the lightest exotic lepton state to be neutral. For example, for the specific choice $M_1 = M_2 = M_3$, $m_1 = m_2$ and $m_3 = m_4$, the lightest charged state has mass $M - m_1$ while the lightest neutral state $M - m_3$; we therefore could take $m_1 < m_3$. In the exotic quark sector, the lightest state is charged and colored, so some additional mechanism must be provided to assure it decays to ordinary particles. Since we are working in the context of models in which the Planck scale is low, we can make the lightest exotic quark unstable by considering possible higher-dimension operators, allowed by the symmetries of the theory and suppressed by the cutoff. As there is some freedom in how we may accomplish this, let us restrict our subsequent discussion to a specific example. Let us choose the charge assignment in which $\Delta_Q = -3/2$. The choice $b_Q = -2/3$ and $b_{\bar{Q}} = -5/6$ is consistent with this condition, and also allows the superpotential operator

$$\frac{1}{M_{Pl}} q\, q\, Q\, \ell \ , \tag{5.12}$$

where lower-case superfields are those of the standard model. This operator allows for three-body decays for the lightest exotic quark field (for example, to a normal lepton and two squarks). Even if the superpartners are heavy, so that this decay is not kinematically allowed, one can obtain a four-fermion operator by "dressing" Eq. (5.12) with a gaugino exchange. In this case, the decay proceeds to two quarks and a lepton, with a width of order

$$\Gamma \sim \frac{1}{64\pi^3}\left(\frac{1}{16\pi^2}\right)^2\left(\frac{M_Q}{M_{Pl}}\right)^2 M_Q \ . \tag{5.13}$$

The first factor is from three-body phase space, the second from the fact that the amplitude occurs at one-loop, and the rest follows from dimensional analysis. The lightest exotic quark decays well before nucleosynthesis providing that $M_{Pl} < 10^{13}$ GeV; this is not a problem in our scenario. Note that the charge assignments $b_Q = -2/3$ and $b_{\bar{Q}} = -5/6$ assure that potentially dangerous mass mixing terms like $q\overline{Q}$, and $QH_D d$ have $\mathrm{U}(1)_B$ charges of $-1/2$ and -1, respectively. Since this is not an integral multiple of 3/2 (the magnitude of the exotic Higgs' $\mathrm{U}(1)_B$ charges) such operators are forbidden by the gauge symmetry. We will adopt the present choice of b_Q and $b_{\bar{Q}}$ for the subsequent discussion. However, the reader should keep in mind that other possible assignments may render the exotic matter unstable, given the presence of higher-dimension operators at the relatively low cutoff of the theory.

Orthogonality. The only charges we have not yet fixed are b_L and $b_{\bar{L}}$, which have been constrained such that $b_L + b_{\bar{L}} = 3/2$. Since we wish to restrict our discussion to models that satisfy $Tr(BY) = 0$, we fix our remaining degree of freedom by imposing this constraint. It is straightforward to check that $Tr(BY) = 9 \cdot \frac{1}{3} \cdot (2 \cdot \frac{1}{6} + \frac{2}{3} - \frac{1}{3}) = 2$ for the ordinary matter, where the overall factor of 9 is the multiplicity due to color and number of generations. For the exotic matter, the quark fields contribute $Tr(BY) = 3 \cdot (b_Q - b_{\bar{Q}}) \cdot (2 \cdot \frac{1}{6} + \frac{2}{3} - \frac{1}{3}) = 1/3$ given our previous choice of $b_Q = -2/3$ and $b_{\bar{Q}} = -5/6$. We now choose $b_L = 4/3$ and $b_{\overline{L}} = 1/6$. The exotic lepton contribution is then $Tr(BY) = (b_L - b_{\overline{L}})(2 \cdot [-\frac{1}{2}] - 1) = -7/3$. Hence, the orthogonality of $\mathrm{U}(1)_B$ and hypercharge is maintained. Notice that our choice for b_L and $b_{\bar{L}}$ is such that no dangerous mass mixing terms between exotic and standard model leptons are generated after $\mathrm{U}(1)_B$ is spontaneously broken. Now that all our charges have been fixed, we summarize them here for convenience:

$$\begin{array}{ll} b_Q = -2/3 & b_{\bar{Q}} = -5/6 \\ b_L = 4/3 & b_{\overline{L}} = 1/6 \end{array} \quad . \tag{5.14}$$

Symmetry Breaking. It is customary in model building to avoid discussing the origin of symmetry breaking scales, given the model-dependence that this issue often entails. Here we only aim to emphasize that the scale of $\mathrm{U}(1)_B$ breaking may be tied quite naturally to the scale of supersymmetry breaking. This point is worth mentioning given that we have constructed our model specifically to allow for the decoupling of the nonstandard sector, to avoid bounds from precision electroweak measurements. One way in which the supersymmetry breaking and $U(1)_B$ scale may be related is if the potential for the nonstandard Higgs fields S_B and $S_{\bar{B}}$ develops its vacuum expectation value as a consequence of a soft scalar squared mass running negative, the analog of the radiative breaking scenario in the MSSM. This scenario can be implemented in the present context since the exotic Higgs fields couple to a sector of new matter fields with large Yukawa couplings. The exotic Higgs fields have the superpotential coupling

$$W = \mu_s S_B S_{\bar{B}}, \tag{5.15}$$

the analog of the μ term in the MSSM. Introducing soft supersymmetry breaking masses, and D-terms, the scalar potential for the exotic Higgs fields is given by

$$\begin{aligned} V &= \frac{1}{2}(\mu_s^2 + m_B^2)(s_B^2 + p_B^2) + \frac{1}{2}(\mu_s^2 + m_{\bar{B}}^2)(s_{\bar{B}}^2 + p_{\bar{B}}^2) \\ &+ \mu_s B_s(s_B s_{\bar{B}} - p_B p_{\bar{B}}) + \frac{9}{32} g_B^2 (s_B^2 + p_B^2 - s_{\bar{B}}^2 - p_{\bar{B}}^2)^2 \ , \end{aligned} \tag{5.16}$$

where $s_{B,\bar{B}}$ and $p_{B,\bar{B}}$ represent the scalar and pseudoscalar components of each of the fields, and m_B, $m_{\bar{B}}$, and B_s are soft, supersymmetry-breaking masses. It is straightforward to show that this potential has stable (local) minima in which one scalar squared mass is negative and both S_B and $S_{\bar{B}}$ acquire vacuum expectation values. For example, for the parameter choice $g_B = 0.3$, $\mu_s = 1$ TeV $B_s = -1$ TeV, $m_B^2 = -1.48$ TeV^2, and $m_{\bar{B}}^2 = 2.81$ TeV^2, we find the vevs

$$\langle s_B \rangle = 3 \text{ TeV} \quad \langle s_{\bar{B}} \rangle = 1 \text{ TeV},$$

the scalar squared masses

$$0.99 \text{ TeV}^2 \quad 4.37 \text{ TeV}^2 \ ,$$

and the pseudoscalar squared mass

$$3.33 \text{ TeV}^2 \ .$$

These are acceptable values. Another possible form for the potential is that of the next-to-minimal supersymmetric standard model, in which both the ordinary μ parameter and the parameter μ_s could have a common origin, the vev of a singlet field. We will not study the issue of possible potentials any further here, though such an investigation would be required if experimental evidence for the model became available.

5.3 Phenomenology

In this section, we explore the Z' phenomenology of our model. We will assume for simplicity that the scale of exotic matter, Λ_B, and of superpartner masses is 1 TeV. The compactification scale, which we call Λ below, is a free parameter. In the case where all non-chiral matter (i.e. the Higgs and gauge fields) are allowed to propagate in the bulk, we require Λ to be greater than a few TeV, to satisfy the constraints from precision electroweak measurements [96]. In this case, the phenomenology that we study is that of the new zero mode gauge field. However, we will also consider the (non-unifiable) possibility that only $\mathrm{U}(1)_B$ lives in the bulk, in which case the bounds on Λ are substantially weakened. For this choice, the Z' zero mode and first few KK excitations become relevant at planned collider experiments, and will be the focus of our discussion. For concreteness, we perform our numerical analysis in the case of one extra dimension.[2] For more than one extra dimension, the sums involving the KK modes are divergent and must be regulated by some additional,

[2] Of course, gravity also lives in the bulk. Our model does not preclude the possibility that gravity propagates in a larger number of dimensions than $\mathrm{U}(1)_B$.

string-theoretic mechanism. We restrict ourselves to one extra dimension to avoid this model-dependent issue; however, the reader should keep in mind that our bounds on the $U(1)_B$ KK modes may be overestimates if there is a mechanism, *e.g.* brane recoil effects [97], that suppresses the KK couplings.

One of the interesting properties of this class of models, regardless of which case we consider, is the strong leptophobia of the Z' and its KK excitations. Given our assumption of a vanishing kinetic mixing parameter, c_B, at the string scale, c_B remains vanishing down to the scale of exotic matter, since $Tr(BY) = 0$. At lower scales, the exotic states are integrated out of the theory, and the orthogonality constraint is no longer satisfied. With our choice of energy scales, c_B remains small down to the Z' mass, so we may treat Eq. (5.1) as a perturbative interaction. Thus, the Feynman rule for the Z'-hypercharge vertex is given by

$$- i\, c_B \left(p^2 g^{\mu\nu} - p^\mu p^\nu\right) . \tag{5.1}$$

Since we assume that the scale of superpartner masses is the same as the scale of exotic matter, we evaluate the non-supersymmetric running of c_B; at one-loop we obtain the renormalization group equation (RGE)

$$\mu \frac{\partial}{\partial \mu} c_B = -\frac{1}{3\pi}\sqrt{\alpha_Y \alpha_B}\left[\frac{5}{6}N_u - \frac{1}{6}N_d\right] , \tag{5.2}$$

where N_u and N_d are the number of standard model up-type and down-type quarks propagating in the loop. This RGE is solved subject to the boundary condition $c_B(\Lambda_B) = 0$, for the reasons described above. Notice that the running of c_B is controlled entirely by the standard model particle content, since these are the only fields relevant below the scale Λ_B. Thus, our analysis is independent of the specific exotic sector introduced to cancel anomalies.

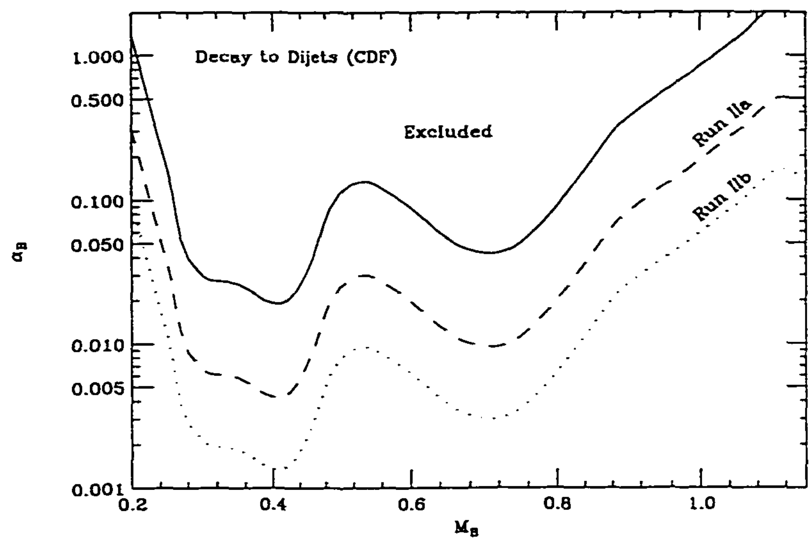

Figure 5.1 Bound on α_B from the cross section times branching fraction to dijets. The solid line corresponds to the bound obtained from Run I with a Luminosity of 106 pb^{-1}. The dashed line corresponds to a luminosity of 2 fb^{-1} for Run IIa and the dotted line to a luminosity of 20 fb^{-1} for Run IIb.

We may now consider the phenomenology of the model by determining bounds in the M_B-α_B plane. We will assume $M_B > m_{top}$ (which was not studied in Refs. [65, 64]) and first consider the case in which all non-chiral superfields live in the bulk. For most of the mass range of interest, the Z' will be sufficiently heavier than the Z so that the most stringent bounds are obtained from direct collider searches. We consider the limits on Z''s decaying to dijets and dileptons at the Fermilab Tevatron Collider:

Decays to Dijets. The CDF Collaboration has placed bounds on narrow resonances decaying to dijets in $p\bar{p}$ collisions at $\sqrt{s} = 1.8$ TeV [98]. They present the 95% C.L. upper limits on cross section times branching ratio as a function of the Z' mass in the range $0.2 - 1.15$ TeV. Since the kinetic mixing effects are small (as we will see below), the branching fraction to dijets in our model is nearly 100%; thus we compare the CDF bounds to the Z' production cross section in our model, which we estimate using the narrow width approximation:

$$\sigma(p\bar{p} \to Z' \to dijets) = \frac{4\pi^2}{9}\frac{\alpha_B}{s}\int dy \sum_{i,j} f_i^p(y, \sqrt{s}, M_B) f_j^{\bar{p}}(y, \sqrt{s}, M_B)\,. \tag{5.3}$$

Here y is the rapidity, $\sqrt{s}$ is the center of mass energy, and f^p ($f^{\bar{p}}$) represents the appropriate parton distribution functions for $p\bar{p}$ collisions. Using the CTEQ 4M structure functions [99] at $\sqrt{s} = 1.8$ TeV for our numerical analysis, we obtain a bound on $\alpha_B(M_B)$ as a function of M_B, shown in Fig. 5.1. The solid line corresponds to the Run I luminosity ($\mathcal{L}$) of $\sim$0.1 fb^{-1} and is the strongest bound on the model. We also estimate the ability of the Tevatron to probe additional parameter space at Run II. Note that the shape of the excluded region in Fig. 5.1 depends on a detailed analysis of both statistical and experimental systematic uncertainties; the latter are difficult to extrapolate with precision to Run II. Therefore, we rely instead on the observation that statistical and systematic uncertainties generally both scale as $\sqrt{\mathcal{L}}$ (*i.e.* the systematic uncertainties can be reduced by higher statistics). Thus, we make a simple extrapolation, scaling the bound from Run I down by $\sqrt{\mathcal{L}_I}/\sqrt{\mathcal{L}_{II}}$ using the expected luminosities at Run IIa and Run IIb, 2 and 20 fb^{-1} respectively; this yields the two other curves shown in Fig. 5.1. We see that, for example, it is possible to have a new gauge boson in the region between 500 and 600 GeV with a coupling of electromagnetic strength that could be observed at Run II.

Decays to Dileptons. Given the construction of our model, the specification of M_B and α_B is sufficient to determine the magnitude of $c_B(M_B)$, up to a small uncertainty. For each point in the parameter space, $M_B/\sqrt{4\pi\alpha_B}$ is of order the scale of $U(1)_B$ breaking. However, this scale also determines the masses of the exotic fermions, and the point at which c_B begins to run. The only uncertainty is in the Yukawa couplings of the exotic matter, which we assume is of order one (say, between 1/3 and 3); this

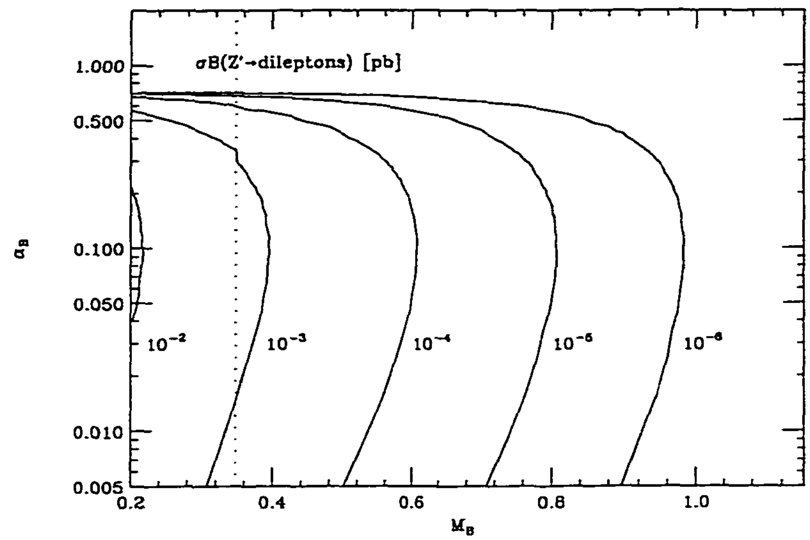

Figure 5.2 Contours of constant cross section times branching fraction to dileptons. The dotted line shows the threshold $M_B = 2m_{top}$.

only affects the result logarithmically. To account for the mixing, we use Eq. (5.2) to run c_B from the $\mathrm{U}(1)_B$ breaking scale $\Lambda_B = rM_B/g_B$, where r is an $\mathcal{O}(1)$ uncertainty, down to M_B with the condition $c_B(\Lambda_B) = 0$. We show some typical values of c_B in Table 1 for different choices of M_B and α_B. The results are uniformly small, due to two competing effects: if the coupling g_B is reduced with M_B held fixed, then the 'starting' scale Λ_B is increased, while the rate of running, *i.e.* the right-hand side of

M_B (TeV)	$\alpha_B(M_B)$	$c_B(M_B)$
0.2	0.1	0.00688
0.5	0.1	0.00694
1.0	0.1	0.00699
0.2	0.01	0.00469
0.5	0.01	0.00471
1.0	0.01	0.00473

Table 5.1 Kinetic mixing for $r = 3$.

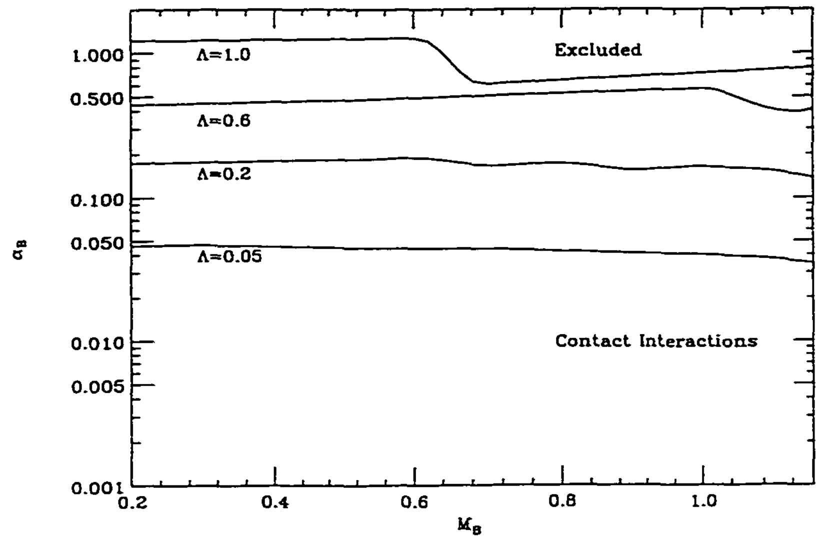

Figure 5.3 Bounds obtained from the contribution of KK modes heavier than 1.15 TeV to contact interactions for several values of Λ.

Eq. (5.2), is reduced. As a consequence, the branching fraction to leptons

$$B = \frac{\frac{3}{2}c_B^2\alpha_Y}{\frac{N_f}{9}\alpha_B + \frac{3}{2}c_B^2\alpha_Y}, \tag{5.4}$$

is highly suppressed throughout the parameter space in Fig. 5.1. Here N_f is the number of quarks lighter than $M_B/2$. In Fig. 5.2 we show contours of constant σB; note that σB vanishes when $\Lambda_B(\alpha_B) = M_B$. The CDF bound on this product in no stronger than 0.04 pb for dilepton invariant masses above $\sim$ 400 GeV, and is significantly weaker for smaller masses [100]; as a consequence, no additional bound can be placed on our parameter space. It is possible, however, that a dilepton signal could be discerned at Run II, if the Z' were already discovered in the dijet channel. For example, for $M_B \approx$ 400 GeV, where the current bound is 0.04 pb, a simple rescaling by $\mathcal{L}$ suggests that the bound could become 0.0028 pb after 20 fb^{-1} of integrated luminosity. The results in Fig. 5.2 imply that this would be sufficient to see the model's tiny dilepton signal.

KK-modes. The Z' phenomenology we have discussed thus far has related to the zero-mode gauge field, and is independent of how the model is configured in extra dimensions. As we mentioned earlier, if all the non-chiral fields propagate in the bulk, then the first Z' KK mode is outside the reach of the Tevatron, and the zero-mode is of principle interest to us. Here, we wish to consider an alternative possibility, that the compactification scale is low enough such that the first few KK modes are also within the kinematic reach of the Tevatron. This can be the case if only $U(1)_B$ and its associated exotic Higgs fields live in the bulk. The usual strong bounds on Λ are evaded in this situation since there are *no* exotic Higgs fields charged under both $U(1)_B$ and any of the standard model electroweak gauge factors – the vev of such a field would lead to mixing at tree-level between the Z and Z' KK modes. In order to determine the relevant bounds, let us consider the following terms in the Z' Lagrangian:

$$\begin{aligned}\mathcal{L}_{KK} &= -\frac{1}{4}\sum_{n=0} F^{(n)}_{\mu\nu}F^{\mu\nu}_{(n)} + \frac{1}{2}\sum_{n=0}\left(M_B^2+\Lambda^2 n^2\right) Z'^{\mu(n)}Z'^{(n)}_{\mu} \\ &\quad -\frac{g_B}{3}\bar{q}\gamma^{\mu}\left(Z'^{(0)}_{\mu}+\sqrt{2}\sum_{n=1}Z'^{(n)}_{\mu}\right)q\,. \end{aligned} \tag{5.5}$$

Notice that the KK modes have contributions to their masses from both the symmetry breaking and the compactification scale. If $\Lambda \ll M_B$, there is effectively a 'pile-up' of states with masses of order M_B and multiplicity M_B/Λ. This is one way in which low-energy bounds are enhanced. In addition, the coupling of the KK modes to quarks has an extra factor of $\sqrt{2}$ compared to the coupling of the zero mode; this results from the field rescalings necessary to put the four-dimensional kinetic terms in canonical form, and to give the zero-mode gauge coupling its conventional normalization. Hence, the appropriate dijet bound on a given KK mode may be obtained from Fig. 5.1 by scaling down the exclusion limit shown by a factor of 2.[3] If Λ is sufficiently small,

[3]The running of α_B in the range shown in Figure 5.1 is small, and can be neglected in this

the zero mode and first few KK modes could be unobserved in Run I, but discovered at Run II. We therefore consider whether Λ can be small enough for this interesting situation to be obtained.

Aside from the KK modes that are within the reach of the Tevatron, there is also an infinite tower of heavier modes that are integrated out of the low-energy theory. Thus, the new physics manifests itself as a series of narrow resonances, together with effective contact interactions that lead to smoothly growing cross sections. We may use the bounds on four-quark contact interactions to bound the compactification scale. If we integrate out all the modes with mass $M_B > M_{min} = 1.15$ TeV (the endpoint of the dijet invariant mass spectrum in Ref. [98]) we obtain operators of the form

$$\mathcal{L}_{\bar{q}q\bar{q}q} = -\sum_{n_{min}}^{\infty} \frac{g_B^2}{9M_n^2} \bar{q}_L \gamma_\mu q_L \bar{q}_L \gamma^\mu q_L + \cdots \tag{5.6}$$

where $M_n^2 = M_B^2 + n^2\Lambda^2$, and n_{min} corresponds to the first KK mode above M_{min}. We show only the purely left-handed operator, which is the one most tightly constrained of those listed in the Review of Particle Physics [1], *viz.*, $\Lambda_{LL}^-(qqqq) > 2.4$ TeV at 95% C.L., with $\Lambda_{LL}^-(qqqq)$ defined therein. The sum shown in Eq. (5.6) can be evaluated analytically so that the bound may be written as

$$\alpha_B < \frac{9M_B\Lambda}{(2.4\mathrm{TeV})^2} \left[i\Psi(n_{min} - \frac{iM_B}{\Lambda}) - i\Psi(n_{min} + \frac{iM_B}{\Lambda}) \right]^{-1} \tag{5.7}$$

where $\Psi(x) = \frac{\partial}{\partial x}[\ln \Gamma(x)]$ is the digamma function. We plot Eq. (5.7) for several values of Λ in Fig. 5.3. The mild steps in these contours occur each time a KK mode becomes more massive than M_{min}, and is included in the contact term.

In the case where Λ is small, we can also determine whether the pile-up of states at M_B is significantly bounded by Z-pole observables. The most stringent constraint

discussion.

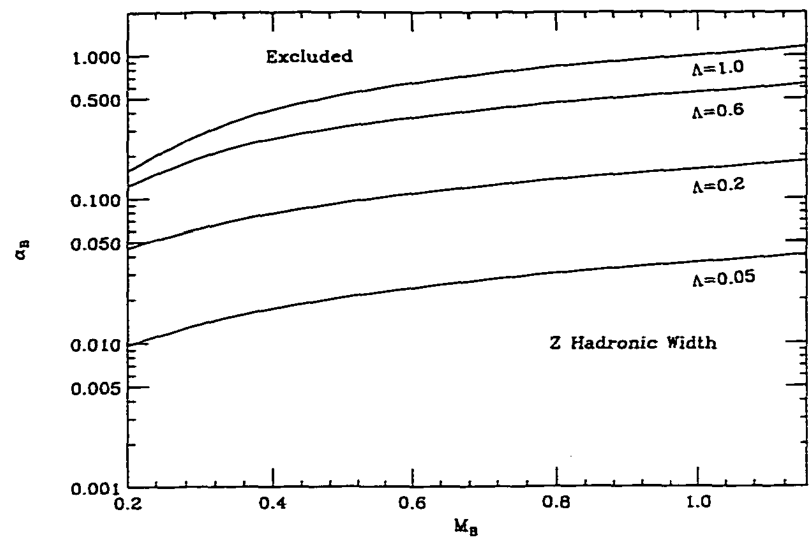

Figure 5.4 Bound obtained from the contribution of the first 1000 KK modes to the Z hadronic width.

for this type of model comes from the measurement of the Z hadronic width [65], which is known to approximately 0.1% [1]. We include contributions from the Z$-Z'$ mixing [65] and from the one-loop $q\bar{q}Z$ vertex correction [64]. The total effect is given by

$$\frac{\Delta\Gamma_{had}}{\Gamma_{had}} \approx -1.194\, c_B(m_Z)\,\sqrt{\alpha_B}\, m_Z^2 \left(\frac{1}{m_Z^2 - M_B^2} + 2\sum_{n=1}^{\infty}\frac{1}{m_Z^2 - M_n^2}\right)$$
$$+\frac{\alpha_B}{18\pi}\left(F_2(M_B) + 2\sum_{n=1}^{\infty} F_2(M_n)\right), \tag{5.8}$$

where $c_B(m_Z)$ is found by solving Eq. (5.2), and $F_2(M)$ is a loop integral factor that can be found in Ref. [64]. The sums appear linearly in Eq. (5.8) since the effects of new physics appear in an interference term at lowest order. Figure 5.4 shows the 2σ bound for several choices of Λ, where the sum includes the first 1000 KK modes. Generally, the bound obtained from the Z hadronic width supersedes the one obtained from contact interactions. Figs. 5.3 and 5.4 in conjunction with Fig. 5.1 show that the compactification scale Λ can be made small enough so that the Z' zero mode and first few KK excitations could be undetectable at Run I and discovered at Run II, without requiring the coupling α_B to be inexplicably small. For example, the parameter choice $\alpha_B = 0.01$, $M_B = 400$ GeV, and $\Lambda = 200$ GeV is consistent with all our constraints.

5.4 Conclusions

We have shown in this article that it is possible to construct viable models with a non-anomalous U(1) symmetry that is orthogonal to hypercharge and that preserves proton stability, a concern when the quantum gravity scale is low. While exotic chiral fields are required to cancel anomalies, we show that these fields may nonetheless be vector-like under the standard model subgroup, so that constraints from the S parameter are evaded, and may appear in complete SU(5) representations, so that power-law unification may be preserved. The new gauge boson and its KK excitations exhibit a high degree of leptophobia, which is only violated by kinetic mixing with hypercharge, which is small and calculable, given our assumed boundary conditions. If power-law unification is sacrificed, then one may consider the case in which only the extra U(1) lives in the bulk. In this case, the most important bounds on the compactification scale come from processes associated with the exchange of the Z' and its KK excitations, and were found to be relatively weak. This allows the Z' and its first few KK modes to be within the kinematic reach of the Tevatron. In both versions of the model, we considered bounds from collider searches for new particles decaying to dijets and dileptons, and, in the second case, bounds on the compactification scale from contact interactions and contributions to the Z hadronic width. For gauge couplings comparable to that of hypercharge, we showed that this scenario is allowed by current experiments, and that the new gauge boson, and perhaps some of its KK excitations could be discovered by the Tevatron at Run II.

BIBLIOGRAPHY

[1] Review of Particle Physics, D.E. Groom *et al.*, Eur. Phys. J. C15 (2000) 1.

[2] Super-Kamiokande Collaboration (Y. Fukuda *et al.*), Phys. Rev. Lett. **81**, (1998) 1562.

[3] H. N. Brown *et al.*, [Muon g-2 Collaboration], Phys. Rev. Lett. **86**, (2001) 2227, hep-ex/0102017.

[4] G. G. Ross, *Grand Unified Theories*, The Benjamin/Cummings Publishing Company, Inc., Menlo Park, California, USA, 1985.

[5] S. Weinberg, *Quantum Theory of Fields. Vol. 3: Supersymmetry*, Cambridge University Press, Cambridge (2000).

[6] C. D. Hoyle, U. Schmidt, B. R. Heckel, E. G. Adelberger, J. H. Gundlach, D. J. Kapner and H. E. Swanson, Phys. Rev. Lett. **86**, 1418 (2001) [hep-ph/0011014].

[7] J. Polchinski, *String Theory Vols. I and II*, Cambridge University Press, Cambridge (1998).

[8] K. R. Dienes, E. Dudas and T. Gherghetta, Phys. Lett. **B436**, 55 (1998) [hep-ph/9803466]; Nucl. Phys. **B537**, 47 (1999) [hep-ph/9806292].

[9] N. Arkani-Hamed, S. Dimopoulos, G. Dvali, Phys. Lett. **B429** (1998) 263; Phys.

Rev. D **59** 086004 (1999); I. Antoniadis, N. Arkani-Hamed, S. Dimopoulos and G. Dvali, Phys. Lett. **B436**, 257 (1998) [hep-ph/9804398].

[10] R. Barbieri, G. Dvali, and L.J. Hall, Phys. Lett. B **377**, 76 (1996); R. Barbieri, L.J. Hall, and A. Romanino, Phys. Lett. B **401**, 47 (1997); R. Barbieri, L.J. Hall, S. Raby and A. Romanino, Nucl. Phys. **B493**, 3 (1997).

[11] See, for example:
Y. Nir and N. Seiberg, Phys. Lett. B **309**, 337 (1993); M. Leurer, Y. Nir, and N. Seiberg, Nucl. Phys. **B420**, 468; D.B. Kaplan and M. Schmaltz, Phys. Rev. D **49**, 3741 (1994); M. Dine, R. Leigh, and A. Kagan, Phys. Rev. D **48**, 4269 (1993); L.J. Hall and H. Murayama, Phys. Rev. Lett. **75**, 3985 (1995); C.D. Carone, L.J. Hall, and H. Murayama, Phys. Rev. D **53**, 6282 (1996); P.H. Frampton and O.C.W. Kong, Phys. Rev. Lett. **77**, 1699 (1996).

[12] F. Gabbiani, E. Gabrielli, A. Masiero and L. Silvestrini, Nucl. Phys. **B477**, 321 (1996).

[13] R. Barbieri, G. Dvali, and L.J. Hall, Phys. Lett. B **377**, 76 (1996).

[14] R. Barbieri, L.J. Hall, and A. Romanino, Phys. Lett. B **401**, 47 (1997).

[15] R. Barbieri, L.J. Hall, S. Raby and A. Romanino, Nucl. Phys. **B493**, 3 (1997).

[16] M. Green and J. Schwarz, Phys. Lett. B **149**, 117 (1984).

[17] C.D. Carone and L.J. Hall, Phys. Rev. D **56**, 4198 (1997).

[18] L.J. Hall and N. Weiner, Phys. Rev. D **60**, 033005 (1999).

[19] LSND Collaboration, C. Athanassopoulos *et al.*, Phys. Rev. Lett. **81**, 1774 (1998).

[20] A. Aranda, C.D. Carone and R.F. Lebed, Phys. Rev. D **62**, 016009 (2000).

[21] C.D. Carone and R.F. Lebed, Phys. Rev. D **60**, 096002 (1999).

[22] A.D. Thomas and G.V. Wood, *Group Tables*, Shiva Publishing, Orpington, UK, 1980.

[23] L.E. Ibáñez and G.G. Ross, Phys. Lett. B **260**, 291 (1991).

[24] T. Banks and M. Dine, Phys. Rev. D **45**, 1424 (1992);
J. Preskill, S.P. Trivedi, F. Wilczek, and M.B. Wise, Nucl. Phys. **B363**, 207 (1991).

[25] H. Georgi and C. Jarlskog, Phys. Lett. B **86**, 297 (1979).

[26] M. Dine, A.E. Nelson, Phys. Rev. D **48**, 1277 (1993); M. Dine, A.E. Nelson, Y. Shirman, Phys. Rev. D **51**, 1362 (1995).

[27] L. Randall and R. Sundrum, Nucl. Phys. **B557**, 79 (1999).

[28] G.F. Giudice, M.A. Luty, H. Murayama, and R. Rattazzi, JHEP **9812**, 027 (1998)

[29] I. Antoniadis, S. Dimopoulos, A. Pomarol, M. Quiros, Nucl. Phys. **B544**, 503 (1999).

[30] See, for example:
Y. Nir and N. Seiberg, Phys. Lett. B **309**, 337 (1993); M. Leurer, Y. Nir, and

N. Seiberg, Nucl. Phys. **B420**, 468; L.E. Ibáñez and G.G. Ross, Phys. Lett. B **332**, 100 (1994); P. Binetruy and P. Ramond, *ibid.* **350**, 49 (1995); V. Jain and R. Shrock, *ibid.* **352**, 83 (1995); Stony Brook Report No. ITP-SB-95-22, hep-ph/9507238 (unpublished); Y. Nir, Phys. Lett. B **354**, 107 (1995); E. Dudas, S. Pokorski, and C.A. Savoy, *ibid.* **356**, 45 (1995); M.M. Robinson and J. Ziabicki, Phys. Rev. D **53**, 5924 (1996); E. Dudas, S. Pokorski, and C.A. Savoy, Phys. Lett. B **369**, 255 (1996); A. Pomarol and D. Tommasini, Nucl. Phys. **B466**, 3 (1996).

[31] See, for example:
D.B. Kaplan and M. Schmaltz, Phys. Rev. D **49**, 3741 (1994); M. Dine, R. Leigh, and A. Kagan, Phys. Rev. D **48**, 4269 (1993); L.J. Hall and H. Murayama, Phys. Rev. Lett. **75**, 3985 (1995); C.D. Carone, L.J. Hall, and H. Murayama, Phys. Rev. D **53**, 6282 (1996); P.H. Frampton and O.C.W. Kong, Phys. Rev. Lett. **77**, 1699 (1996); P.H. Frampton and A. Rašin, Phys. Lett. B **478**, 424 (2000), hep-ph/9910522 (unpublished).

[32] See, for example, H. Arason, D.J. Castaño, E.J. Piard, and P. Ramond, Phys. Rev. D **47**, 232, (1993).

[33] A. Aranda, C.D. Carone, R.F. Lebed,Phys. Lett. B **474**, 170 (2000), hep-ph/9910392.

[34] S. Coleman, Nucl. Phys. **B310**, 643 (1988);
S. Giddings and A. Strominger, *ibid.* **B307**, 854 (1988);
G. Gilbert, *ibid.* **B328**, 159 (1989).

[35] R. Barbieri, P. Creminelli, A. Romanino, Nucl. Phys. **B559**, 17 (1999).

[36] R. Dermisek, S. Raby, Phys. Rev. D **62**, 015007 (2000), hep-ph/9911275.

[37] T. Banks, Nucl. Phys. **B323**, 90 (1989).

[38] L.M. Krauss and F. Wilczek, Phys. Rev. Lett. **62**, 1221 (1989).

[39] J. Preskill, *P. Ramond and R. Stora, eds Les Houches, Session XLIV, 1985-Architecture des interactions fondamentales à courte distance/Architecture of fundamental interactions at short distances*, 235, Elsevier Science Publishers B.V., 1987

F. Wilczek, and M.B. Wise, Nucl. Phys. **B363**, 207 (1991).

[40] R. Barbieri, L.J. Hall, D. Smith, A. Strumia and N. Weiner, JHEP **9812**, 017, (1998).

[41] J.N. Bahcall, P.I. Krastev, A.Y. Smirnov, Phys. Rev. D **58**, 096016 (1998).

[42] V. Barger, M.S. Berger, P. Ohmann, Phys. Rev. D **47**, 1093 (1993).

[43] I. Antoniadis, C. Kounnas, R. Lacaze, Nucl. Phys. **B211**, 216 (1983).

[44] W.H. Press, S.A. Teukolsky, W.T. Vetterling, B.P. Flannery, *Numerical Recipes in Fortran 77*, 2nd ed. (Cambridge University Press, New York, 1992).

[45] K.S. Babu, C.N. Leung, J. Pantaleone, Phys. Lett. B **319**, 191 (1993).

[46] A.G. Cohen, D.B. Kaplan, A.E. Nelson, Phys. Lett. B **388**, 588 (1996).

[47] A. Kagan and S. Samuel, Phys. Lett. **B252** (1990) 605; Phys. Lett. **B284** (1992) 289.

[48] E.H. Simmons, Nucl. Phys. **B312** (1989) 253; C.D. Carone and E.H. Simmons, Nucl. Phys. **B397** (1993) 591; C.D. Carone and E.H. Simmons, Phys. Lett. **B344** (1995) 287.

[49] C.D. Carone and H. Georgi, Phys. Rev. D **49** (1994) 1427.

[50] See the review "Electroweak Model and constraints on new physics" in Ref. [1].

[51] W.A. Bardeen, C.T. Hill and M. Lindner, Phys. Rev. D **41** (1990) 1647.

[52] C.T. Hill, Phys. Lett. **B266** (1991) 419.

[53] D. Delepine, J.M. Gerard, R. Gonzalez Felipe, Phys. Lett. **B372** (1996) 271.

[54] D.E. Clague and G.G. Ross, Nucl. Phys. **B364** (1991) 43.

[55] N. Arkani-Hamed, S. Dimopoulos, and G. Dvali, Phys. Lett. **B429** (1998) 263; K. R. Dienes, E. Dudas and T. Gherghetta, Phys. Lett. **B436** (1998) 55.

[56] B. A. Dobrescu, hep-ph/9903407; H-C Cheng, B. A. Dobrescu, C. T. Hill, Nucl. Phys. **B589** (2000) 249, hep-ph/9912343.

[57] C.D. Froggatt and R.G. Moorhouse, Phys. Rev. D **45** (1992) 2471.

[58] LEP working group for Higgs boson searches, CERN EP/2000-055.

[59] CLEO Collaboration, M.S. Alam *et al.*, Phys. Rev. Lett. 73 (1994) 1895.

[60] A. Aranda, in progress.

[61] K.S. Babu, C. Kolda and J. March-Russell, Phys. Rev. D **54** 4635 (1996).

[62] P. Chiappetta, J. Layssac, F.M. Renard, C.Verzegnassi, Phys. Rev. D **54** 789 (1996).

[63] G. Altarelli, N. Di Bartolomeo, F. Feruglio, R. Gatto, M. Mangano, Phys. Lett. **B375**, 292 (1996).

[64] C. D. Carone and H. Murayama, Phys. Rev. Lett. **74**, 3122 (1995).

[65] C. D. Carone and H. Murayama, Phys. Rev. D **52**, 484 (1995).

[66] S. Davidson and D. Bailey, Phys. Lett. **B348**, 185, (1995).

[67] I. Antoniadis, N. Arkani-Hamed, S. Dimopoulos, and G. Dvali, SLAC-PUB-7801, April 1998, Phys. Lett. **B436**, 257, (1998), hep-ph/9804398.

[68] K. Dienes, E. Dudas, and T. Gherghetta, CERN-TH-98-100, Jun 1998, Nucl. Phys. **B537** (1999) 47, hep-ph/9806292.

[69] A. Nelson and N. Tetradis, Phys. Lett. **B221**, 80, (1989).

[70] H. Albrecht, *et al.* (ARGUS Collaboration), Z. Phys. C **31** 181 (1986).

[71] P. B. Mackenzie and G. P. Lepage, Phys. Rev. D **47**, 1244 (1981).

[72] K-T Chao, H-W Huang and Y-Q Liu, Phys. Rev. D **53** 221 (1996).

[73] C. Edwards, *et al.*, SLAC-PUB-5160, January 1990.

[74] Z. Jakubowski, *et al.* Z. Phys. C **40**, 49 (1988).

[75] M. Ciuchini, E. Franco, G. Martinelli, L. Reina, and L. Silvestrini, Phys. Lett. **B334**, 137, (1994).

[76] C. Amsler, *et al.* (Crystal Barrel Collaboration), Z. Phys. C **70** 219 (1996).

[77] See, for example, the compilation of collider parameter in Ref. [1].

[78] V. Luth, *et al.*, Phys. Rev. Lett. **35** 1124, (1975).

[79] A.S. Artamonov, *et al.*, Phys. Lett. **B137**, 272, (1984).

[80] See, for example, H. Georgi, Ann. Rev. Nucl. Part. Sci. **43**, 209 (1993).

[81] N. Arkani-Hamed, S. Dimopoulos, G. Dvali, Phys. Lett. **B429** (1998) 263; Phys. Rev. D **59** 086004 (1999); I. Antoniadis, N. Arkani-Hamed, S. Dimopoulos and G. Dvali, Phys. Lett. **B436**, 257 (1998) [hep-ph/9804398].

[82] Z. Berezhiani and G. Dvali, Phys. Lett. **B450**, 24 (1999) [hep-ph/9811378].

[83] F. C. Adams, G. L. Kane, M. Mbonye and M. J. Perry, hep-ph/0009154.

[84] Y. Hayato *et al.* [SuperKamiokande Collaboration], Phys. Rev. Lett. **83**, 1529 (1999) [hep-ex/9904020].

[85] C. D. Carone, L. J. Hall and H. Murayama, Phys. Rev. D **53**, 6282 (1996) [hep-ph/9512399].

[86] N. Arkani-Hamed and M. Schmaltz, Phys. Rev. D **61**, 033005 (2000) [hep-ph/9903417].

[87] For a list of references, see I. Antoniadis and K. Benakli, Int. J. Mod. Phys. **A15**, 4237 (2000) [hep-ph/0007226].

[88] D. Bailey and S. Davidson, Phys. Lett. **B348**, 185 (1995) [hep-ph/9411355].

[89] A. Aranda and C. D. Carone, Phys. Lett. **B443**, 352 (1998) [hep-ph/9809522].

[90] I. Antoniadis, Phys. Lett. **B246**, 377 (1990); I. Antoniadis and K. Benakli, Phys. Lett. **B326**, 69 (1994) [hep-th/9310151].

[91] K. R. Dienes, E. Dudas and T. Gherghetta, Phys. Lett. **B436**, 55 (1998) [hep-ph/9803466]; Nucl. Phys. **B537**, 47 (1999) [hep-ph/9806292].

[92] K. R. Dienes, C. Kolda and J. March-Russell, Nucl. Phys. **B492**, 104 (1997) [hep-ph/9610479].

[93] J. Erler, Nucl. Phys. **B586**, 73 (2000) [hep-ph/0006051]; H. Cheng, B. A. Dobrescu and K. T. Matchev, Nucl. Phys. **B543**, 47 (1999) [hep-ph/9811316]; Phys. Lett. **B439**, 301 (1998) [hep-ph/9807246].

[94] C. D. Carone, Phys. Lett. **B454**, 70 (1999) [hep-ph/9902407]; P. H. Frampton and A. Rasin, Phys. Lett. **B460**, 313 (1999) [hep-ph/9903479]; A. Delgado and M. Quiros, Nucl. Phys. **B559**, 235 (1999) [hep-ph/9903400]; Z. Kakushadze, Nucl. Phys. **B548**, 205 (1999) [hep-th/9811193]; A. Perez-Lorenzana and R. N. Mohapatra, Nucl. Phys. **B559**, 255 (1999) [hep-ph/9904504].

[95] K. R. Dienes, A. E. Faraggi and J. March-Russell, Nucl. Phys. **B467**, 44 (1996) [hep-th/9510223].

[96] P. Nath and M. Yamaguchi, Phys. Rev. D **60**, 116004 (1999) [hep-ph/9902323]; Phys. Rev. D **60**, 116006 (1999) [hep-ph/9903298]; M. Masip and A. Pomarol, Phys. Rev. D **60**, 096005 (1999) [hep-ph/9902467]; A. Strumia, Phys. Lett. **B466**, 107 (1999) [hep-ph/9906266]; R. Casalbuoni, S. De Curtis, D. Dominici and R. Gatto, Phys. Lett. **B462**, 48 (1999) [hep-ph/9907355]; T. G. Rizzo and J. D. Wells, Phys. Rev. D **61**, 016007 (2000) [hep-ph/9906234]; C. D. Carone, Phys. Rev. D **61**, 015008 (2000) [hep-ph/9907362].

[97] M. Bando, T. Kugo, T. Noguchi and K. Yoshioka, Phys. Rev. Lett. **83**, 3601 (1999) [hep-ph/9906549].

[98] F. Abe *et al.* [CDF Collaboration], Phys. Rev. D **55**, 5263 (1997) [hep-ex/9702004].

[99] H. Plothow-Besch, Int. J. Mod. Phys. **A10**, 2901 (1995).

[100] F. Abe *et al.* [CDF Collaboration], Phys. Rev. Lett. **79**, 2192 (1997).

VITA

Alfredo Aranda

Born in Ciudad Juárez, Chih., México, August 28, 1973. Graduated from the University of Texas at El Paso, El Paso, Texas, with a bachelor degree in Physics. He entered the graduate program at the College of William & Mary, Williamsburg, Virginia, in August 1996.